Development of a Dynamic Biomechanical Model
for Load Carriage: Phase VI:

Assessing Physiological and Biomechanical Loading Using the Portable Measurement System and the Dynamic Biomechanical Model

by
E. Morin, Ph.D., P.Eng.
S.A. Reid, M.Sc, P.Eng
J.M. Stevenson, Ph.D.
A. Lee, M.Sc.
C. Hare, M.Sc.

Project Manager:
J.M. Stevenson, PhD. (613) 533-6288
E.L. Morin (613) 533-6562

Ergonomics Research Group,
Queen's University, Kingston, Ontario, K7L 3N6

December 2007

Author

E. Morin, Ph.D., P.Eng.
Queen's University

Approved by

Captain Philip Snow
Scientific Authority

Approved for release by

K. C. Wulterkens
For, Chair, Knowledge and Information Management Committee

Abstract

In this work, factors affecting the physiological cost of load carriage and models for the estimation of metabolic energy cost during load carriage were examined in detail. The dynamic biomechanical model (DBM), designed to analyse the effects of rucksack parameters on forces experienced by a pack wearer, was used to create a stand-alone interactive software tool.

It was shown that tri-axial accelerations of the upper torso can be used in static and dynamic conditions to determine alterations in posture and gait, including: heel strike and toe off, forward lean angle, double support time and stride duration. These findings will permit assessment of gait in the field using the portable measurement system, allowing assessment of gait parameters over long durations, under varying terrain and loads. Terrain characteristics are also likely to be reflected in signal parameters other than the rms values examined in this work, permitting further improvement of the predictive models without requiring specific field data such as load, speed and topography. The ability to measure gait alterations using upper body accelerations merits further investigation as the present work was limited in this area.

Models to predict metabolic cost during load carriage under conditions of variable speed, load and incline were developed. A model similar to Pandolf's (Pandolf et al. 1977), using field specific data: load, speed and incline, had the highest correlation coefficient ($r^2 = 0.823$) but under-predicted energy cost both at low values and at high values of measured VO_2. A second model using upper body acceleration alone showed reasonable predictive ability ($r^2 = 0.554$) but under predicted VO_2 at high energy cost levels. Review of the results showed that the energy effect of incline is not captured in the rms acceleration parameters used in the model. Heart rate is well correlated to metabolic cost and a model using it and acceleration parameters successfully achieved the predictive power of the model based on load, speed and incline with $r^2 = 0.811$.

The Dynamic Biomechanical Model body of work consists of a general dynamic biomechanical model of human backpack load carriage based on the characteristics of the Canadian Clothe the Soldier Rucksack with the ability to assess injury risk potential across as range of activities and loads. Output from this program is expected to provide input to a load carriage limit predictive equation.

Résumé

Dans cette étude, les facteurs qui ont une incidence sur le coût physiologique lié au transport de charges et sur les modèles servant à évaluer la dépense d'énergie métabolique durant le transport de charges ont été examinés en détail. Le modèle biomécanique dynamique (MBD), élaboré dans le but d'analyser les effets des paramètres relatifs aux havresacs sur les forces ressenties par le porteur d'un sac, a été utilisé pour créer un outil logiciel interactif autonome.

Il a été démontré que les accélérations triaxiales de la partie supérieure du torse peuvent être utilisées dans des conditions statiques et dynamiques pour déterminer les changements au niveau de la posture et de la démarche, y compris l'impact du talon au sol et le décollement des orteils, l'angle d'inclinaison avant, la durée du double appui et la durée des enjambées. Ces résultats permettront d'évaluer la démarche sur le terrain à l'aide du système de mesure portatif ainsi que les paramètres relatifs à la démarche sur une longue période, sur différents terrains et avec des charges variées. Les caractéristiques des terrains doivent également pouvoir être prises en considération dans les paramètres des signaux autres que les valeurs quadratiques moyennes examinées dans cette étude, en vue d'améliorer davantage les modèles prédictifs sans recourir à des données de terrain précises comme la charge, la vitesse et la topographie. La capacité à mesurer les changements dans la démarche en utilisant les accélérations du haut du corps mérite une analyse plus poussée, la présente étude ayant à peine effleuré cet aspect.

Des modèles servant à prédire la dépense d'énergie métabolique durant le transport de charges dans des conditions de vitesse, de charge et d'inclinaison variables ont été élaborés. Un modèle similaire à celui de Pandolf (Pandolf *et coll.*, 1977), qui utilise des données de terrain précises, par exemple la charge, la vitesse et l'inclinaison, avait le coefficient de corrélation le plus élevé ($r^2 = 0,823$), mais une dépense d'énergie sous-estimée à des valeurs mesurées de VO_2 faibles et élevées. Un deuxième modèle utilisant seulement une accélération du haut du corps a montré une valeur prédictive raisonnable ($r^2 = 0,554$), mais une valeur de VO2 sous-estimée à des niveaux de dépense énergétique élevés. Un examen des résultats montre que l'effet de l'énergie liée à l'inclinaison n'est pas pris en considération dans les valeurs quadratiques moyennes des paramètres d'accélération utilisés dans le modèle. Il existe une bonne corrélation entre le rythme cardiaque et la

dépense métabolique; un modèle qui tient compte de cette corrélation ainsi que des paramètres d'accélération a montré la valeur prédictive du modèle basée sur la charge, la vitesse et l'inclinaison avec un coefficient de corrélation $r^2 = 0,811$.

Le modèle biomécanique dynamique consiste en un modèle biomécanique dynamique général de transport de charges dans un havresac par un être humain, basé sur les caractéristiques du havresac du programme canadien Habillez le soldat (HLS), qui permet d'évaluer les risques de blessures potentiels en fonction d'une gamme d'activités et de charges. On s'attend à ce que les données issues de ce programme soient utilisées dans une équation prédictive des limites de transport de charges.

Executive Summary

Development of a Dynamic Biomechanical Model for Load Carriage: Phase VI: Assessing Physiological and Biomechanical Loading Using the Portable Measurement System and the Dynamic Biomechanical Model

E. Morin, Ph.D., P.Eng. Et-Al, Queens University;
DRDC Toronto CR 2008-009, Defence R&D Canada – Toronto; December 2007

The purpose of the DRDC research program on human load carriage has been to improve our understanding of the physiological and biomechanical effects on humans of carrying heavy loads, to determine the effects of load carriage design features on human health and mobility, and to establish acceptable load carriage limits. A load carriage limit (LCL) equation (LCL = (SCL×DF×PF×BF×RF)×Time), which includes factors that have an impact on load carriage performance, has previously been introduced. The starting load constant (SLC), which is the current upper limit on load carried, is modified by the factors: DF, RF, PF and BF. The demographic factor (DF) and readiness factor (RF) are determined by physical and psychological characteristics of the individual. PF and BF are determined by the physiological effects (e.g. metabolic energy cost, cardiovascular load) and biomechanical effects (e.g. contact pressures and forces experienced due to the presence of the load carriage system), respectively. This research program has focused on identifying PF and BF via direct measures and a dynamic biomechanical model (DBM).

Load carriage results in measurable alterations in posture and gait to accommodate the load. These effects interact with physiological changes to increase the metabolic energy cost of walking during load carriage relative to the cost of walking with no load. In this work, postural and gait changes were tracked using upper body accelerations measured using a Crossbow accelerometer mounted over the sternum. Forward body lean angles estimated from upper body accelerations were validated against lean angles measured using an inertial sensor and digital images. It was found that lean angles can be reasonably well estimated from upper body accelerations, where forward body lean increases with load carried. Using accelerometry to estimate body lean has the advantage that the lean angle can be tracked over time and when the subject is in the field performing normal duties or training exercises.

The determination of gait events – heel strike and toe-off – using upper body accelerations was examined in subjects walking with no load and walking with one of three loads in a CTS backpack. It was found that heel strike and toe-off timing can be reliably detected from the upper body accelerations. Using this timing information and kinematic information from the Optotrak® motion analysis system, it was found that cadence (the number of strides per second) did not change with load carried, but velocity and stride length decreased. The amount of time spent in double support (both feet planted) during the gait cycle increased with load, as did the maximum knee angle at heel strike. These results are in agreement with previous findings, that gait changes during load carriage occur to increase stability and reduce the impulsive forces on the lower limb.

Several models to predict energy cost from upper body accelerations, alone or in combination with heart rate or load carried, were derived. The validity of these models to predict metabolic energy cost was assessed by examining the predicted vs. measured values and the characteristics of the residuals. In all but one model (the model with HR only as the independent variable), energy cost was under-predicted at high values of $\dot{V}O_2$. This appears to be because the effects of increased incline are not reflected in the upper body accelerations. If incline and other terrain factors can be predicted from upper body accelerations (e.g. using pattern recognition techniques) then it may be possible to determine a correction factor and improve the energy cost estimate.

The dynamic biomechanical model (DBM) has been used to generate a stand-alone program that permits assessment of the effects of varying load magnitude, centre of gravity location, speed of walking, tightness of shoulder straps and use or non-use of a waist belt. The geometric and inertial properties of the rucksack modeled are based on the current issue Clothe the Soldier (CTS) rucksack. This program has applications in quantifying the biomechanical loading of different CTS rucksack configurations which may be a variable in studies attempting to assess physiological strain on subjects. The model provides estimated reaction forces and moments on the lumbar spine, shoulder reaction force and total load experienced by the body as a ratio of load carried. The model also calculates the distribution of force to the upper and lower torso and the total contact force. A visual analogue scale is used to indicate the acceptability of each rucksack configuration to a user,

based on the rucksack load carriage parameters determined in the course of the Clothe the Soldier program.

The final result of this body of work consists of a general dynamic biomechanical model of human backpack load carriage based on the geometry and characteristics of the Canadian Clothe the Soldier Rucksack with the ability to assess injury risk potential across as range of activities and loads.

Sommaire

L'objectif du programme de recherche de R & D pour la défense Canada (RDDC) sur le transport de charges par l'être humain est d'améliorer notre compréhension des effets physiologiques et biomécaniques sur les êtres humains transportant de lourdes charges afin de déterminer l'incidence des caractéristiques liées au transport de charges sur la mobilité et la santé de ces derniers, et d'établir des limites de transport de charges acceptables. L'équation des limites de transport de charges (LCL = (SCL × DF × PF × BF × RF) × durée), qui comprend des facteurs qui ont une incidence sur le transport de charges, a déjà été présentée. La constante de charge initiale (SLC), qui est la limite supérieure réelle de la charge transportée, est modifiée par les facteurs suivants : DF, RF, PF et BF. Le facteur démographie (DF) et le facteur état de préparation (RF) sont déterminés par les caractéristiques physiques et psychologiques des individus. Les facteurs PF et BF sont déterminés par les effets physiologiques (p. ex. la dépense d'énergie métabolique, la charge cardiovasculaire) et par les effets biomécaniques (p. ex. les pressions et les forces de contact exercées par la présence d'un système de transport de charges). Ce programme de recherche met l'accent sur l'identification des facteurs PF et BF au moyen de mesures directes et d'un modèle biomécanique dynamique (MBD).

Le transport de charges se traduit par des changements mesurables au niveau de la posture et de la démarche en fonction de la charge imposée. Ces effets interagissent avec les changements physiologiques pour augmenter la dépense d'énergie métabolique liée à la marche durant le transport de charges par rapport à la dépense d'énergie liée à la marche sans aucune charge. Dans cette étude, les changements dans la posture et la démarche ont été enregistrés en utilisant les accélérations du haut du corps mesurées à l'aide d'un accéléromètre de Crossbow monté sur le sternum. Les angles d'inclinaison avant du corps, qui sont estimés à partir des accélérations du haut du corps, ont été validés en les comparant aux angles d'inclinaison mesurés à l'aide d'un capteur à inertie et d'images numériques. On a trouvé que les angles d'inclinaison peuvent être estimés avec une exactitude raisonnable à partir des accélérations du haut du corps, tandis que l'inclinaison avant du corps augmente proportionnellement à la charge transportée. Le recours à un accéléromètre pour estimer l'inclinaison du corps permet de suivre l'angle d'inclinaison en

fonction du temps et de le différencier selon que le sujet exécute sur le terrain des tâches normales ou des exercices d'entraînement.

La détermination des effets liés à la démarche – impact du talon au sol et décollement des orteils – en utilisant les accélérations du haut du corps a été étudiée chez des sujets qui marchaient sans aucune charge et chez des sujets qui marchaient avec une des trois charges placées dans un havresac du programme HLS. Il a été démontré que la synchronisation de l'impact du talon au sol et du décollement des orteils peut être détectée de façon fiable à partir des accélérations du haut du corps. À partir de cette information sur la synchronisation et de l'information sur la cinématique du système d'analyse des mouvements Optotrak®, on a trouvé que la cadence (le nombre d'enjambées par seconde) ne change pas en fonction de la charge transportée, mais que la vitesse et la longueur des enjambées diminuent. La durée du double appui (les deux pieds sur le sol) durant le cycle de la marche augmente avec la charge, tout comme l'angle maximal du genou lorsque le talon touche le sol. Ces résultats sont conformes aux résultats antérieurs, c'est-à-dire que les changements dans la démarche durant le transport de charges visent à augmenter la stabilité et à réduire les efforts exercés sur les membres inférieurs.

Plusieurs modèles servant à prédire la dépense d'énergie à partir des accélérations du haut du corps, seules ou en combinaison avec le rythme cardiaque ou la charge transportée, ont été dérivés. La validité de ces modèles pour prédire la dépense d'énergie métabolique a été évaluée en examinant les valeurs prévues par rapport aux valeurs mesurées ainsi que les caractéristiques des variations résiduelles. Pour tous les modèles sauf un (le modèle prenant le rythme cardiaque comme seule variable indépendante), la dépense d'énergie était sous-estimée à des valeurs élevées de VO_2. Ce résultat semble s'expliquer par le fait que les conséquences de l'augmentation de l'inclinaison ne sont pas prises en considération dans les accélérations du haut du corps. Si l'inclinaison et d'autres caractéristiques du terrain peuvent être prévues à partir des accélérations du haut du corps (p. ex. en utilisant les techniques de reconnaissance des tendances), il est alors possible de déterminer un facteur de correction et d'améliorer l'estimation de la dépense d'énergie.

Le modèle biomécanique dynamique (MBD) est utilisé pour générer un programme autonome qui permet d'évaluer les effets (l'amplitude) de la variation des charges, de l'emplacement du centre de gravité, de la vitesse de marche, de la tension des courroies

d'épaule et de l'utilisation ou non d'une ceinture de taille. Les propriétés relatives à la géométrie et à l'inertie du havresac modélisé sont basées sur le havresac actuel du programme HLS. Ce programme est utile pour quantifier les charges biomécaniques des différentes configurations d'havresacs HLS qui peuvent constituer une variable dans les études qui tentent d'évaluer l'effort physiologique demandé aux sujets. Le modèle fournit une estimation des moments et des forces exercés sur la colonne lombaire, des forces exercées sur les épaules et de la charge totale exercée sur le corps, qui se traduit par un rapport de la charge transportée. Le modèle calcule également la distribution de la force exercée sur la partie supérieure du torse et la partie inférieure du torse, ainsi que la force de contact totale. Une échelle analogique visuelle est utilisée pour indiquer à l'utilisateur si la configuration de ses havresacs est acceptable. Cette échelle est basée sur les paramètres de transport de charges dans un havresac, déterminés dans le contexte du programme Habillez le soldat.

Il résulte finalement de ces travaux un modèle biomécanique dynamique général de transport de charges dans un havresac par l'être humain fondé sur la géométrie et les caractéristiques du havresac du programme canadien Habillez le soldat, qui permet d'évaluer les risques de blessures potentiels dans toute la gamme des activités et des charges envisagées.

Table of Contents

List of Figures

List of Tables

Section 1: Physiological Loading

1   Introduction

In a previous contract[1], the objectives were to assess our ability to predict metabolic energy cost from upper body accelerations under conditions of different loads carried, changing speed and changing incline and to advance the development of the dynamic biomechanical model. The ultimate goal of our research program is to identify the parameters of the load carriage limit (LCL) equation, introduced in the previous report (Morin et al., 2004):

$$LCL = (SCL \times DF \times PF \times BF \times RF) \times Time$$

Where SLC is the heaviest load currently used in the field, DF is a demographic factor, PF is the physiological factor, BF is the biomechanical factor and RF is the readiness factor. DF and RF are determined by characteristics of the individual, including physical (age, gender, height, weight and fitness level) and psychological (motivation and acceptance) variables. The PF is determined primarily by factors which affect the metabolic energy cost, such as load carried, speed of locomotion and terrain factors. The BF is determined by the reaction forces and moments due to the presence of a backpack, contact pressures and backpack motion relative to body motion.

Transporting a loaded backpack results in alterations in body posture and gait pattern, which can impact the energy cost of locomotion. In backpack load carriage, the load volume is situated dorsal to the body and the load is transferred onto the body through the pack suspension system (shoulder straps and waist belt). The centre of gravity (CoG) of the body plus load is behind the CoG of the body alone, thus the load bearer must lean forward to bring the CoG over the base of support. Bloom and Woodhull-McNeal (1987) looked at forward body lean for an internal and an external frame backpack, where the centre of the load volume is lower and closer to the body for the internal frame pack than for the external frame pack. The total load mass was 14 kg for women and 19 kg for men (giving a range of 22% - 32% body weight). Subjects were photographed as they stood with

---

[1] Contract # W7711-03-7863 Call-up #1

no pack, the internal frame pack and the external frame pack. The positions of the joint centres of the ankle, knee, hip and shoulder joints and the external auditory meatus for each subject were measured. From Fig. 2 (p. 1427), the average position of the hip is approximately 6 cm ahead of the ankle for no load, 7.8 cm ahead of the ankle for the external frame pack load, and 8.4 cm ahead of the ankle for the internal frame pack load; the average position of the shoulder is approximately 4.8 cm ahead of the ankle for no load, 13.8 cm ahead of the ankle for the external frame pack load, and 17 cm ahead of the ankle for the internal frame pack load. The torque present at the hip with forward lean and the torque which would have been present had the subjects not leaned forward were also calculated. It was found that body lean compensated for 74% of the torque for the external frame pack, but only 52% of the torque for the internal frame pack. To maintain stability, the body must compensate for the excess applied torque in some other way. This implies muscular effort, which may lead to increased energy cost and cardiovascular load. Holewijn (1990) reported that metabolic cost did not increase when standing with a loaded backpack (5.4 or 10.4 kg load), but that average heart rate increased significantly by 9 beats per minute (bpm).

Abe et al. (2004) hypothesized that the rotational torque induced about the hips by a backpack load, aids in forward momentum, thereby saving energy. The rotative torque, about the CoG of the body functions to push the hips forward while walking. The positive effect on metabolic energy cost is partially negated and eventually overcome (as load increases) by the extra burden placed on the leg muscles by the load. The cost of walking per unit distance was obtained as the ratio of net VO_2 (steady state VO_2 minus resting VO_2) to walking speed: $C_w = netVO_2/v$ for four loads (0, 6, 9 and 12 kg) and nine walking speeds (0.67, 0.83, 1, 1.17, 1.33, 1.5, 1.67, 1.83 and 2 m/s). The energy cost curves for walking at different speeds are u-shaped with a minimum at 1.33 m/s, which is very close to natural walking speed. The cost of walking with the loaded backpack was lower than walking without a backpack, except at the highest speed for the 12 kg load. The average C_w for the 9 and 12 kg loads was significantly lower than for no load at the slowest walking speeds (0.67, 0.83 and 1 m/s). Abe et al. (2004) suggest that the gravitational potential energy (E_p) increases when a load is carried on the back. If the transfer efficiency between E_p and kinetic energy (E_k) during walking, and the time course of E_p are not altered by the

presence of the load, then there is a greater transfer of E_p to E_k resulting in a lower metabolic energy cost. This effect is based on the concept of 'free-ride' whereby the metabolic energy cost of walking with loads does not increase for loads less than 20% of body mass (Charteris et al., 1989). The loads used by Abe et al. (2004) were approximately 9.7%, 14.5% and 19.3% of the average body weight of the subjects (62.1 ± 1.2 kg). Holewijn (1990) also noted that the energy cost per kg load of walking with a 5.4 kg backpack was lower than the energy cost per kg of body mass when walking with no load, but increased when carrying a 10.4 kg pack.

Several studies examining the effect of backpack load carriage on biomechanical parameters, principally gait parameters, have been done. Martin and Nelson (1986) examined temporal and kinematic characteristics of walking gait while carrying different loads. Eleven male and eleven female subjects participated in the study. The subjects walked at 1.78 m/s while carrying one of five loads; however only the two highest loads (30 kg and 36.8 kg for men; 29.26 kg and 36.06 kg for women) included a loaded external frame backpack[2], weighing 12.34 kg and 19.14 kg respectively. It was reported that stride length did not change with load for men, but decreased with increasing load for women, with a consequent increase in stride frequency to maintain velocity. Single leg contact time did not change, but swing time decreased with increased load in both men and women. Double support time increased with load in women, and displayed a slight increase with load in men. For the two heaviest loads, the forward lean angle of the trunk increased, as expected, since these two loads included a backpack. In the male subjects, the average trunk angle increased by 6.4° between load 3 (no backpack) and load 4 (12.34 kg backpack) and a further 1.4° for load 5 (19.14 kg backpack); in the female subjects, the average trunk angle increased by 8.8° between load 3 (no backpack) and load 4 (12.34 kg backpack) and a further 1.8° for load 5 (19.14 kg backpack).

In a study done by Harmon et al. (2001), sixteen male volunteers walked at three speeds (1.1, 1.3 and 1.5 m/s) while carrying four loads (6, 20, 33 and 47 kg) in a specially designed backpack (12 experimental conditions). Gait kinetics, kinematics and EMG at the

---

[2] The lowest three loads included items such as clothing (including a helmet and protective vest for the 3rd load), webbing, a water filled canteen, tools and small sand bags. These loads were distributed relatively evenly on the front and back of the body.

shoulder, back and legs were measured. Several gait parameters were found to increase significantly with increasing load carried including stride frequency, double support time, knee bend and forward trunk inclination. Stride time decreased significantly and stride length tended to decline but the effect was not significant. EMG activity increased significantly in the trapezius, quadriceps, hamstrings, tibialis anterior and gastrocnemius, which supports Abe et al.'s (2004) statement that there is an extra burden placed on the legs as a result of supporting a load. Activity in the erector spinae muscles decreased as load increased from 6 to 20 kg, but then increased again as load increased above 20 kg. Gait parameters which increased significantly for increased walking speed included stride length and stride frequency, and the vertical excursion of the body CoG. Double support time decreased significantly with increased speed. Franduti-Polcyn et al. (2001) reported on the results of four load carriage studies carried out at the Center for Military Biomechanics (Natick, Mass.) involving five load carriage systems: the ALICE (All-purpose Lightweight Individual Carrying Equipment); LW I (first generation Land Warrior prototype); LW II (second generation Land Warrior prototype); MLS (Modular Load System prototype); and MOLLE (Modular Lightweight Load-carrying Equipment). The packs were loaded with fighting (range: 11.82 – 23.45 kg), approach (range: 23.41 – 35.47 kg) and sustainment (range: 37.54 – 50.11 kg) loads. Gait kinetics and kinematics were measured on male subjects carrying the loaded backpacks. Vertical ground reaction force (GRF), joint reaction forces, knee bend, range of hip angle and forward trunk lean increased with weight supported (body weight plus load weight). There was a slight trend towards decreasing stride rate and increased double support time. The biomechanical adaptations to load carriage observed in these studies tend to keep the body lower to the ground, with the CoG over the base of support thereby increasing stability, and to reduce the impulsive forces on the lower limbs. When individuals are required to walk at higher speeds and carry heavy loads, however, they cannot adapt as well to the demands of the load and this may lead to higher risk of injury or fatigue during load carriage (Harmon et al., 2001).

LaFiandra et al. (2003) examined rotation of the pelvis and upper thorax in the transverse plane in twelve subjects (7 female and 5 male) while carrying no load or carrying a backpack loaded to 40% body weight, and walking on a treadmill at speeds of 0.6 – 1.6 m/s (increasing in 0.2 m/s steps). Without a backpack, increasing the speed of

walking resulted in greater pelvic rotation to increase stride length, thus causing increased counter rotation of the thorax. When the backpack was worn, pelvic and thoracic rotation decreased and tended to remain in-phase as walking speed increased. This indicates that pelvic rotation does not contribute to increased stride length at increased walking speed during backpack load carriage. To increase velocity, subjects wearing the backpack increased their hip excursion angle and stride frequency. Subjects also tended to minimize torque production in the upper body during load carriage and relative torque between the upper and lower body (LaFiandra et al., 2002). Holewijn (1990) noted that for relatively light loads (5.4 and 10.4 kg) the force generated by the trapezius increased when the load was borne primarily on the shoulders. This occurred in order to generate a higher rotational force on the shoulder and maintain thoracic rotation during gait.

There has also been considerable study on the effect of heavy load carriage on metabolic energy cost. In the studies reported by Franduti-Polcyn et al. (2001) it was found that O_2 consumption increased with load carried when subjects walked at 4.8 km/h on a treadmill. Their regression equation was: $y = 0.0162x + 14.874$ where y is the metabolic energy cost per body weight and x is the load weight (N). Approximately 40% of the variance in O_2 consumption was accounted for by load. Hong et al. (2000) examined walking with a backpack in fifteen 10-year old children. Subjects walked on a treadmill at 1.1 m/s for 20 min. while carrying 0, 10%, 15% or 20% body weight (BW) loads. VO_2 significantly increased after walking for 5 min., then gradually increased over the duration of the walk. VO_2 for the 20% BW load was significantly higher, and recovered more slowly, than for the 0 or 10% loads, but there were no significant differences in VO_2 between 0, 10% and 15% BW loads. Heart rate (HR) also increased significantly during walking, but there were no significant differences between loads carried. Systolic blood pressure (BP) increased during walking for all loads, but recovered more slowly for the 15% and 20% BW loads. Diastolic BP increased significantly during walking for the 15% and 20% BW loads only. Holewijn (1990) reported that VO_2 increased significantly when walking with a 5.4 kg or a 10.4 kg load versus walking with no load. The energy cost of walking with no load was 4.2 W/kg BW; the additional cost of walking with a 5.4 kg backpack was 1.1 W/kg load mass and with a 10.4 kg backpack was 6.3 W/kg load mass. As well, HR increased by 8 beats per min. (bpm) when walking with the 5.4 kg load and by

an additional 6 bpm when walking with the 10.4 kg load. Holewijn (1990) and Hong et al. (2000) both noted that metabolic cost did not increase when subjects simply supported the loads while standing, but that HR did increase – by 9 bpm in adults and 8.12 bpm in children respectively. These results indicate that there is both a metabolic and a cardiovascular cost to carrying loads in backpacks.

Pierrynowski et al. (1981) examined load carriage in six male subjects, in order to determine the optimal load based on metabolic considerations. Subjects walked at 5.54 km/h on a treadmill carrying loads of 0, 15.16, 19.3, 22.65, 28.63 or 33.85 kg in a modified backpack. The metabolic task cost (MTC) was computed as the cost per unit distance and mass supported, where the mass supported comprised the load mass and 0%, 25%, 50%, 75% or 100% body mass. As higher percentages of body mass were taken into account the optimal load, which corresponded to the minimum on the MTC vs mass supported curve, decreased. Pierrynowski et al. (1981) suggested that credit for 50% body mass should be included when determining optimal load, which gave an optimal load value of 18 kg. Falola et al. (1999) looked at optimal walking speed when carrying a load of 10% body mass versus no load. They calculated energy cost as:

$$C_w = \left[\frac{\dot{V}O_2(walking) - \dot{V}O_2(resting)}{walking\_speed} \right] \times 60 \ \mathrm{ml \cdot kg^{-1} \cdot km^{-1}}$$

and obtained u-shaped C_w vs speed curves[3]. The optimum walking speeds, which corresponded to the minima on the C_w vs speed curves, were 4±0.2 km/h and 3.5±0.5 km/h for the unloaded and loaded cases respectively. It was suggested that during walking with a load, there is a trade-off between stability and metabolic cost, resulting in a reduced optimum speed.

Lloyd and Cooke (2000) examined the effect of incline and load carriage on the energy cost of walking. Nine subjects (five female and four male) completed four tests: walking downhill at 3 km/h (–27°, –22°, –17°, –12° and –5° inclines) and walking uphill at 3 km/h (0°, 5°, 10°, 15° and 20° inclines) wearing each of two backpacks – a traditional backpack and a pack with front load balance pockets – loaded to 25.6 kg. In all cases, VO_2 and HR were significantly higher for walking with a load than with no load and VO_2 was

---

[3] Typically energy cost vs speed curves for walking are u-shaped with a minimum at the optimal speed, e.g. see Saibene and Minetti (2003)

higher for uphill versus downhill walking. VO$_2$ was generally lower for the new pack design, with front load balance pockets, than for the traditional pack, but the difference was significant only at 0°, 5°, 10° and 20° uphill.

It is apparent from the foregoing discussion, that there are measurable biomechanical and physiological changes when humans carry loads. Biomechanical alterations occur to increase stability and reduce impulsive forces on the body (Franduti-Polcyn et al., 2001), but the presence of an external load still leads to increased ground reaction force, joint forces and muscular activity. Optimal walking speed may decrease with load carried, but soldiers may be required to walk at relatively high speeds while carrying heavy loads, depending on mission requirements, increasing the potential for fatigue and injury (Harmon et al., 2001).

The overall goal of this work was to assess biomechanical and physiological factors that can be monitored in humans, using the portable measurement system, and to examine how these factors interact to affect performance during load carriage exercises. The specific objectives of the work are:

- to determine the accuracy and reliability of static and dynamic forward body lean angle estimates using upper body accelerations;
- to assess alterations in the gait pattern during load carriage using upper body accelerations;
- to estimate metabolic energy cost using upper body accelerations alone and in combination with heart rate.

2   Computation of Forward Lean Angle during Load Carriage

2.1   Forward Lean Angles Reported by the Xsens Motion Sensor

2.1.1   Data Collection and Analysis
In a treadmill study done under a previous contract (Morin et al., 2004), upper body accelerations were measured using a triaxial accelerometer (Crossbow model CXL10LP3)

and an Xsens MT9 inertial motion sensor[4] mounted on the sternum of the upper torso of the subjects (see Appendix D of Morin et al., 2004).

The Xsens is a miniature inertial measurement unit that provides serial digital output of three-dimensional (3D) acceleration, 3D rate-of-turn and 3D earth-magnetic field data. Combined with the MT9 Software it provides 3D orientation data in real-time. The Xsens stores its measurement data in two files. The first is a calibrated MT9 data log-format file called MT9_cal_SID_XXX.log. The file contains nine columns of data: three columns of acceleration data (x, y and z-axis respectively); three columns of rate-of-turn (gyroscope) data (x, y and z-axis respectively); and three columns of earth-magnetic field data (x, y and z-axis respectively). The second file is an orientation coordinate system file called MT9_Euler_SID_XXX.log. By default the earth-fixed coordinate system is defined as a right handed cartesian co-ordinate system with the x-axis positive when pointing to the local magnetic north, the z-axis positive when pointing up and the y-axis positive according to the right hand rule as shown in Figure 1-1. The rotation about the x-axis, defined as the roll, is represented by Φ and ranges from -180° to 180°. The rotation about the y-axis, defined as the pitch, is represented by θ and ranges from -90° and 90°. The rotation about the z-axis, called the yaw, is represented by Ψ and ranges from -180° to $+180^{o}$. The four columns of the orientation coordinate system file contain the SID (the ID of the Xsens), roll (in degrees), pitch (in degrees) and yaw (in degrees).
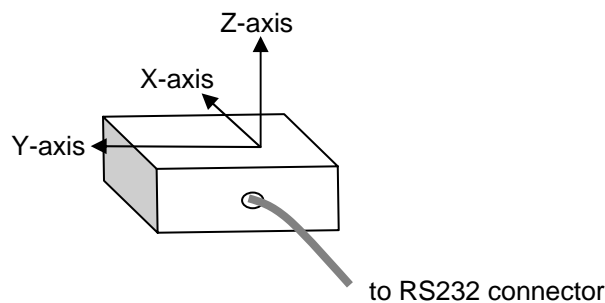
Figure 1-1.   Xsens co-ordinate system orientation

---

[4] Manufactured by Xsens Technologies B.V., Capitool 50, Postbus 545, 7500 AM Enschede, The Netherlands. 1www.xsens.com

The accuracy of the Xsens MT9 sensor has been tested and the results have been reported previously (Fergenbaum et al., 2003). In the current study, the Xsens data obtained from the treadmill study (Morin et al., 2004) were analyzed to confirm the angles obtained using upper body accelerations. The Xsens was oriented on the chest such that the x-axis was horizontal, the y-axis pointed downwards and the z-axis pointed outwards from the body. Upper body lean results in rotation about the x-axis and is reflected in the roll angle.

A Matlab$^®$ program was written to extract the Euler angles (roll, pitch and yaw) from the Xsens data for the two testing conditions – change in treadmill speed (3.22, 4.83 and 6.44 km/h) and change in treadmill incline (0°, 5° and 10°)) for four load conditions (no load or 16.6, 25.9 or 38.7 kg carried in the Canadian CTS backpack). A 1-second segment of Euler angle data was extracted from the middle of the ten-second recording of stationary data, while the subject was standing upright prior to testing, per condition for all four loads. Two 5-second segments of Euler angle data were extracted for the each of the walking trials – one segment was extracted from near the start of each test condition and the second was extracted from near the end of each test condition. All three Euler angles (roll, pitch and yaw) for each segment of extracted data were averaged. The average roll angles for each condition for all four loads were used to determine the forward lean angles – static average lean angles were computed from the standing data and dynamic average lean angles were computed from the walking data. These angles were compared to the forward lean angles previously calculated from upper body accelerations recorded during the treadmill study (Morin et al., 2004).

Results

Average static forward lean angles, relative to body lean angle in the no load case, calculated using upper body accelerations and Xsens data are shown versus load in Figure 1-2 a) and b) respectively. As expected, given the results of earlier studies (Stevenson et al., 2002), there is an increase in forward lean angle as load increases. The forward lean angles calculated using upper body accelerations and those calculated from Xsens data, were compared using t-tests and the means were found to be not significantly different. After outliers were removed from each data set (two from the accelerometer angles and two from the Xsens angles – see Appendix B), the mean angles for the 25.9 kg load were found to be

significantly different ($p < 0.05$) and it was noted that the mean relative angles from the accelerometer data were consistently larger than the angles from the Xsens data.
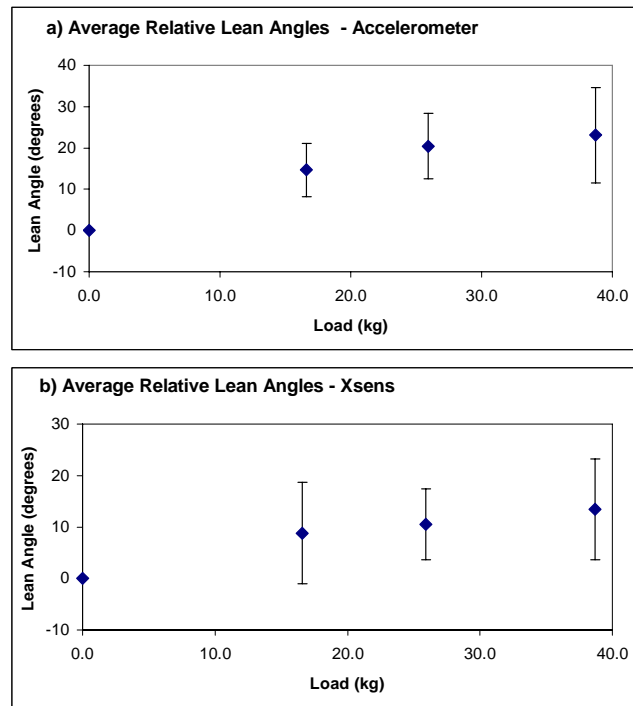
Figure 1-2.   Average static relative lean angles for changing backpack loads calculated from: a) upper body accelerations and b) Xsens data. Relative lean angles were obtained by subtracting the lean angles for no load from the angles for all loads. Error bars represent ±1 standard deviation. Note the y-axis scales are different.

Dynamic forward lean angles, for each combination of load, speed and incline were computed using 5 sec of Xsens data from the beginning and the end of each condition. Relative angles, averaged across subjects, are given in Table 1-I and plotted versus load in Figure 1-3. Examination of Table 1-I and Figure 1-3 reveals that there is no difference in the forward lean angle from the beginning to the end of each trial condition, except at the slowest speed, where the lean angle decreases, indicating that subjects straightened slightly as they walked.

Table 1-I. Average relative forward body lean angles (in degrees) calculated from Xsens data at the start and end of each trial condition. Number of values for each average, N = 7.

Load		Speed					
		3.22		4.83		6.44	
		Mean	Std dev	Mean	Std dev	Mean	Std dev
0	Start	0	0	0	0	0	0
	End	0	0	0	0	0	0
16.6	Start	12.35	7.14	8.24	7.24	8.54	7.18
	End	9.78	6.32	8.92	6.42	9.07	6.00
25.9	Start	13.24	6.59	10.18	7.94	9.65	7.03
	End	11.21	4.60	10.96	6.13	10.11	5.61
38.7	Start	17.49	8.70	11.19	7.25	9.73	6.37
	End	14.28	4.30	12.82	5.08	10.87	4.99

Load		Incline					
		0		5		10	
		Mean	Std dev	Mean	Std dev	Mean	Std dev
0	Start	0	0	0	0	0	0
	End	0	0	0	0	0	0
16.6	Start	14.36	9.45	13.15	13.35	9.94	12.26
	End	12.39	14.11	12.62	14.07	9.85	12.74
25.9	Start	14.11	6.92	16.78	10.02	14.50	9.05
	End	14.52	8.27	15.77	9.30	14.98	11.04
38.7	Start	15.23	5.29	15.39	7.00	12.88	6.53
	End	13.90	5.26	14.80	6.83	11.80	5.85
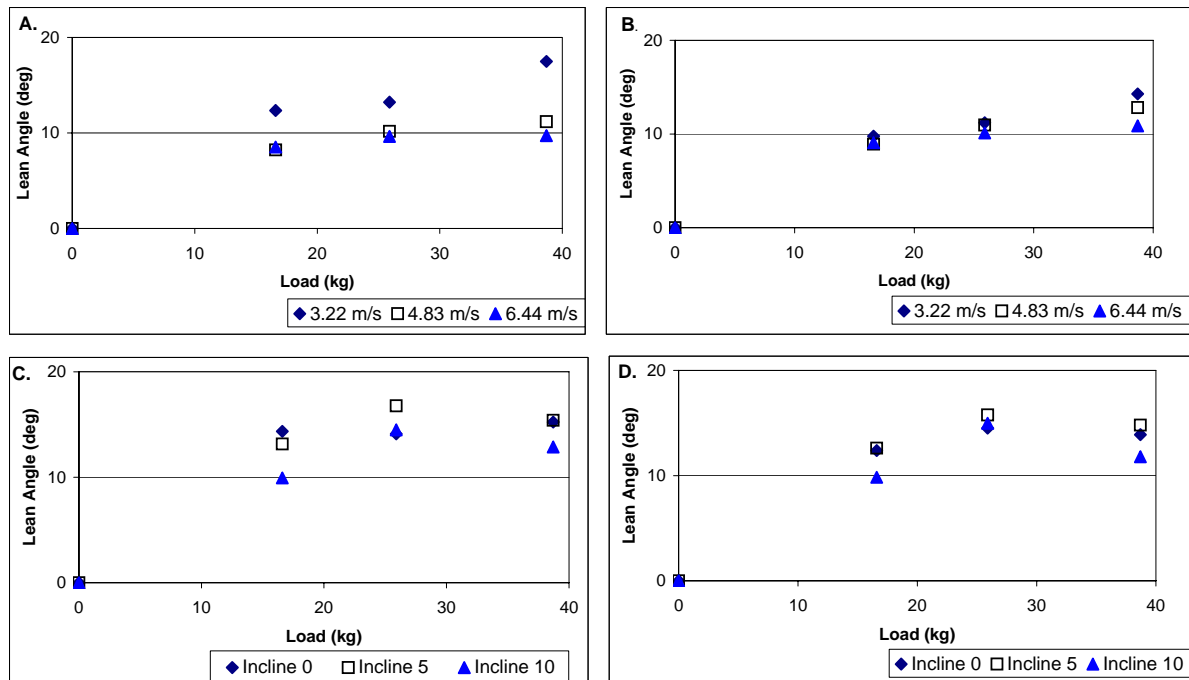
Figure 1-3. Relative average forward lean angle versus load computed from Xsens data at A. the beginning and B. the end of the changing speed trials; and C. the beginning and D. the end of the changing incline trials. Lean angles for zero loads have been subtracted from all angles. Error bars are not shown because of overlap.

Angles computed using the Xsens data were compared to angles previously computed using upper body accelerations (Morin et al., 2004). Angles computed using Xsens data from the end of each trial were used and relative forward lean angles for all subjects are given in Appendix B (Table B-II and B-III). Average relative lean angles, computed from accelerometer data are given in Table 1-II.

Table 1-II. Average relative lean angles (in degrees) computed from accelerometer data.

Load	Speed (km/h)						No of values: N
	3.22		4.83		6.44		
	Mean	Std dev	Mean	Std dev	Mean	Std dev	
0	0	0	0	0	0	0	
16.6	13.90	5.61	14.19	6.53	10.83	8.56	4
25.9	19.04	7.05	19.84	7.97	17.09	3.31	4
38.7	28.82	7.93	27.52	5.30	22.79	5.57	6
Load	Incline (deg)						No of values: N
	0		5		10		
	Mean	Std dev	Mean	Std dev	Mean	Std dev	
0	0	0	0	0	0	0	
16.6	20.19	7.55	22.76	7.58	23.48	4.37	5*
25.9	29.14	8.27	28.90	8.13	30.15	9.87	4
38.7	30.47	19.15	29.94	20.72	26.50	9.72	6*

* Some data values are missing

Relative forward lean angles computed using both accelerometer and Xsens data are shown in Figure 1-4. There is a pattern of increasing forward body lean with increasing load carried, for both the accelerometer and Xsens data and with both changing speed and incline. A series of statistical tests were performed on the data. Using single factor Anova's, speed and incline were found to have no significant effect on forward lean angle, for angles computed from both the accelerometer and the Xsens data. Thus angle data were grouped by load, for the changing speed and changing incline tests independently and a single factor Anova was computed to determine the effect of load. Load had a significant effect on the forward lean angle computed from the accelerometer data for changing speed tests only. The load effect was not significant in all other cases (forward lean angle computed using accelerometer data for the changing incline tests, forward lean angle computed using Xsens data for the changing speed tests and for the changing incline tests). The angles computed from accelerometer and Xsens data were compared using t-tests. The means were found to be significantly different ($P < 0.001$) for the 25.9 and 38.7 kg loads. It is apparent from Figure 1-4 that the angles reported by the accelerometer are higher than those reported by the Xsens.
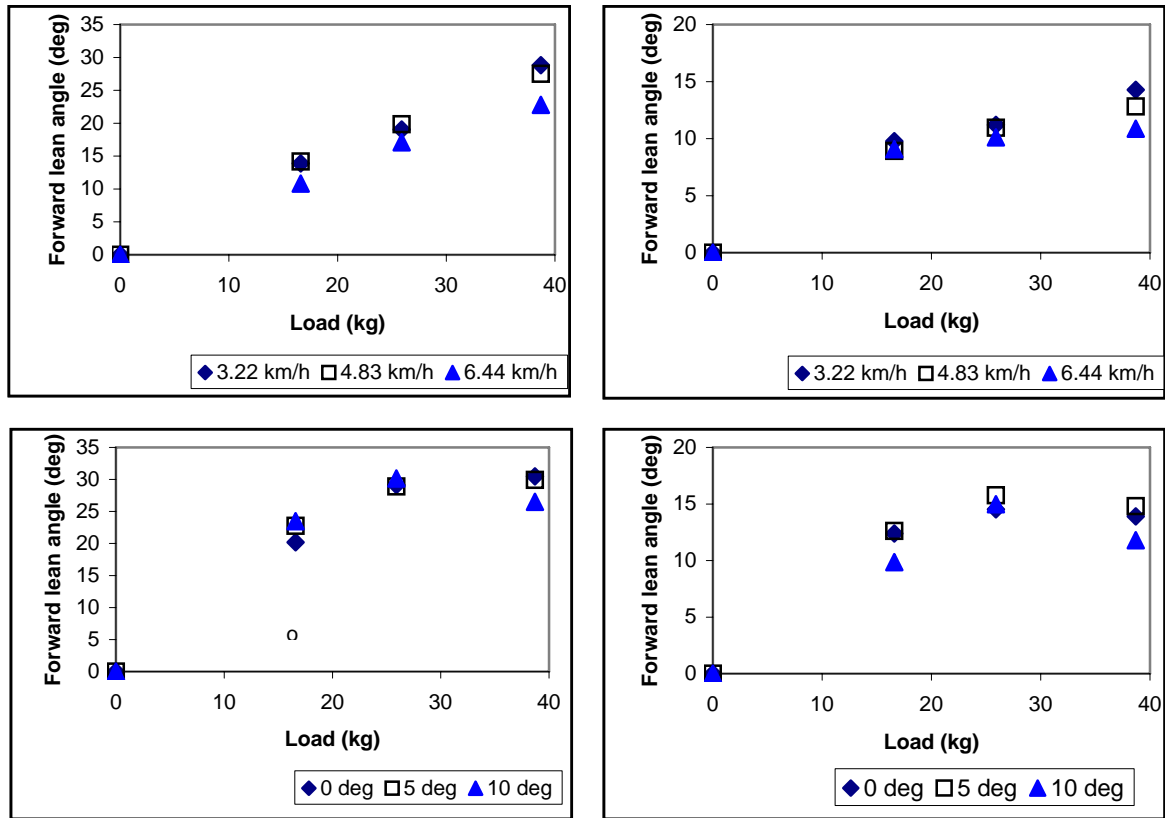
Figure 1-4. Forward lean angles computed using accelerometer data (left) and Xsens data (right) for changing speed (top) and changing incline (bottom) tests. Error bars are not shown because of overlap.

2.1.2 Discussion

There was a tendency for the static forward lean angles computed using accelerometer data to be larger than those computed using Xsens data, however, the angles were only significantly different for the 25.9 kg load. The computed static lean angles were similar to angles computed using digital images in a previous study (Stevenson et al., 2002), where these angles fell between the angles computed using the accelerometer and the Xsens data (see Appendix B). For the dynamic case, forward lean angles computed from accelerometer data were again higher than angles computed using Xsens data and in this case, values were significantly different for the 25.9 and 38.7 kg loads. In both cases, the angle data exhibited high intersubject variability.

Speed and incline were found to have no effect on forward body lean angle. Load carried was found to have a significant effect only in the case of lean angles computed

using accelerometer data for the changing speed tests. This was surprising, since it is known that donning a loaded backpack causes the body's CoG to shift dorsally. In order to position the CoG over the base of support, the load bearer must lean forwards and the forward lean increases as load mass increases. That load was not a significant factor affecting forward body lean may be due to the high variability in the data. For example, in the Xsens angles for the changing speed tests, there were two cases in which the lean angle declined with load. If these anomalous cases are removed, the load effect becomes significant. In the changing incline tests, the average forward lean angle does not increase monotonically with load, but declines from the 25.9 kg to the 38.7 kg loads. This occurs for all incline angles, but is most pronounced for the 10° incline. Comparing the lean angle results for the changing incline tests, with results for the 4.83 km/h speed test (where subjects walked at 4.83 km/h for the changing incline tests), it is apparent that the lean angle for the 25.9 kg load is higher for all incline tests. It is this increase at the 25.9 kg load that primarily counteracts the increasing trend in lean angle with load for the changing incline tests.

Given the variability in the results and the differences in lean angle values obtained from the accelerometer, Xsens and digital image data, it is desirable to further explore the accuracy of the forward body lean angle estimate from upper body accelerations. In the following study, upper body movements were measured using an Optotrak motion analysis system and using an accelerometer mounted on the sternum. This permitted a comparison of forward lean angles estimated from upper body accelerations and measured position data.

2.2   Forward Lean Angles During Gait

An experimental study was done to determine how carrying different loads in a backpack affects gait, and to determine if changes in gait are reflected in upper body accelerations. Upper body acceleration data collected during this study were analysed to determine forward lean angles while subjects were standing or walking carrying no load, or one of three different loads in a backpack (the Canadian CTS pack).

2.2.1 Data Collection

Twelve young, physically fit adult males were recruited to participate in this study. Subjects completed a PAR-Q and You questionnaire and read and signed a Letter of Information and Informed Consent From (included in Appendix A) before participating in the study. Subject age, height and weight were recorded. To protect subjects' identities, all participants were assigned a subject number and were only identified subsequently by this number.

The subjects' gait patterns under the no load and three loaded conditions were tracked using an Optotrak gait analysis system (NDI OPTOTRAK 3020) and force plate and subjects' upper body movements were tracked using the Optotrak system and a triaxial accelerometer (Crossbow® model CXL10LP3). Subjects were outfitted with 11 Optotrak infrared markers. Four markers were affixed to the skin on the lateral surface of the right leg: two thigh markers were attached over the greater trochanter and the lateral femoral epicondyle; two shank markers were attached over the head of fibula and the lateral ankle malleolus. Two rigid extensions, with infra-red markers affixed to the ends, were attached to the skin on the ventral surfaces of the thigh and shank segments. These were located half way between the other two segment markers, and extended outward in the sagittal plane. Two additional markers were placed on the lateral side of the right shoe to track movement of the foot. The remaining three markers were used to track the movement of the upper body. These markers and a triaxial accelerometer were affixed to a plexiglass plate, which was attached over the sternum and extended outwards in the sagittal plane. This allowed for the upper body movement to be tracked by the accelerometer and to be validated by the Optotrak system. All markers were attached to the skin using medical grade tape.

Four load carriage (LC) conditions were tested: no load, or a CTS pack loaded to a total mass of 16.6, 25.9 or 38.7 kg. The LC conditions were tested in randomized order. A side view digital photograph of each subject was taken for each load condition prior to testing (a set of photographs for one subject is shown in Appendix B). Subjects then completed the tests outlined in Table 1-III. The LC condition was randomized, but subjects completed the tests in the order given in Table 1-III. The fixed paced walk was at a cadence of 2 steps per second (regulated by a metronome) corresponding to a velocity of

approximately 1.34 m/s. During each test kinematic and kinetic gait data were recorded using the Optotrak system and force plate and upper body accelerations were recorded from the chest-mounted accelerometer. A total of 81 data sets, including standing data, were collected for each subject. Subjects wore each load for approximately fifteen minutes, and the time to complete the experimental session was approximately two hours.

Table 1-III. Tests completed by each subject in the gait analysis study

Test	Load carried (kg)	Data Collection Duration per Load	Number of Repetitions per Load
Comfortable standing	0, 16.6. 25.9, 38.7	10 s	1
Self-paced walk across the room – one step on force plate (right foot)	0, 16.6. 25.9, 38.7	15 s	10
Fixed paced walk across the room – one step on force plate (right foot)	0, 16.6. 25.9, 38.7	15 s	10

The forward lean angles were computed, for each test, from the recorded acceleration data as described previously [1].[5]

2.2.2 Results

The average and average relative forward lean angles of subjects, calculated using upper body accelerations, are shown in Figure 1-5 and Figure 1-6 respectively. A forward lean angle is represented by a positive angle and a backward lean angle is represented by a negative angle. There is an increase in forward lean angle as load increases for both the average lean angles and the average relative lean angles. Single factor ANOVA analysis was done on the computed lean angles and load was found to be a significant factor affecting the stationary lean angle ($p<0.001$) and lean angles during self-paced and fixed-

---

[5] In the gait study, the accelerometer data were not collected using the Embla recorder and it was not necessary to attenuate the accelerometer voltage before sampling. Thus, the accelerometer voltages were converted to g's of acceleration using the following equation: accel = (data_value – zero_g_voltage)/sensitivity. The zero g voltage and sensitivity for the accelerometer used are given in Appendix B.

paced walking (p<0.001 for both). The Pearson correlation coefficients between load and lean angle were: 0.59, 0.60 and 0.61 for the stationary, self-paced and fixed-paced angles respectively, indicating that 35-38% of the variance in the angle values is explained by load.

It can be noted from Figure 1-5 that the forward body lean is greater when the subjects are walking than when they are stationary. This is also true for the lean angles from the treadmill study, as shown in Appendix B. In walking, it is necessary for an individual to move his/her CoG outside (anterior to) the base of support. One way to do this is to lean forward with respect to vertical, and this is reflected in the greater forward lean detected during walking. This effect is not present for the relative lean angle, indicating that the forward body lean due to walking and the lean induced by wearing a backpack are independent effects.
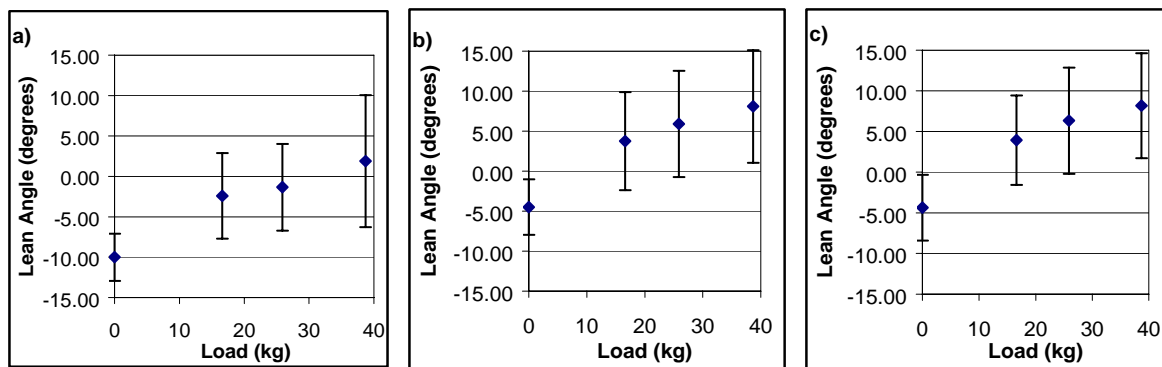
Figure 1-5. Average lean angle versus load for 12 subjects for a) stationary, b) self paced walking and c) fixed paced walking. Error bars are ±1 standard deviation.
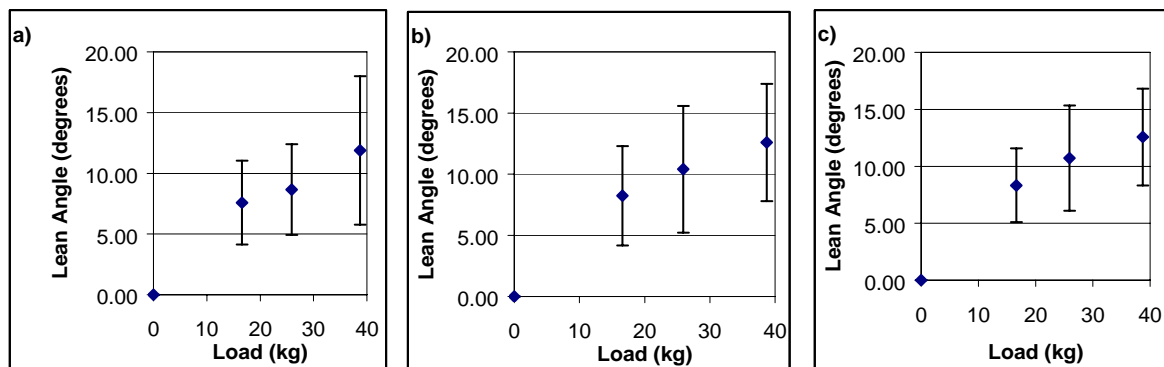
Figure 1-6. Average relative forward lean angle versus load for 12 subjects for a) stationary, b) self paced walking and c) fixed paced walking. Relative lean angles were obtained by subtracting the forward lean angle at 0 load. Error bars are ±1 standard deviation.

Comparing Figure 1-6 to Figure 1-4, it is apparent that the forward lean angles computed from upper body accelerations in the gait analysis study are smaller than those computed from upper body accelerations in the treadmill study, and comparable to the angles reported by the Xsens in the treadmill study. Angle values from the treadmill study, for walking at 3.22 km/h, 0° incline, computed from both the accelerometer and Xsens, and angles from the gait study for self-paced walking were grouped and analysed for significant differences. There were no significant differences for the 16.6 kg load. For the 25.9 and 38.7 kg loads, however, the angles computed using the accelerometer for the treadmill versus the gait study were significantly different ($p<0.05$ for 25.9 kg; $p<0.001$ for 38.7 kg). There was no significant difference between the Xsens angles from the treadmill study and the angles from the gait study for these loads.

Stationary forward lean angles computed using upper body accelerations were compared to lean angles computed using position information from the Optotrak. Three markers were affixed to an extension on the Plexiglas plate that was attached overtop of the subject's sternum, such that the markers were in the sagittal plane. Position data from one marker gives the orientation of the subject's upper body in two dimensions and this can be compared to the vertical reference for the Optotrak to determine the forward lean of the body. This was done using two seconds of position data as the subjects stood with no load or the three backpack loads. Because the Plexiglas plate extends outwards from the body, the absolute angles are artificially large, but the relative lean angles can be computed by subtracting the angle at zero load. A plot of the relative stationary forward lean angles determined from the position marker and from the upper body accelerations is shown in Figure 1-7. The angles computed using the position data are significantly higher ($p<0.01$ in all cases) than the angles computed using the accelerometer data.
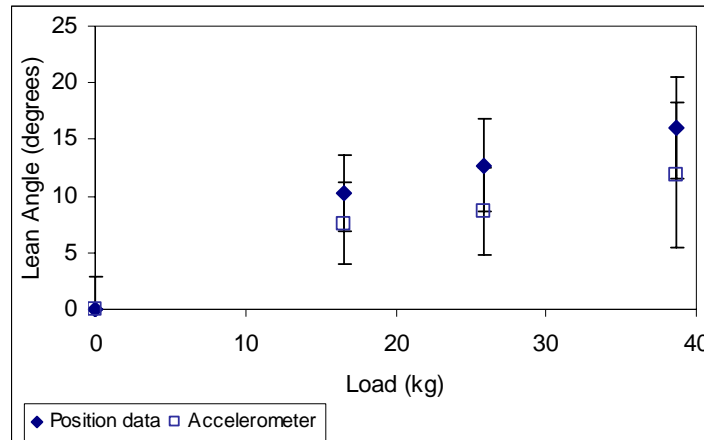
Figure 1-7. Relative stationary forward lean angles, with respect to vertical, computed from Optotrak marker (position) data and from upper body accelerations.

2.2.3 Discussion

There is a discrepancy between lean angles computed from upper body accelerations for the two studies presented here. However, the forward lean angles obtained in the gait analysis study were in agreement with the angles reported by the Xsens inertial sensor in the treadmill study. Examining the static relative lean angles (given in Tables B-I and B-VI in Appendix B), it can be seen that the angles computed from upper body accelerations in the treadmill study are highly variable – with the outliers removed, the range of relative lean angle for each load is: 5.29-24.47° (16.6 kg); 8.83-23.32° (25.9 kg) and 5.56-40.48° (38.7 kg). There is less variability in the static relative lean angles for the gait analysis study where the ranges are: 0.02-13.11° (16.6 kg); 3.02-14.4° (25.9 kg) and 3.29-22.53° (38.7 kg). As well, considering Tables B-II and B-VI, the standard deviations for the lean angles averaged across subjects for the gait analysis study are about half the standard deviations for the treadmill study. This indicates that there is some confounding factor (or factors) contributing to the variability in the forward lean angles computed in the treadmill study. One possible source may be the movement of the treadmill which may induce vibrations in the subject which are detected by the accelerometer and appear as an offset in the acceleration record. This would introduce a bias in the angle estimate. Since the Xsens includes a gyroscope and magnetic sensor, as well as an accelerometer, it may be

less prone to this error, and thus the reported lean angles are smaller than for the Crossbow accelerometer.

Given that the lean angle estimates obtained for the gait analysis study are more consistent than those obtained from the treadmill study, and are in agreement with the angles reported by the Xsens, it appears that these values are more accurate. In the walking tests (both self-paced and fixed paced), which included 10 trials, the forward lean angles were found to be highly repeatable within subjects (see Appendix B, Table B-V). However, the relative static forward lean angles obtained from the accelerometer were significantly different from lean angles computed from Optotrak marker data, where the angles from the position data were higher. Calibration of the accelerometer against a standard measurement of body lean (e.g. from digital images, as done by Stevenson et al., 2002) would improve the accuracy of the forward lean angle estimate.

The use of upper body accelerations in determining forward lean during load carriage is advantageous, because forward lean can be tracked both during static (standing) and dynamic (walking or running) activities and the subject can be moving freely in his/her environment. The results presented here indicate that a reasonable estimate of forward body lean can be obtained from upper body accelerations, with calibration of the accelerometers in the gravitational field, and with some knowledge of the terrain factors, e.g. treadmill walking versus walking on a hard, flat surface, such as a floor.

3   Changes in Gait Parameters during Load Carriage

The upper body accelerations obtained in the study described above (sec. 1.2.2) were analysed and compared to the kinematic (Optotrak) and kinetic (force plate) data recorded using the gait analysis system. The goal was to determine if the acceleration patterns were related to specific gait events and to assess the alterations in the gait pattern during load carriage.

3.1   Determination of Gait Events

Upper body accelerations can provide useful information for gait analysis. Comparing synchronized vertical force plate and upper body accelerometer data, it was found that both left and right heel strike and toe-off exhibit distinct acceleration patterns.

The force plate captures ground reaction force (GRF) information for a single right footfall. Right heel strike occurs when the vertical GRF exceeds five percent of the maximum; toe-off is defined as the point when the vertical GRF falls to below five percent maximum, following heel strike. The upper body accelerations recorded at the sternum in the vertical, mediolateral and anteroposterior planes are plotted against the vertical GRF in Figure 1-8. Comparing the accelerations and vertical GRF, it can be seen that heel strike is characterized by a small plateau preceding a local maximum in the vertical acceleration and a subsequent deceleration in the anteroposterior acceleration. The characteristics of toe-off include a local minimum in the anteroposterior acceleration pattern and a small decrease following maximal vertical acceleration. Mediolateral acceleration patterns can be used to distinguish between left and right side events, where a decrease in the mediolateral acceleration between successive heel strike and toe-off indicates a right heel strike followed by a left toe-off. Similarly, an increase between consecutive heel strike and toe-off indicates a left heel strike and a right toe-off. These events are shown in Figure 1-8.
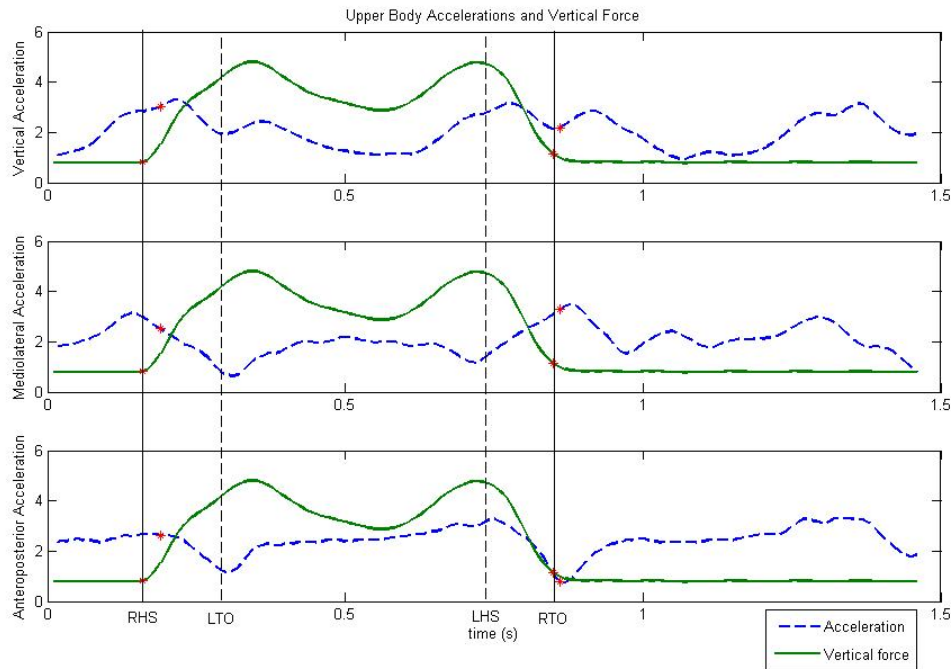
Figure 1-8. Accelerometer and vertical force plots where right heel strike (RHS) and right toe-off (RTO) have been identified from the force plate data. Left heel strike (LHS) and left toe-off (LTO) have been identified from upper body acceleration data. Positive vertical acceleration is upwards, positive mediolateral acceleration is to the right and positive anteroposterior acceleration is backwards.

22

A Matlab® program was written to detect the timing of heel strike and toe-off from the accelerometer records. The event times were compared to times determined from force plate data to assess the accuracy of this method. Table 1-IV presents the average time differences between right heel strike and right toe-off timing, determined from the force plate and from the accelerometer, and the Pearson's Correlation Coefficient between the data obtained from the two methods. On average, there is less than half a data point difference (data were sampled at 100Hz, therefore the sampling period is 0.01 seconds) between methods for all gait events, which shows a high level of consistency. The precision of the force plate estimate is limited to 0.01 seconds. There is strong correlation between methods for both heel strike and toe-off detection. The larger error and lower correlation coefficient observed for the subsequent right heel strike and stride duration is because the time of the second right heel strike must be estimated based on hand switch information, where an observer depressed a hand switch whenever a right heel strike occurred. This method assumes the human error associated with the hand switch is consistent from one heel strike to the next, but this is not always the case. Stride duration has a similar margin of error as the second right heel strike but a lower correlation coefficient.

Table 1-IV. Average error in terms of data points and msec, between event timing from force plate and from accelerometer data, and the correlation coefficient between values obtained using the two methods.

	Mean ± St. Deviation		Correlation Coefficient
	Data Points	msec	
Right Heel Strike	0.02 ± 2.81	0.16 ± 28.1	0.99
Right Toe-off	0.19 ± 2.49	1.85 ± 24.9	0.99
Next Right Heel Strike	0.37 ± 9.31	3.71 ± 93.1	0.93
Stride duration	0.36 ± 9.12	3.55 ± 91.2	0.67

3.1.1 Effects of Load Carried on Gait Parameters

Load carriage causes a number of alterations in gait parameters. For both the fixed and self-paced walking trials, an increase in load carried in the backpack caused a decrease in stride length and velocity, while cadence remained constant. The percentage of gait cycle spent in double leg support and the maximum knee angle during the absorption phase of the

gait cycle also increased with load. The trials regulated by a metronome had a lower stride frequency as well as a decreased velocity. Table 1-V provides a summary of these results.

Table 1-V.   Effects of carrying a load on gait characteristics

	Load (kg)		Stride length (m)	Cadence (#steps/s)	Velocity (m/s)	% double support	Max Knee Angle
Self-paced	0	Avg	1.44	0.83	1.20	23.98	18.72
		Std dev	*0.11*	*0.08*	*0.13*	*2.81*	*6.22*
	15.6	Avg	1.41	0.83	1.17	26.41	20.61
		Std dev	*0.13*	*0.09*	*0.10*	*2.87*	*5.60*
	25.9	Avg	1.40	0.82	1.14	27.49	21.43
		Std dev	*0.11*	*0.08*	*0.09*	*2.46*	*5.43*
	35.4	Avg	1.39	0.83	1.14	28.39	24.36
		Std dev	*0.13*	*0.09*	*0.09*	*3.26*	*5.15*
Fixed paced	0	Avg	1.46	0.78	1.14	23.07	18.37
		Std dev	*0.11*	*0.07*	*0.12*	*3.62*	*6.12*
	15.6	Avg	1.40	0.80	1.12	25.32	21.05
		Std dev	*0.13*	*0.07*	*0.09*	*3.17*	*5.63*
	25.9	Avg	1.43	0.78	1.11	26.98	21.89
		Std dev	*0.10*	*0.07*	*0.09*	*3.11*	*6.28*
	35.4	Avg	1.37	0.80	1.09	28.13	23.62
		Std dev	*0.13*	*0.07*	*0.10*	*3.20*	*5.20*

An ANOVA using a repeated measures general linear model was performed on the data using SPSS version 12.0. Velocity, stride length and knee angle displayed a linear relationship with load, and percent of double leg support had both a linear and quadratic relationship with load carried at the 0.05 significance level. Linear regression was then performed to determine the percentage of parameter variance attributed to the load carried. This is an attempt to express a linear relationship between load and different gait characteristics and does not take into account other between subject factors such as height and weight variations or differences in fitness levels. The percentage of double support gave highest correlation with load carried ($R=0.5$), indicating that 25 percent ($R^2=0.25$) of variation in double leg support is explained by load carried. The other parameters have lower correlations with load, with values ranging from 0.3 to 0.05. The linear regression equations and correlation coefficients are presented in Table 1-VI.

Table 1-VI. Correlation Coefficients and Linear Regression Equations for Gait Parameters expressed as a function of load carried.

	Variable	R	Regression Equation
Self-paced	Velocity (m/s)	0.200	y = -0.002x + 1.196
	Cadence (cycles/s)	0.050	y = -0.000x + 0.837
	Stride Length (m)	0.135	y = -0.001x + 1.433
	% Double Support	0.496	y = 0.124x + 24.182
	Knee Angle (degrees)	0.328	y = 0.149x + 18.430
Regulated Pace	Velocity (m/s)	0.156	y = -0.001x + 1.140
	Cadence (cycles/s)	0.058	y = 0.000x + 0.784
	Stride Length (m)	0.222	y = -0.002x + 1.457
	% Double Support	0.503	y = 0.145x + 23.099
	Knee Angle (degrees)	0.308	y = 0.143x + 18.491

3.1.2   Discussion

It has been established that features in the upper body acceleration record represent events in the gait cycle – in particular, heel strike and toe-off. Using upper body accelerations recorded at the mid-line (over the sternum), it is possible to identify both right and left heel strike and toe-off, where the mediolateral accelerations can be used to determine the side on which the events occur. This finding is important as it will allow us to monitor gait in the field using the portable measurement system and it will permit assessment of gait over long durations, for different terrain conditions and under different load carriage requirements.

Changes in particular gait parameters were found as load carried in a backpack increased. The most significant changes were an increase in per-cent double support and in the maximum knee bend. There was also a slight decrease in stride length and decrease in velocity for self-paced walking; where the walking pace was regulated, the stride length did decrease slightly but velocity was maintained. These results agree with previous findings that alterations to stabilize gait occur as heavier loads are carried and that there is more strain on the lower limbs, hence more need for shock absorption in the knees. It should be noted that, in this study, subjects carried each load for a relatively short time period (approximately a few minutes). There may be more substantial changes in the gait pattern over time as load is carried for long durations and for long distances – these changes can be assessed using upper body accelerations.

4 Energy Cost Prediction during Load Carriage

In the previous contract (Morin et al., 2004), mathematical models were developed to predict energy cost ($\dot{V}O_2$) during backpack load carriage, given known parameters – load carried, speed of walking and incline – and/or measured values – upper body accelerations. These models were based on two minute segments of data extracted during steady state O_2 consumption during a treadmill test, where the test conditions (changing load, speed and incline) are summarized in Appendix C. In this work, the data from the treadmill study have been re-examined to determine if more accurate models for energy cost prediction can be developed. To this end, heart rate has been included as an independent parameter in the modeling process.

4.1.1 Data Analysis

In the study done previously, subjects walked on a treadmill while carrying a loaded backpack for eight 18-minute tests. During each test, either speed or positive incline was increased at 6-minute intervals (see Table C-I). With each adjustment, the subject's VO_2 generally displayed a transient rise which leveled off within two minutes. O_2 consumption was measured at 20 s intervals using a TEEM 100 metabolic cart. These values were processed as described previously (Morin et al., 2004) to obtain normalized in VO_2 ml/min/kg body weight. Heart rate (HR) was detected using a Polar heart rate monitor and recorded at 1-minute intervals. Upper body accelerations (mediolateral, vertical and VO_2 anteroposterior) were detected using a Crossbow triaxial accelerometer and sampled at 100 Hz. The root mean-square (rms) values of the accelerations were computed over 1 minute intervals and the rms magnitude per minute was computed as:

$$rms_{mag} = \sqrt{rms_x^2 + rms_y^2 + rms_z^2} \ .$$

Data collected in the treadmill study were examined to assess the inter-relationship between the test parameters, the measured variables and measured O_2 consumption. Because of variability in measured VO_2, it should be averaged over a relatively long interval, thus it was decided to average all parameters over the final 4 minutes of each test condition. Good data were not recorded from all subjects from all tests, and the number of steady state data values for the changing speed tests (for all loads) was $n_{sp} = 81$, and for the changing incline tests was $n_{in} = 82$. Correlation analysis was performed on the changing

speed and changing incline test data independently and the results are given in Table 1-VII. VO_2 and HR are highly correlated and both are correlated with speed and incline and moderately correlated with load. In terms of the acceleration parameters, VO_2 is highly correlated with anteroposterior accelerations in the changing speed tests, but less well correlated with acceleration parameters in the changing incline tests. Speed is correlated with all acceleration parameters, in particular vertical accelerations, but incline is only moderately correlated with the vertical and anteroposterior accelerations. Measured parameters (HR and acceleration rms values) have been plotted against VO_2 in Figure C-1 (Appendix C). Averaged data for the changing speed and changing incline tests were grouped for analysis using SPSS v. 12.0. Single factor ANOVA's were run on the data with load, speed and incline as factors and HR, VO_2, AccelX, AccelY, AccelZ and Accel_mag as variables. All variables varied significantly with load ($p<0.05$), except AccelY and Accel_mag. All variables varied significantly with speed ($p<0.001$) and all variables varied significantly with incline ($p<0.01$) except AccelX. These results indicate that there is a relationship between metabolic energy cost during load carriage and the measured variables and it should be possible to predict energy cost given upper body accelerations and/or HR.

Table 1-VII. Correlation coefficients (R values) for energy cost (VO2), test parameters (load, speed and incline) and measured quantities (upper body accelerations and heart rate) averaged over the final four minutes of each test condition. AccelX, AccelY and AccelZ are the average rms accelerations in the mediolateral, vertical and anteroposterior directions respectively. Accel_mag is the magnitude of the average rms accelerations in the three directions.

Correlation analysis for all subjects - changing speed tests								
	Load	**Speed**	**HR**	**VO2**	**AccelX**	**AccelY**	**AccelZ**	**Accel_mag**
Load	1							
Speed	0.0000	1						
HR	0.4367	0.7019	1					
VO2	0.4701	0.7571	0.8661	1				
AccelX	-0.2778	0.6061	0.2723	0.4631	1			
AccelY	-0.1180	0.9278	0.6174	0.6586	0.6194	1		
AccelZ	0.1710	0.7843	0.7006	0.8533	0.5782	0.6759	1	
Rms_mag	-0.0796	0.9377	0.6488	0.7598	0.7509	0.9528	0.8419	1
Correlation analysis for all subjects - changing incline tests								
	Load	**Incline**	**HR**	**VO2**	**AccelX**	**AccelY**	**AccelZ**	**rms_mag**
Load	1							
Incline	0.0000	1						
HR	0.4278	0.7451	1					
VO2	0.4860	0.7711	0.8918	1				
AccelX	-0.2996	0.2022	0.2292	0.1347	1			
AccelY	0.0283	0.6113	0.4006	0.6348	0.2656	1		
AccelZ	0.2306	0.4765	0.5383	0.5836	0.0977	0.4854	1	
rms_mag	0.0831	0.6492	0.5360	0.7009	0.3605	0.9258	0.7555	1

4.1.2 Energy Cost Models

Models for energy cost prediction were derived using regression analysis on the grouped data for changing speed and changing incline tests in SPSS v. 12.0. A number of models were generated for different combinations of the independent variables. Stepwise regression analysis was done, such that the variables with the highest correlations were preferentially included in the model and variables which did not improve the correlation were removed. A summary of the models is given in Table 1-VIII.

Table 1-VIII. Models to predict energy cost from test parameters and measured variables.

Model #	Equation	R^2	Independent variables
1	VO2 = -13.791+0.286(HR)	0.76	HR only
2	VO2 = -5.79+1.148(I)+3.202(S)+0.204(L)	0.823	Load, Speed, Incline
3	VO2 = 7.579(AccelZ)+4.345	0.482	AccelZ
4	VO2 = 2.627+5.9(AccelZ)+2.801(AccelY)-2.65(AccelX)	0.554	AccelX, AccelY, AccelZ, Accel_mag
5	VO2 = -13.652+0.212(HR)+0.186(AccelZ)+1.16(AccelY)	0.811	AccelX, AccelY, AccelZ, Accel_mag, HR
6	VO2 = -2.35+3.871(AccelZ)+0.185(L)+3.233(AccelY)	0.683	AccelX, AccelY, AccelZ, Accel_mag, Load

The R^2 values for Model 2 indicate that, if load, speed and incline are known, 82% of the variance in the energy cost is explained by these variables[6]. However, since these parameters are not known under field conditions, other models involving the measured parameters should be considered. Since HR was well correlated with VO_2, a model involving HR only as a VO_2 independent variable was generated and this model explains 76% of the variance in the data. An initial model involving the acceleration parameters indicated that the anteroposterior accelerations (AccelZ) explained the highest percentage of variance in the VO_2 measurements, thus Model 3 involving AccelZ only was generated (Model 3). This model explains 48% of the variance in VO_2 [7]. If AccelX and AccelY are included (Model 4), the proportion of variance explained increases to 55% and if load is included as well, the proportion of variance explained is 68% (Model 6). If HR is included with the acceleration parameters in the energy cost model, the model explains 81% of the variance in VO_2 (Model 5), which is very close to the proportion of variance explained by Model 2.

The goodness of the fit of the above models to the VO_2 data was examined using graphical analysis, since high R^2 values do not necessarily guarantee that a model fits the data well (NIST/SEMATECH, 2005; Bland and Altman, 1986). This graphical analysis is presented in Appendix C and from the analysis, it can be seen that Model 1, based on HR, gives a good estimate of VO_2 but has a constant error (or bias error) of approximately 2

---

[6] In the previous report, the following model was derived: $VO_2 = 2.559 + 0.107(I^2) + 0.335(S^2)+0.182(L)$ and $R^2 = 0.833$. Given that the R^2 value is not substantially different from the linear model reported here, it was felt that the linear model is sufficient.

[7] Energy cost models generated AccelX and AccelY only as independent variables explained 7% and 37.8% of the variance in VO_2 respectively.

ml/min/kg. VO_2 is well predicted from load, speed and incline, but these parameters are known only in a well controlled laboratory environment. VO_2 can be predicted from upper body accelerations, but it is under-predicted at high VO_2 levels. Including HR or load with the acceleration parameters as the independent variables in the model improves the agreement between measured and predicted VO_2, but values are still under-predicted at high VO_2 levels. This lack of agreement disappears however, if predicted vs measured VO_2 is plotted only for the changing speed tests. Thus, increasing incline results in increased energy cost, but this is not reflected in the upper body accelerations.

4.1.3 Discussion

The results presented here demonstrate that VO_2 can be reliably predicted for walking with a loaded backpack under conditions of different loads carried, changing speed of walking and changing incline if load, speed and incline are known. These parameters can be controlled in a laboratory setting but cannot be accurately known during field trials, e.g. military training exercises[8] where it is desirable to track energy cost over time, and VO_2 must be estimated using measured variables. Heart rate is well correlated with VO_2, but was found to overestimate VO_2 by approximately 2 ml/kg/min, across the range of measured VO_2. Upper body accelerations, in the anteroposterior and vertical directions, are also correlated with VO_2 and models to predict VO_2 from the rms values of the accelerations were developed. It was found that these models underestimate energy cost at increasing values of measured VO_2 when both the changing speed and changing incline tests are included in the prediction. If the changing incline tests are excluded from the predictions, however, the agreement between the measured VO_2 and predicted VO_2 is very good. This suggests that the effort required to walk uphill is not reflected in the rms values of the upper body accelerations. Changing incline or changes in terrain may be affect body accelerations in other ways, however. For example, gait patterns may be altered when walking uphill or downhill and it may be possible to detect these alterations, given the relationship between upper body accelerations and gait parameters presented in Section 3.1. If a relationship between the effects of terrain on walking and measured upper body

---

[8] The load carried (including backpack, load carriage vest, rifle, protective gear and clothing) at the outset of a training exercise can be determined. However, the total load may vary over the course of the exercise, particularly if the exercise will last more than a few hours.

accelerations can be established, terrain characteristics could be predicted from measured accelerations and correction factors for VO_2 estimation can be identified, similar to the terrain factor included in Pandolf's energy cost model (Pandolf et al., 1977). Until these correction factors have been established, it is possible to obtain reasonable estimates of metabolic energy cost from variables which can be measured using the portable measurement system.

5 Conclusions & Recommendations

5.1 Postural and gait adjustments during load carriage

The results presented here confirm published findings that, when bearing loads in backpacks, individuals alter their posture and gait to maintain stability and minimize propulsive forces on the body. These alterations include leaning forward to bring the CoG over the base of support, decreasing stride length, increasing double support time and increasing knee bend during load carriage. It has been demonstrated that the magnitude of these changes can be estimated in both the static case (standing while supporting a load) and the dynamic case (walking while carrying a load) using recorded upper body accelerations.

How metabolic energy cost during walking is affected by load carried, increasing speed of walking and increasing incline has also been documented in this report. Several models to predict the energy cost of load carriage from known parameters and from measured variables were generated. The model involving load, speed and incline as independent variables had the highest correlation coefficient but graphical analysis reveals that the model under-predicts energy cost both at low values and at high values of measured VO_2 (see Fig. C-6)[9]. Heart rate and VO_2 are well correlated but there is an offset or bias error in the VO_2 estimate of approximately 2 ml/kg/min. Models involving upper body accelerations predict VO_2 reasonably well, however, these models under-predict VO_2 at high energy cost levels. This under-prediction disappears if VO_2 is predicted for the changing speed tests only, indicating that the energy cost of walking uphill is not reflected

in upper body accelerations. Nevertheless, metabolic energy cost during walking while carrying a load can be reasonably well predicted using Model 4:

$$\dot{V}O_2 = 2.627 + 5.9(\mathrm{AccelZ}) + 2.8(\mathrm{AccelY}) - 2.65(\mathrm{AccelX})$$

The estimate can be supplemented by considering HR, however, other factors such as anxiety or arousal can cause increased HR, which would decrease the accuracy of an energy cost estimated involving HR.

To improve the capability of the portable measurement system to accurately detect changes in gait, posture and metabolic energy cost during load carriage, it is recommended that the following be done:

- calibration of the Crossbow accelerometers for forward body lean estimates. A simple static calibration rig, in which the accelerometer can be positioned at known angles, would permit easy calibration of the accelerometer prior to use in human testing.
- assess the accuracy of using the mean accelerations to estimate the proportion of the gravitational vector on each accelerometer axis in the dynamic case, in the presence of other factors, e.g. vibrations, which may alter the mean values
- further investigate gait alterations during load carriage and how these are reflected in upper body accelerations. The should include a study of the effects on gait, of load carriage over long durations and the effects of varying terrain, e.g. hard, flat surfaces such as paved roads, rocky terrain and sandy or snowy terrain.
- determine whether terrain characteristics are reflected in parameters of upper body accelerations, other than the rms values. If terrain characteristics can be estimated during walking, determine a correction factor for the metabolic energy cost equation.

---

[9] For three subjects, the 16.6 kg load was less than 20% BW (17.1, 18.2 and 18.6%). For these subjects, the energy cost while carrying the pack may not have been higher (or only slightly higher) than the energy cost of walking with no load (Charteris et al., 1989; Holewijn, 1990) resulting in a lower than expected energy cost.

SECTION 2: DYNAMIC BIOMECHANICAL MODEL

1 Introduction

The purpose of this work was to create a standalone interactive program based on the existing Dynamic Biomechanical model (DBM) for estimating biomechanical loading during load carriage. This interactive program can be used either to control for biomechanical load factors during various types of physiological stress testing or as an educational tool to demonstrate the biomechanical effect of varying load carriage parameters. In addition, a general model of the CTS rucksack was created in the Visual Nastran4D (VN4D) platform. This general model can be used to explore the effect of varying a wide variety of model parameters including the pack geometry, shoulder strap attachment points, material properties, and body motions.

2 Description of RUCKMAN™ Model

The RUCKMAN Model was developed using the Dynamic Biomechanical Model (DBM report, 2004). It is an interactive program that enables a researcher to estimate biomechanical loading due to a range of rucksack configurations and load carriage factors. Users are provided with a complete analysis of predetermined combinations of: load carried, load position, waist belt tightness, shoulder strap tension and walking speeds.

RUCKMAN can be used to quantify biomechanical factors and would allow a researcher to control for these variables during physiological measurements in load carriage situations. In this manner, an investigator can control for these factors during human trials.

The software can be also be used to demonstrate a number of capabilities of the DBM model and can educate users in the effects on soldiers of varying load carriage parameters.

Visual Nastran is a special purpose engineering analysis program and the DBM subsequently requires a significant level of user skill. RUCKMAN was undertaken to create a tool that is easy to use and provides ready access to quantifying and understanding the biomechanical effects of typical load carriage conditions. RUCKMAN was developed by

first performing a series of 152 analyses with the DBM in Visual Nastran 4D, creating a load carriage results database. This database is accessed through a user interface in LabView® that requires no special training for the user. RUCKMAN was then compiled so that it is fully transportable and non-corruptible. It may be installed on any personal computer running a current Windows® operating system, (Windows 98, Window NT, and Windows XP).

2.1   Characteristics of RUCKMAN™

Load mass and COG

RUCKMAN™ was developed to provide analyses that span the more common load carriage conditions occurring in a military setting and are set at 15, 25 and 35 kg, (33, 55 and 77 lbs). Although in certain instances, military requirements have necessitated greater loads, these represent the majority of operational demands for the Canadian Forces Rucksack.

Figure 2-1 shows the physical geometry of RUCKMAN's pack person model. It includes an articulating waist belt, fitted shoulder straps, upper back pad, lumbar pad and a tripartite pack volume to permit specification of the centre of gravity (COG) location.
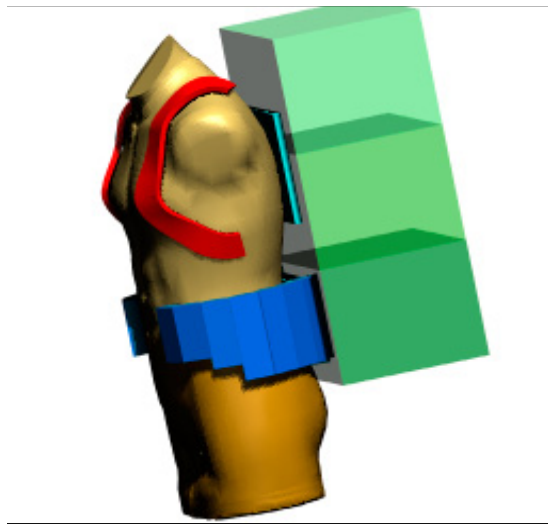
Figure 2-1.   RUCKMAN Model Physical Components
The physical objects and geometries were developed from the Dynamic Biomechanical model (DBM) reported on in Reid et al, 2003, Reid et al 200).

The COG of a load has a direct influence on the force distribution to the torso and can be selected in RUCKMAN as either high, mid height or low in the rucksack. Figure 2-2 illustrates the mass distribution for the three COG configurations. These choices exist for each of the possible mass selections, giving rise to 9 different combinations of load and COG location.
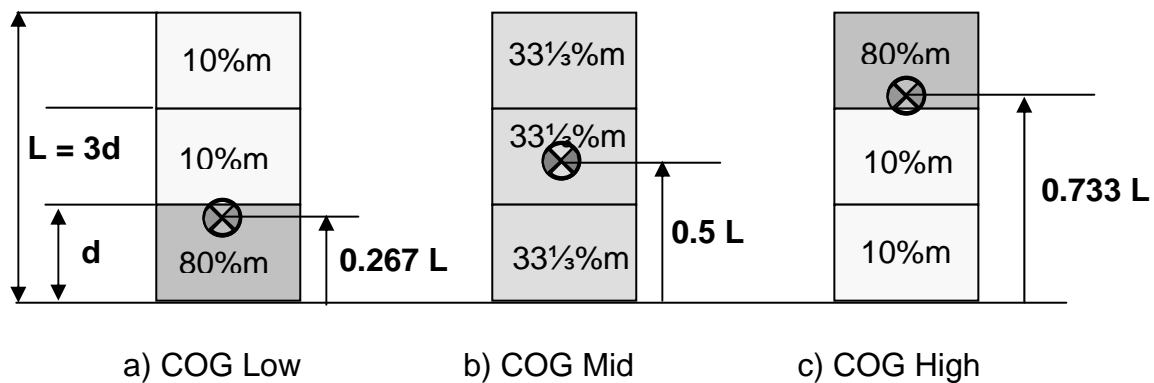
Figure 2-2.   Rucksack Load Distributions
2a) 80% of the mass located in the lower 1/3 of the ruck volume, 20% of the mass distributed within the upper 2/3 of the ruck.
2b) mass equally distributed within the ruck volume.
2c) 80% of the mass located in the upper 1/3 of the ruck volume, 20% of the mass distributed evenly in the lower 2/3 of the ruck.

Forward lean angle

Rucksack users typical lean their upper torso forward to counter balance any moment created by the weight of rucksack. Correspondingly, the upper torso of the model is weighted anthropometrically and by varying the amount of torso lean, a moment about the hip can be balanced. Each COG position and mass requires a different forward lean angle to reduce the hip moment to zero.   In order to determine the appropriate torso lean angles, a torque motor was created at the location of the hip. Each load configuration was then tested to determine the angle of lean that would reduce the motor torque required to maintain that posture to less than 1 N.m. This angle was then recorded as the required lean angle for subsequent analyses of that load configuration.

Table 2-I summarizes the calculated torso lean angles for each load, COG location and marching pace.

Table 2-I. Summary of Available RUCKMAN Analyses

Shoulder Strap Tension 100 N Waist Belt Tension 60 N

Mass	COG Position	FWD Lean Angle	Walking Speed Step Cadence 1.8 Hz = 4.0 kph Step Cadence 1.9 Hz = 5.0 kph Step Cadence 2.1 Hz = 6.0 kph		
15 kg	Low	10.7	1.8 Hz	1.9 Hz	2.1 Hz
	Med	9.6	1.8 Hz	1.9 Hz	2.1 Hz
	High	9.5	1.8 Hz	1.9 Hz	2.1 Hz
25 kg	Low	15.3	1.8 Hz	1.9 Hz	2.1 Hz
	Med	13.5	1.8 Hz	1.9 Hz	2.1 Hz
	High	12.2	1.8 Hz	1.9 Hz	2.1 Hz
35 kg	Low	19	1.8 Hz	1.9 Hz	2.1 Hz
	Med	16.5	1.8 Hz	1.9 Hz	2.1 Hz
	High	14.5	1.8 Hz	1.9 Hz	2.1 Hz

Shoulder Strap Tension 100 N **Waist Belt Tension 0 N (Loose)**

Mass	COG Position	FWD Lean Angle	Walking Speed Step Cadence 1.8 Hz = 4.0 kph Step Cadence 1.9 Hz = 5.0 kph Step Cadence 2.1 Hz = 6.0 kph		
15 kg	Low	10.7	1.8 Hz	1.9 Hz	2.1 Hz
	Med	9.6	1.8 Hz	1.9 Hz	2.1 Hz
	High	9.5	1.8 Hz	1.9 Hz	2.1 Hz
25 kg	Low	15.3	1.8 Hz	1.9 Hz	2.1 Hz
	Med	13.5	1.8 Hz	1.9 Hz	2.1 Hz
	High	12.2	1.8 Hz	1.9 Hz	2.1 Hz
35 kg	Low	19	1.8 Hz	1.9 Hz	2.1 Hz
	Med	16.5	1.8 Hz	1.9 Hz	2.1 Hz
	High	14.5	1.8 Hz	1.9 Hz	2.1 Hz

Shoulder Strap Tension 60 N Waist Belt Tension 60 N

Mass	COG Position	FWD Lean Angle	Walking Speed Step Cadence 1.8 Hz = 4.0 kph Step Cadence 1.9 Hz = 5.0 kph Step Cadence 2.1 Hz = 6.0 kph		
15 kg	Low	10.7	1.8 Hz	1.9 Hz	2.1 Hz
	Med	9.6	1.8 Hz	1.9 Hz	2.1 Hz
	High	9.5	1.8 Hz	1.9 Hz	2.1 Hz
25 kg	Low	15.3	1.8 Hz	1.9 Hz	2.1 Hz
	Med	13.5	1.8 Hz	1.9 Hz	2.1 Hz
	High	12.2	1.8 Hz	1.9 Hz	2.1 Hz
35 kg	Low	19	1.8 Hz	1.9 Hz	2.1 Hz
	Med	16.5	1.8 Hz	1.9 Hz	2.1 Hz
	High	14.5	1.8 Hz	1.9 Hz	2.1 Hz

Table 2-I. Summary of Available RUCKMAN Analyses (continued)

Shoulder Strap Tension 60 N   Waist Belt Tension 0 N (Loose)

Mass	COG Position	FWD Lean Angle	Walking Speed Step Cadence 1.8 Hz = 4.0 kph Step Cadence 1.9 Hz = 5.0 kph Step Cadence 2.1 Hz = 6.0 kph		
15 kg	Low	10.7	1.8 Hz	1.9 Hz	2.1 Hz
	Med	9.6	1.8 Hz	1.9 Hz	2.1 Hz
	High	9.5	1.8 Hz	1.9 Hz	2.1 Hz
25 kg	Low	15.3	1.8 Hz	1.9 Hz	2.1 Hz
	Med	13.5	1.8 Hz	1.9 Hz	2.1 Hz
	High	12.2	1.8 Hz	1.9 Hz	2.1 Hz
35 kg	Low	19	1.8 Hz	1.9 Hz	2.1 Hz
	Med	16.5	1.8 Hz	1.9 Hz	2.1 Hz
	High	14.5	1.8 Hz	1.9 Hz	2.1 Hz

Moment of Inertia

Within the VN4D program, the moment of inertial of an object is completely user definable. By default, the program will also calculate the moment of inertia given the assigned material properties, mass distribution and geometry of an object. For the RUCKMAN analyses, the moment of inertia of the three-part pack was automatically calculated by VN4D based on the geometry and mass of each segment.

Shoulder Straps

Shoulder straps for these analyses were modeled in three parts; a middle padded region, an upper strap connecting the pad to the upper section of the pack and a lower webbing strap connecting the lower region of the pad to the lower portion of the pack. The mid portion consisted of the conforming shoulder pads described in (Reid et al., 2003). These pads were created by capturing the geometry of the body surface and extruding this shape outwards along the local surface normals. Therefore by definition, they are in contact with the underlying shoulder shape along their entire length. In practice, the center region of a loaded shoulder strap does not move with respect to the underlying shoulder although the ends or edges may. For that reason shoulder pads were modeled as fixed to the body at the midpoint of the pad leaving the edges of the pad free to move under the

influence of webbing straps. This approach greatly reduces the complexity of the shoulder contact solution.

Flexible strapping above and below the pad were modeled as damped springs with user variable stiffness. Positioning a slider control sets a value of 50, 100 or 150. This value provided a scale factor to the upper and lower spring 'K' values. The stiffness was then calculated as:

$$K = 100 \text{ x SF N/m}, \qquad K_{low} = 5,000 \text{ N/m}, \ K_{mid} = 10,000 \text{ N/m}, \ K_{high} = 15,000 \text{ N/m}$$

These scale factors, which resulted in upper strap tensions of approximately 100 and 60 N, were determined iteratively for the different loads carried.

Waist Belt

The geometry and material properties of the segmented waist belt are fully described in a previous report (Reid et al., 2003). The RUCKMAN Model used this belt with two minor modifications to model the specific cases required.

The general Dynamic Biomechanical Model (DBM) showed some initial solution instability related to the contact complexity between the minimally constrained waist belt segments and the lower body. This was resolved by controlling waist belt tension with a time dependant force actuator. During the first 3 seconds of each analysis, waist belt tension ramps up from 10 N to the final value of 60 N. This gradual application of tension facilitates numerical solution of the waist belt multi-body contact problem.

In cases where a loose belt is analyzed, the waist belt buckle was modeled as a rope with minimal tension (0 to 3 N).

Walking Speeds

Three different walking speeds were analysed for RUCKMAN. They were 4 kph (2.48 mph), 5 kph (3.10 mph) and 6 kph (3.73 mph). These speeds represent relaxed, moderate and brisk walking with a loaded rucksack. The two faster speeds bracket the pace of approximately 5.6 kph necessary to complete the Canadian Forces standard Battlefield Readiness Test in the required time.

Running an analysis

All analyses listed in Table 2.1 have been completed using Visual Nastran 4D and the results are included with the RUCKMAN model in a library of results. This permits RUCKMAN to exist as a stand-alone program for comparison of speed effect, load position effect and strap tension effect on the calculated biomechanical parameters.

To use RUCKMAN, a user selects the RUCKMAN icon or selects the filename *RUCKMAN.exe*. The user is presented with a sequence of input screens that directs their selections. The order of selection follows this pattern:
1. Choose a Load Magnitude
2. Choose a Load Location
3. Choose a Shoulder Strap Tension
4. Choose a Waist Belt Tension
5. Choose a Walking Speed.

Once these selections have been made, the program will select the appropriate case from the results library, import the data and display the results in both real time and summary form. A description of this process is illustrated in the following sections.

Opening the program evokes the display of the main screen. This display is shown in Figure 2-3 and consists of three parts - an input screen area where selection of the analysis parameters begins, a video display area where motion picture files (.avi files) are displayed as part of the analysis output and a graphical output section where all numerical data is plotted against time.

A user begins selection of the analysis parameters by responding to questions displayed in Screen B – Input area. As the user responds to screen prompts in Screen B, the program will renew this display area. Figure 2-4 (a – e) shows an enlarged view of the input area and illustrates the parameter selection process.

Once all parameters are chosen, the program pauses to allow the user to confirm the selected parameters. If the user is satisfied with the selected parameters, they select the button marked GO, found immediately beneath the input screen. Alternatively, should the user wish to change a parameter, they can select the red RESET button and re-enter the parameters. These controls are indicated in Figure 2-4(e).

When the GO button is selected, the program will begin to display the results for the selected analyses.

Figure 2-3. RUCKMAN Main Screen at Program Initiation
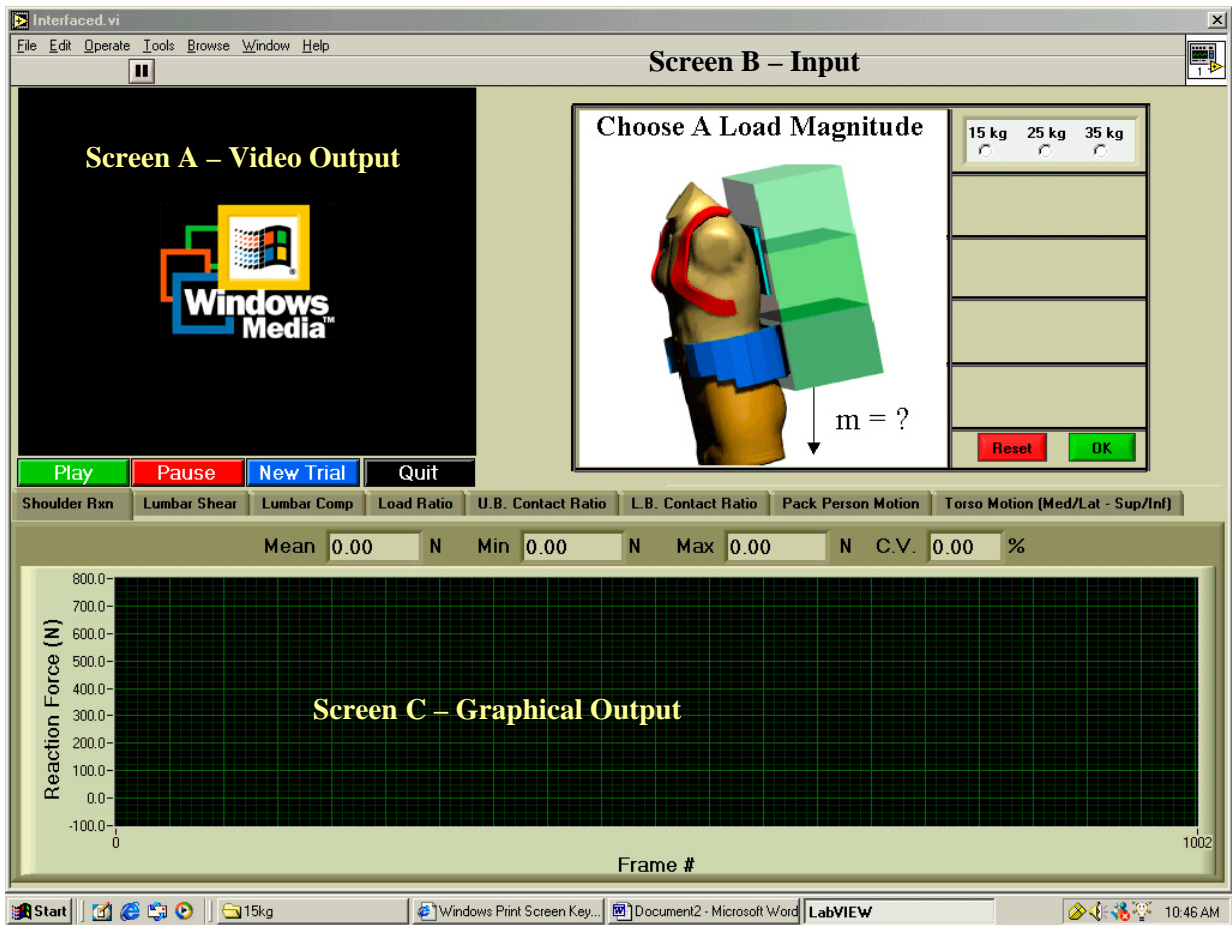
Figure 2-4. (a) Screen B – Input, Choose a Load Magnitude
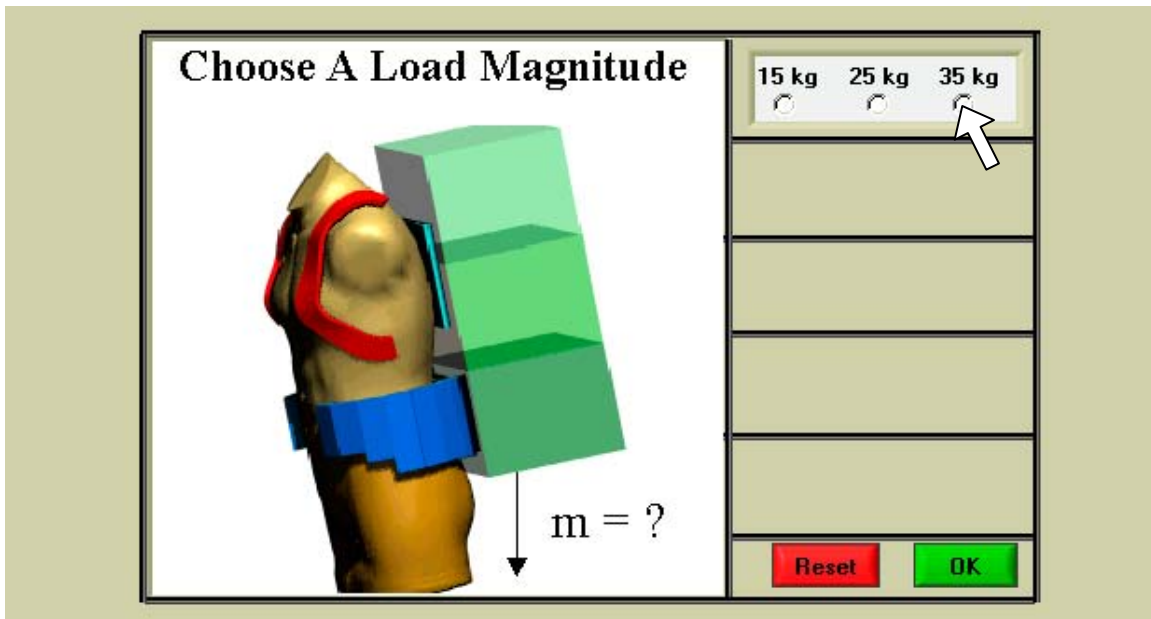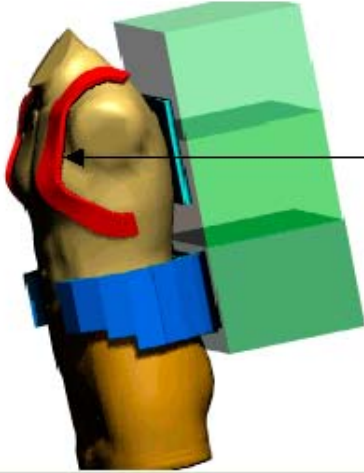
(b) Screen B – Input, Choose a Centre of Gravity Location
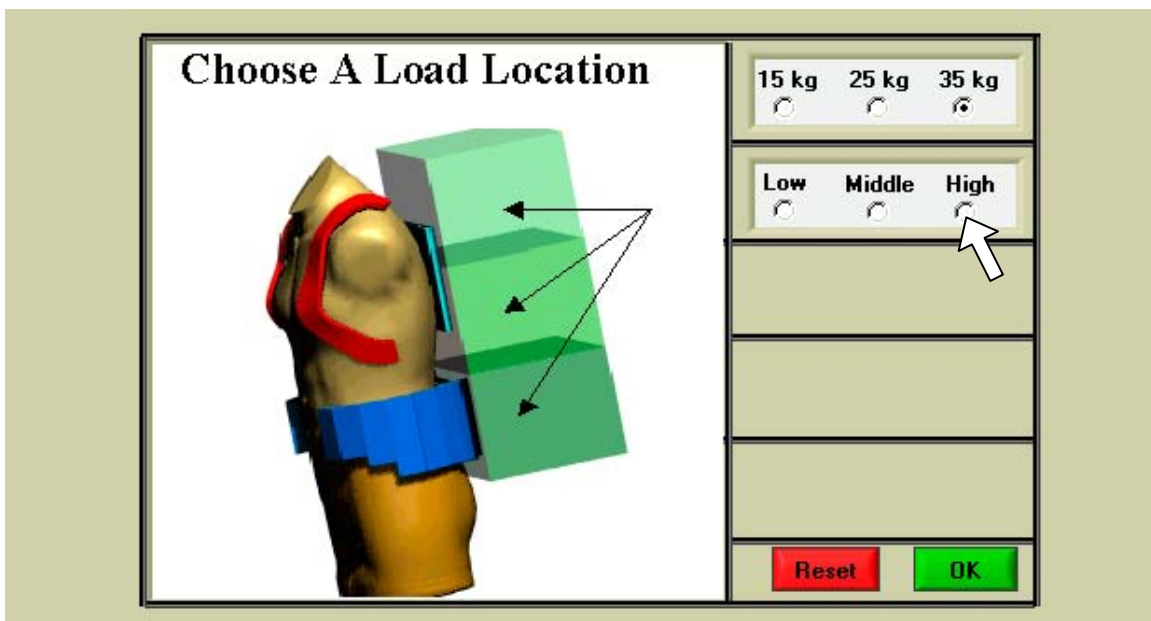
(c)   Screen B – Input, Choose a Shoulder Strap Tension
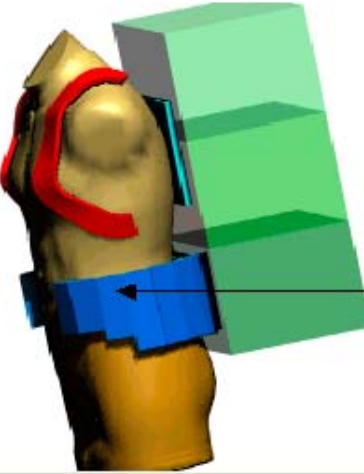
(d)   Screen B – Input, Choose a Waist Belt Tension

(e)	Screen B – Input, Choose a Walking Speed
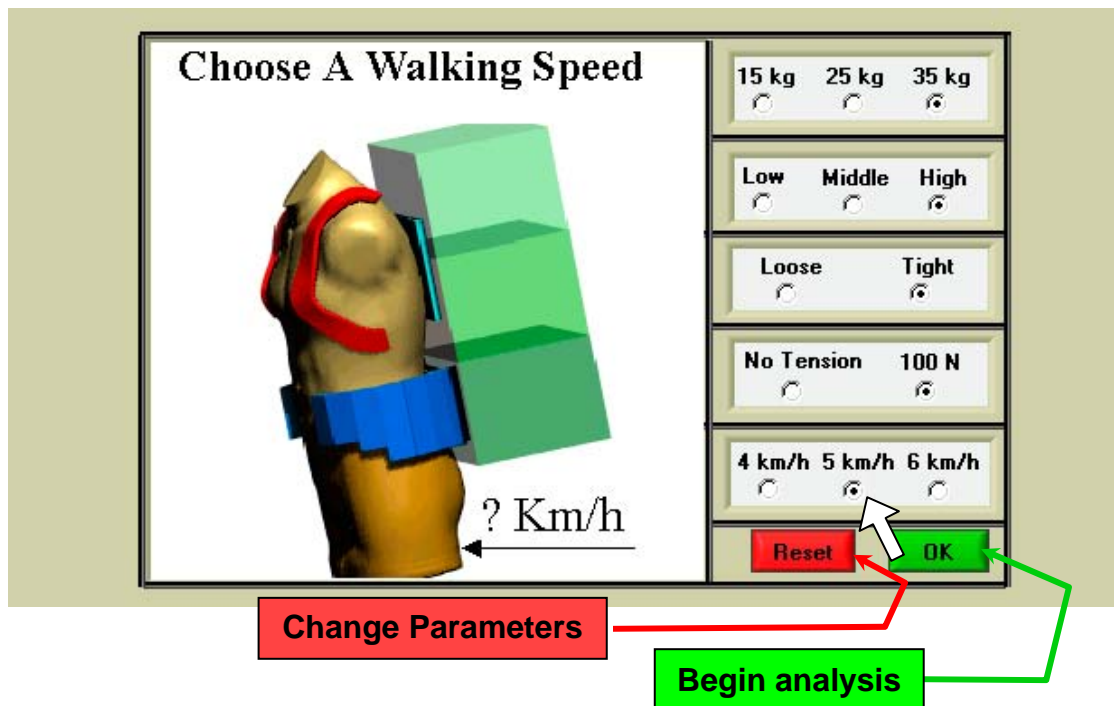
Figure 2-5. RUCKMAN Final Screen prior to beginning an analysis
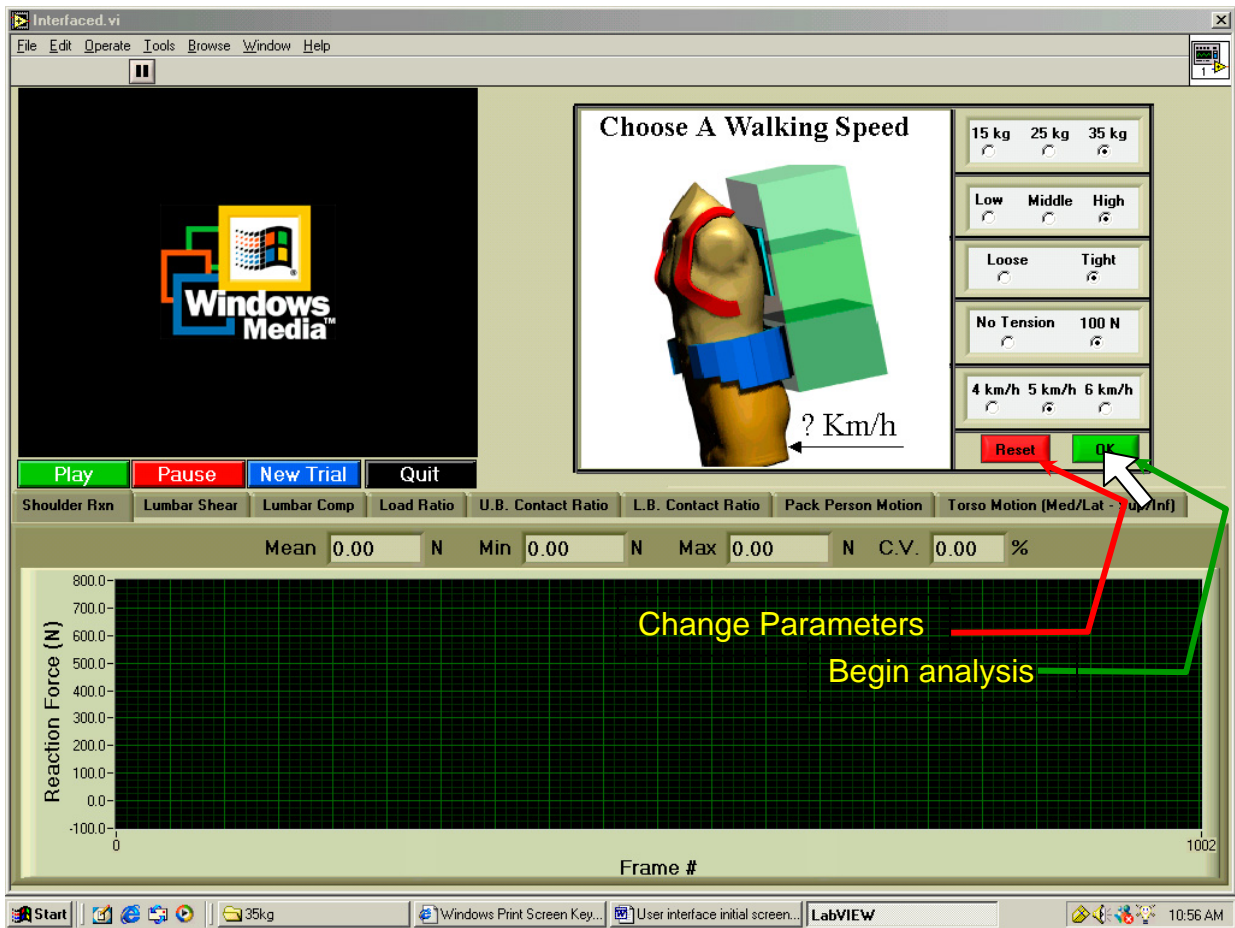
2.2   Description of Model Outputs

RUCKMAN provides a number of results including time histories and summary statistics of the models behaviour under the influence of the different sets of load carriage parameters. This data is presented graphically and is also completely available to the user in the form of text files should a user wish to do additional statistical analyses.

Injury mechanisms

The mechanisms of tissue injury fall into several categories and include dynamic overload causing strains, sprains or tears, impact injury causing tearing or bruising, cumulative mechanical overloading causing micro-tears leading over time to inflammation and scarring, and shearing loads that cause excessive tissue deformation and abrasion. When the mechanical energy to be dissipated or transmitted exceeds the ability of the

particular tissue to maintain its structural integrity, tissue damage results. (Whiting, Zernicke, 1998). This leads to the concept of tissue tolerance limits and the identification of critical injury factors.

Tissue Tolerance and Critical Factors

In the body of research generated around the study of human load carriage a number of biomechanically significant factors have emerged. These factors pertain to the load state of the human and to the response of the rucksack. These include:

Human based Factors
1. Lumbar Shear
2. Lumbar compression
3. Shoulder Reaction Forces
4. Ratio of Load carried to Load experienced

Rucksack Response Factors
1. Relative motion of Ruck with respect to Body
2. Upper Body Load vs Total Body Load
3. Lower Body Load vs Total Body Load

A brief explanation of these parameters and their implications in the context of the results presented in RUCKMAN is offered in the following sections. Additional in-depth discussion of these factors can be found in the reports (Stevenson et al., 2002, Reid et al., 1995).

3 RUCKMAN Results

RUCKMAN results are shown in all three windows and a typical output display is shown in Figure 2-6. These results are presented in videos of the pack person motion, in horizontal bar graphs depicting pack performance parameters and in a series of tab selected real time graphs.

3.1   Screen A – Video Output

Videos of the pack-person motion will appear in Screen A, at the upper left side of the monitor.   Motion is synchronized with the display of results plotted on the graph appearing on the lower part of the monitor display.

3.2   Screen B – Light Graphs

On the upper right side of the screen, the input screen will be replaced with a series of horizontal light graphs.   These horizontal lights reflect the mean values of pack performance parameters and are based on values developed from work with the load carriage simulator.   These parameters were found to be correlated with objective and subjective assessments of pack performance. Table 2-III Contains a summary of these parameters and an explanation.

Correlated LC Simulator and Human Factors Variables
Displacements and Forces

Table 2-II.   Comparison variables. Asterisk indicates LC system measurements which are significantly correlated to human factors measurements.

LC Simulator Measures			*Correlated Human Factors*
Displacement (mm)	x	▲	Posterior Hip Discomfort
	y		
	z	▲	Posterior Hip Discomfort
	r	▲	Posterior Hip Discomfort
Moment (Avg, Nm/kg)	x (-ve)		
	y (-ve)	▲	Forward Flexion Mobility, Overall comfort, Overall Fit
	z		
	r		
Force (Avg, N/kg)	x		
	y (-ve)	▲	Front Mobility, Overhead Mobility, Posterior Shoulder Discomfort, March Thermal Comfort
	z	▲	Front Mobility, Overhead Mobility, March Thermal Comfort
	r		
Moment (Amp, Nm/kg)	x	▲	Torsional Mobility, Overhead Mobility, Lie Function, Balance, Agility, Anterior Shoulder Discomfort, March Acceptability, March Comfort
	y		
	z	▲	Front Mobility
	r	▲	Posterior Neck Discomfort
Force (Amp, N/kg)	x		
	y		
	z	▲	Lie Function, Load Control, March Acceptability, March Integration, Overall Balance, Overall Comfort, Overall Maneuverability
	r	▲	Load Control, March Integration

Correlated LC Simulator and Human Factors Variables
Pressures and Stiffness

Table 2-III.

Shoulder Pressure (ANT)	Av (kPa)	▲	Posterior Hip Discomfort
	Pk (kPa)	▲	Doffing Function
	PDI	▲	Doffing Function
	F (N)	▲	Posterior Neck Discomfort
Shoulder Pressure (POST)	Av (kPa)		
	Pk (kPa)	▲	Doffing Function
	PDI		
	F (N)		
Lumbar Pressure (UPPER)	Av (kPa)		
	Pk (kPa)		
	PDI		
	F (N)	▲	Posterior Discomfort
Lumbar Pressure (LOWER)	Av (kPa)		
	Pk (kPa)		
	PDI	▲	Front Mobility, Posterior Discomfort
	F (N)		
Stiffness (Nm/deg)	Torsion	▲	Overhead Mobility, Front Mobility
	Flexion	▲	Combined Function, Posterior Neck Discomfort, Low Back Discomfort
	Side	▲	Front Mobility, Anterior Shoulder Discomfort, Anterior Hip Discomfort

Table 2-IV.

Rucksack Performance Results

Parameter	Correlated Variable		Superior	Low Decile	Mean	High Decile	Inferior
Relative Displacement (mm)	X ▲	Posterior Hip Discomfort		1.32	6.82	12.33	
	Y			1.06	3.83	6.60	
	Z ▲	Posterior Hip Discomfort		7.47	11.32	15.17	
	R ▲	Posterior Hip Discomfort		8.16	14.06	19.97	
Hip Moment (Avg, Nm/kg)	X (-ve)			0.07	-0.07	-0.21	
	Y (-ve) ▲	Forward Flexion Mobility, Overall comfort, Overall Fit		-0.13	-0.26	-0.39	
	Z			0.01	0.07	0.14	
	R			0.16	0.30	0.43	
Hip Reaction F (Avg, N/kg)	X			7.06	8.72	10.37	
	Y (-ve) ▲	Front Mobility, Overhead Mobility, Posterior Shoulder Discomfort, March Thermal Comfort		-1.06	-1.25	-1.44	
	Z ▲	Front Mobility, Overhead Mobility, March Thermal Comfort		8.85	8.94	9.03	
	R ▲			11.49	12.58	13.66	
Hip Moment (Amp, Nm/kg)	X ▲	Torsional Mobility, Overhead Mobility, Lie Function, Balance, Agility, Anterior Shoulder Discomfort, March Acceptability, March Comfort		-0.01	0.06	0.13	
	Y ▲	Front Mobility		0.07	0.32	0.57	
	Z ▲			-0.01	0.09	0.17	
	R ▲	Posterior Neck Discomfort		0.11	0.35	0.59	
Hip Force (Amp, N/kg)	X ▲	Lie Function, Load Control, March Acceptability, March Integration, Overall Balance, Overall Comfort, Overall Maneuverability		1.40	3.18	4.96	
	Y			-0.19	0.05	0.29	
	Z			5.41	7.32	9.22	
	R ▲	Load Control, March Integration		5.91	8.05	10.18	

3.3 Screen C – Real-Time Graphs

Time histories are shown in Screen C

1. Estimated Shoulder Reaction Force
2. Estimated Lumbar Shear
3. Estimated Lumbar Compression
4. Estimated Ratio of Load carried to Load experienced
5. Estimated Upper Body Contact force
6. Estimated Lower body Contact force

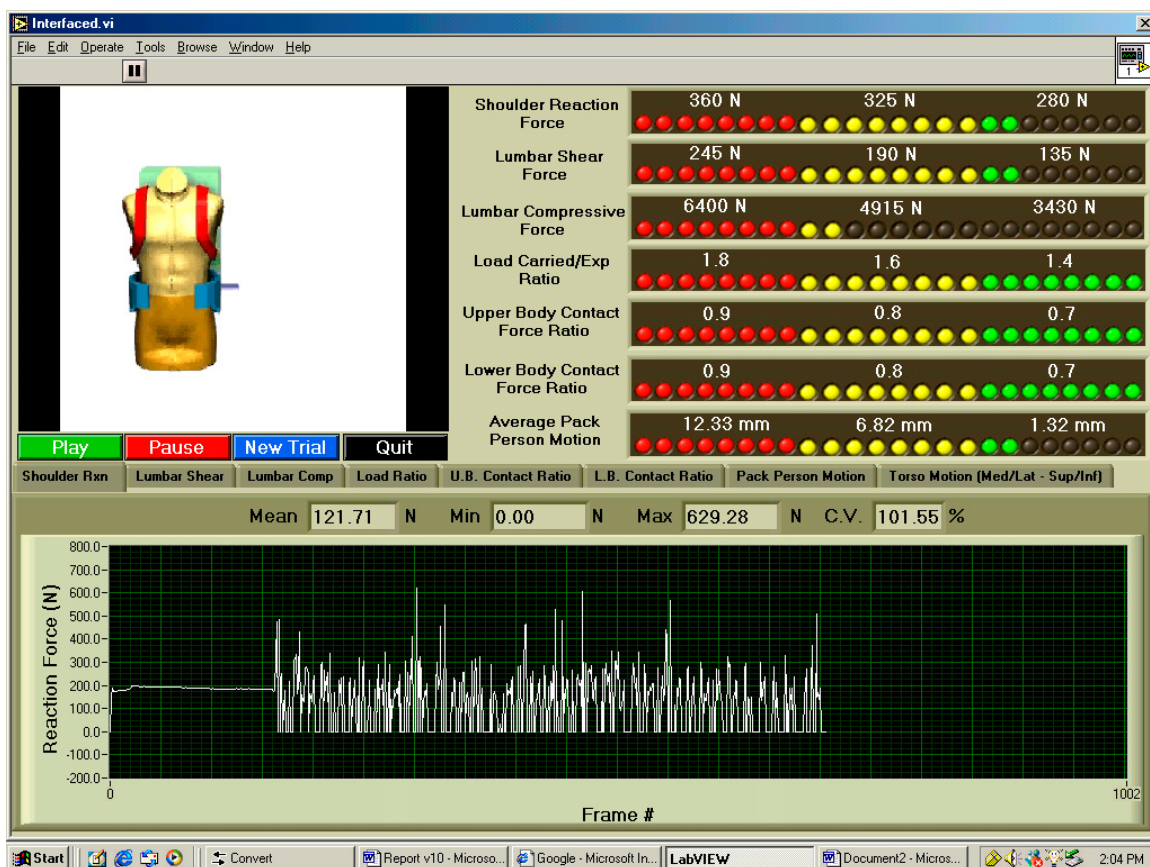**Figure 2-6.**   Shoulder Reaction Force Time History Output

Shoulder Reaction Force Time History Output

The magnitude of the load born by the shoulders has been shown to be a critical factor in the total load carriage capability of a soldier [Stevenson et al, 1996] where a simple 2D static analysis of 4 different military backpacks demonstrated a correlation coefficient of 0.98 between

50

the reaction force magnitude at the shoulders and the perceived level of discomfort reported by soldiers during 6 km marches with 35 kg loads.   Although tested, the data for the American Medium Field Pack (ALICE pack) was not included as results indicated this pack had the highest level of user discomfort with one of the lowest levels of shoulder loading. A linear regression gave the following relationship between shoulder reaction force and discomfort:

Eq. 1   Shoulder Discomfort (%) = 0.6862 * (Shoulder Reaction Force (N)) - 185.7 N
$r^2 = 0.97$

The RUCKMAN light graph output levels for shoulder reaction force of 280, 325 and 360 N therefore correspond to estimated user discomfort levels of approximately 5%, 35% and 60% respectively.
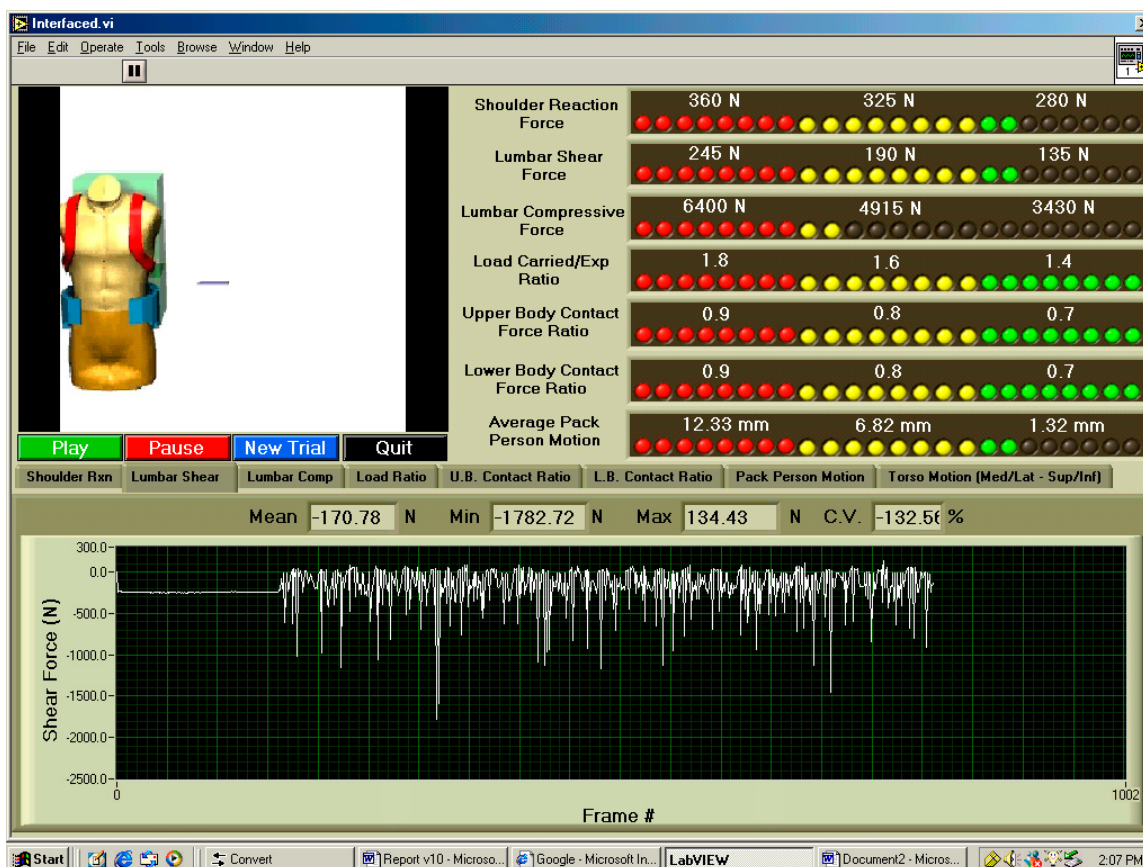
Figure 2-7.   Lumbar Shear Time History Output

3.4   Exporting results

All results shown in the summaries and plots of RUCKMAN can be readily exported for further analysis.   A complete listing of the analyses and the output data files is included in Appendix D-1, RUCKMAN Output Files.   A standardized and intuitive naming strategy has been used to catalogue these files and the explanation is as follows:

Example filename: 25kg100N60N1L5kph.txt

25kg 100N 60N 1L 5kph.txt

a   b   c   d   e   .txt

Where:
a = load carried
b = shoulder strap tension setting
c = waist belt tension setting
d = centre of gravity position
e = walking speed

REFERENCES

Abe, D., Yanagawa, K. and Niihata, S. Effects of load carriage, load position and walking speed on energy cost of load carriage. *Appl. Ergonomics*, **35**: 329-335, 2004.

Bland, J.M. and Altman, D.G. Statistical methods for assessing agreement between two methods of clinical measurement. *Lancet*, **327(8476)**: 307-310, 1986.

Bloom, D. and Woodhull-McNeal, A.P. Postural adjustments while standing with two types of loaded backpack. *Ergonomics*, **30**: 1425-1430, 1987.

Bryant, JT, Doan, J, Stevenson, JM, Pelot, RP. Validation of objective based measures and development of a performance based ranking method for load carriage systems. Proceedings of the RTO – NATO Specialist Meeting, 15; 1-12, 2001.

Charteris, J., Scott, P.A. and Nottrodt, J.W. Metabolic and kinematic responses of African women headload carriers under controlled conditions of load and speed. *Ergonomics*, **32**: 1539-1550, 1989.

Cholewicki, J., McGill, S.M. (1996) Mechanical stability of the in vivo lumbar spine: Implications for injury and chronic low back pain. *Clin. Biomech*. 11(1): 1-15.

Cholewicki, J., Simons, A.P.D., and Radebold, A. (2000). Effects of external trunk loads on lumbar spine stability. *J. Biomech.* 33(11): 1377-1385.

Falola, J.M., Brisswalter, J. and Delpech, N. Effet du port d'une charge sur le tronc sur la détermination d'une vitesse de marche optimale. *Science & Sports*, **14**: 201-204, 1999.

Fergenbaum, M.A., Perry, A., Lin, E., Reid, S.A., and Morin, E.L. *Development of a portable data acquisition system for human performance assessment in the field. Phase IIc: Gait Analysis Module*. DRDC Toronto CR 2008-010. PWGSC Contract # W7711-0-7632-05, 2003.

Franduti-Polcyn, A., Bensel, C.K., Harmon, E.K. and Obusek, J.P. The effects of load weight: a summary analysis of maximal performance, physiological and biomechanical results from four studies of load-carriage systems. *NATO RTO Specialist's Meeting on Soldier Mobility: Innovations in Load Carriage System Design and Evaluation*, 7-1 – 7-11, 2001.

Harmon, E.K., Han, K-P. and Frykman, P. Load-speed interaction effects on the biomechanics of backpack load carriage. *NATO RTO Specialist's Meeting on Soldier Mobility: Innovations in Load Carriage System Design and Evaluation*, 5-1 – 5-16, 2001.

Holewijn, M. Physiological strain due to load carrying. *Eur. J. Appl. Physiol.*, **61**: 237-245, 1990.

Hong, Y., Li, J.X., Wong, A.S.K. and Robinson, P.D. Effects of load carriage on heart rate, blood pressure and energy expenditure in children. *Ergonomics*, **43**: 717-727, 2000.

LaFiandra, M., Holt, K.G., Wagenaar, R.C. and Obusek, J.P. Transverse plane kinetics during treadmill walking with and without a load. *Clin. Biomech.,* **17**: 116-122, 2002.

LaFiandra, M., Wagenaar, R.C., Holt, K.G. and Obusek, J.P. How do load carriage and walking speed influence trunk coordination and stride parameters? *J. Biomech.*, **36**: 87-95, 2003.

Marras, W.S., Lavender, S.A., Leurgans, S.E., Fathallah, F.A., Ferguson, S.A., Allread, W.G., Rajulu, S.L. (1995) Biomechanical risk factors for occupationally related low back disorders. *Ergonomics* 38: 377-410.

McGill, S.M. *Low Back Disorders* , copyright 2002, printer Sheridan Books, USA

McGill, S.M. (1992) A myoelectrically based dynamic three-dimensional model to predict loads on lumbar spine tissues during lateral bending. *J. Biomech.* 25: 395-414.

McGill, S.M. (1997) The biomechanics of low back injury: Implications on current practice in industry and the clinic. *J. Biomech.* 30: 465-475.

Morin, E.L., Stevenson, J.M., Reid, S.A. and Bryant, J.T. *Understanding the Costs of Load Carriage by Means of the Portable Measurement System and Dynamic Biomechanical Model*, DRDC Toronto CR 2005-128. PWGSC Contract # W7711-03-7863-01, 2004.

NIST/SEMATECH, *e-Handbook of Statistical Methods*, http://www.itl.nist.gov/div898/handbook, 2005.

Pandolf, K.B., Givonni, B., Goldman, R.F., "Predicting energy expenditure with loads while standing or walking very slowly", *J. App. Physiol.,* vol. 43, pp. 577-581, 1977.

Pelot, R.P., Rigby, A., Bryant, J.T., Stevenson, J.M. Section C: Phase II of a Biomechanical Model for Load Carriage Assessment. PWGSC Contract # W7711-7-7420/A (45 pgs), 1998.

Pelot, R.P., Rigby, A., Stevenson, J.M., and Bryant, JT. Static biomechanical load carriage model. Proceedings of the RTO – NATO Specialist Meeting, 25; 1-12, 2001.

Pierrynowski, M.R., Winter, D.A. and Norman, R.W. Metabolic measures to ascertain the optimal load to be carried by man. *Ergonomics*, **24**: 393-399, 1981.

Reid, SA, Bryant, JT, Stevenson, J.M., *Phase II Development of a Dynamic Biomechanical Model of Human Load Carriage, DRDC Toronto CR 2005-118. W7711-0-7632-06, June 2002*

Reid, SA., Bryant, JT, Stevenson, J.M., & Abdoli, M. *Phase IV Part A&B: Development of a Dynamic Biomechanical Model Version 2 of Human Load Carriage, DRDC Toronto CR 2005-123. W 7711-0-7632-07, July, 2003.*

Saibene, F and Minetti, A.E. Biomechanical and physiological aspects of legged locomotion in humans. *Eur. J. App. Physiol.*, **88**: 297-316, 2003.

Sanders, J.E., Greve, J.M., Mitchell, S.B, Zachariah, S.G., *Material Properties of commonly used interface properties and their static coefficients of friction with skin and socks*. Journal of Rehabilitation Research and Development, Jn 1998, V35, No.2: 161-176.

Stevenson, J.M., Bryant, J.T., dePencier, R.D., Pelot, R.P., and Reid, J.G. Research and Development of an Advanced Personal Load Carriage System (Phase I-D). DSS Contract # W7711-4-7225/01-XSE (350 pgs). 1995

Stevenson, J.M., Bryant, J.T., Reid, S.A. and Pelot, R.P. Validation of the Load Carriage Simulator: Research and Development of an Advanced Personal Load Carriage system: Section D (Phase 1). DSS Contract #W7711-4-7225/01 (44 pgs). 1996

Stevenson, JM, Bryant, JT, Reid, SA, Pelot, RP, Morin EL *Development of the Canadian Integrated Load Carriage System using Objective Measures*. Proceedings of the RTO – NATO Specialist Meeting, 21; 1-11, 2001.

Stevenson, JM, Reid, SA, Bryant, JT, Hadcock, L.J., Morin, EL *Part A of Phase I: Equipment Upgrades to Accommodate Dynamic Biomechanical Modeling* subsection of: *Development of a Dynamic Biomechanical Model for Load Carriage: Phase I DRDC Toronto CR 2005-115* PWGSC Contract # W7711-0-7632-01/A, March 2001

Stevenson, J.M., Good, J.A., Devenney, I.A., Morin, E.L., Reid, S.A. and Bryant, J.T. *Characterization of load control during a human trials circuit, Phase 3(b), DRDC Toronto CR 2005-120.* PWGSC Contract #W7711-0-7362-06, 2002.

Stevenson, JM, Bryant JT, Reid, SA, Pelot, RP, Morin, EL, Bossi LL. Development and Assessment of the Canadian personal load carriage system using objective biomechanical measures. (Accepted with revisions: Ergonomics, April 2003).

Whiting, William C., Zernicke, Ronald F. *Biomechanics of Musculoskeletal Injury*, published by Human Kinetics, Windsor, ON N8Y 2L5, 1998

Appendix A – Letter of Information and Consent Form

Biomechanical Effects of Load Carriage under Varying Loads

Dear _____

You are being invited to participate in a research study on load carriage being conducted by the Ergonomics Research Group at Queen's University. This study is being completed for Defence Research and Development Canada - Toronto (DRDC). We will read through this consent form with you and describe the procedures in detail. You will be given time to read it yourself and are encouraged to ask questions at any time.

Aims and Purposes of the Study:

The overall aim of our research program is to develop a dynamic biomechanical model for application in load carriage situations. Currently, data is being gathered using accelerometers, and the Optotrak camera system. This optoelectric system consists of 3 cameras and infrared markers. The system collects position data from markers placed on selected skin surface locations and projecting probes attached to the lower limb and sternum. This data will be used to examine walking patterns. Data will also be collected from an accelerometer located on the sternum. The main objective of this study is to assess whether walking patterns vary with changes in load carried and whether these changes are detected in the upper body acceleration patterns. This study is also being conducted to validate the use of accelerometers to determine the forward trunk lean associated with carrying loads in a backpack.

Study Details:

During the session, you will be asked to walk under four load conditions: while carrying no load or while carrying one of 3 loads, ranging from approximately 15 to 35 kg, in a backpack. Eight infrared markers will be attached to the outside of your right leg and an additional three will be located on a projecting surface, attached to a plexiglass plate; this plate will be attached to your sternum using double sided tape. A triaxial accelerometer is affixed to the sternum plate to measure upper body accelerations. You will be asked to walk at your own pace across the length of the room, several times for each load condition. Then you will be asked to walk across the length of the room several times at a regulated pace (corresponding to a speed of approximately 1.34 m/s or 3 mph).

Risks of Participation:

The risks of participating in this study include: back and joint pain, dizziness, fatigue, muscle cramping, shortness of breath, fainting, and heart attack. The risk of these events is minimal for young, healthy and physically fit individuals. If you experience dizziness, fatigue, pain, muscle

cramps or shortness of breath please report them to the research assistant or the principal investigator immediately.

Exclusion Criteria:

To minimize the risks and reduce variation in the subject characteristics, only young, physically fit men are being recruited to participate in this study. Therefore, you will not be considered for this study if you:

- Are not between the ages of 21 and 29 years
- Are female
- Do not pass the PAR-Q and You

Confidentiality:

All information obtained during the course of this study is strictly confidential and your anonymity will be protected at all times. You will be identified by a study number, not your name. Personal information will be stored in a locked file and will be available only to the principal researcher and research assistants who have helped collect the data. Digital photographs will be taken during the experimental session and may be used in publications and presentation of the work. In such cases, care will be taken to protect your identity.

Voluntary Nature of the Study:

Your participation in this study is completely voluntary. You may withdraw from this study at any time without coercion to continue or penalty.

Withdrawal of subject by principal investigator:

You may be withdrawn from this study by the principal investigator if the principal investigator feels that you are unable to safely continue the session.

Payment:

You will receive $20.00 for your participation in this study.

Subject Statement and Signature:

I have read and understand the consent form for this study. The purposes, procedures and technical language have been explained to me. I have been given sufficient time to consider the above information and to seek advice if I chose to do so. I have had the opportunity to ask questions which have been answered to my satisfaction. I am voluntarily signing this form. I will receive a copy of this consent form for future reference.

If at any time I have further questions, problems or adverse events, I can contact:

Dr. E. Morin at (613) 533-6562
Electrical & Computing Engineering

Or

Dr. Janice Deakin at (613) 533-6601
School of Physical & Health Education

If I have any questions regarding my rights as a research subject I can contact

Dr. Albert Clark, Chair, Research Ethics Board at 533-6081

By signing this consent form, I am indicating that I agree to participate in this study.

_____   _____
Signature of Subject   Date

_____   _____
Signature of Witness   Date

Statement of Investigator:

I, or one of my colleagues, have carefully explained to the subject the nature of the above research study. I certify that, to the best of my knowledge, the subject understands clearly the nature of the study and demands, benefits, and risks involved to participants in this study.

_____   _____
Signature of Principal Investigator   Date

Appendix B – Forward Lean Angle Results

B.1 Static and Dynamic Forward Body Lean Angles Computed from Accelerometer and Xsens Data

The average static body lean angles computed from accelerometer data, (as described in Morin et al., 2004) and recorded Xsens data are given in Table B-I. Forward body lean angles are represented as positive, backwards lean or tilt is represented as negative.

Table B-I. Static forward body lean angles computed for all subjects at each load for the changing speed and changing incline tests. Relative lean angles were calculated by subtracting the lean angles for zero load from the angles for all loads. Outliers are in bold.

Subject #	Load (kg)	Relative Lean Angle for Changing Speed Tests (deg)		Relative Lean Angle for Changing Incline Tests (deg)	
		Accelerometer	Xsens	Accelerometer	Xsens
01	0	0	0	0	0
	16.6	24.23	23.60	17.36	6.58
	25.9	26.35	21.89	25.87	11.21
	38.7	38.31	27.72	17.36	10.16
03	0	n/a	0	0	0
	16.6	n/a	16.09	13.80	5.82
	25.9	n/a	16.04	8.83	8.76
	38.7	n/a	7.47	5.56	5.82
06	0	*0*	0	*0*	*0*
	16.6	*-26.15*	-4.07	*-9.79*	*4.91*
	25.9	*-4.21*	2.51	*3.95*	*5.44*
	38.7	*10.18*	26.36	*-4.12*	*-3.09*
07	0	0	0	n/a	0
	16.6	11.39	8.51	n/a	18.10
	25.9	15.45	8.94	n/a	16.81
	38.7	28.09	15.14	n/a	7.81
08	0	0	0	0	0
	16.6	14.98	16.62	24.47	6.16
	25.9	21.19	18.30	33.32	9.29
	38.7	40.48	18.76	28.30	27.12
09	0	0	0	n/a	0
	16.6	5.29	5.50	n/a	16.44
	25.9	10.46	6.06	n/a	12.93
	38.7	20.27	9.93	n/a	18.39
10	0	n/a	0	0	0
	16.6	n/a	14.64	9.56	16.26
	25.9	n/a	19.79	23.19	8.08
	38.7	n/a	10.27	15.38	7.49
12	0	0	*0*	n/a	0
	16.6	10.94	*-16.16*	n/a	2.16
	25.9	19.14	*-4.22*	n/a	6.08
	38.7	14.09	*-0.38*	n/a	26.56

The highlighted values in Table B-I have been identified as anomalous, because the angles indicate that the subject generally leaned backwards, or only slightly forwards, which would produce an unstable posture, especially at the higher loads. These values were removed and the means and standard deviations for the angles were calculated, as given in Table B-II. As well, t-tests were run to compare angles computed using accelerometer data and using Xsens data. The means of the distributions were found to be significantly different only for the 25.9 kg load ($p<0.02$). It does appear, however, that the forward body lean angles reported by the Xsens are consistently lower than angles obtained from the upper body accelerations. All data values (except the anomalous values) were grouped and are plotted in Figure B-1. Linear regressions, with intercept set to zero, were performed on the data. The regression lines have positive slopes, indicating that the forward lean angle increases with load. It can be noted that the slope for the accelerometer regression line is higher than for the Xsens regression line. However, given the variability in the data, it is not possible to conclude that the slopes are significantly different.

Table B-II. Average and standard deviation for relative static forward lean angles computed using accelerometer and Xsens data.

Load (kg)	Accelerometer		Xsens	
	Mean Angle (deg)	Std dev	Mean Angle (deg)	Std dev
0	0.00	0.00	0.00	0.00
16.6	14.67	6.47	10.89	7.59
25.9	20.42	7.90	11.91	5.83
38.7	23.09	11.59	15.64	8.37

Figure B-1. Relative forward body lean angles obtained from the Crossbow accelerometer (left) and Xsens data (right) during the treadmill tests. Note the scales on the y-axes are different.
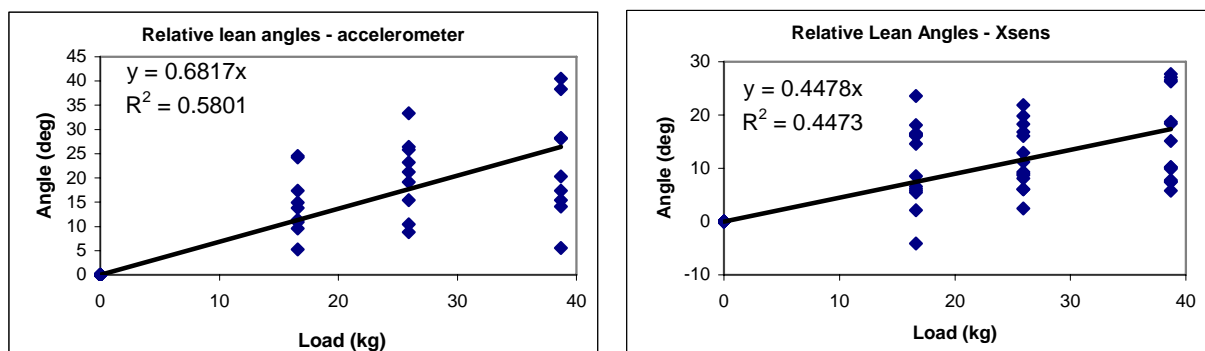
Static forward body lean angles were computed for a previous study (Stevenson et al., 2002) using digital images. The angle computed is total body lean versus true vertical. The average angles and standard deviations are given in Table B-III. These values display less intersubject variability than values computed using both the accelerometer and Xsens data. For the accelerometer and Xsens angles, the coefficients of variation (CoV = standard deviation / mean) range from 0.49 to 1.11; for the image data, CoV's range from 0.16 to 0.98 and if CoV values for the lowest load are removed, the range is 0.16 to 0.43.

Table B-III.　Average body lean angles computed using digital images for subjects participating in a previous load carriage trial (Stevenson et al., 2002).

Load Mass	CTS Pack			DFS Pack		
	Average Angle	Std Dev	Number of Subjects	Average Angle	Std Dev	Number of Subjects
5.5	3.98	3.91	13	4.88	2.99	9
15.7	14.96	3.88	13	18.17	4.38	8
25.5	16.09	6.23	12	20.98	4.10	8
34.3	18.67	8.10	9	23.45	3.76	7

A plot of the forward lean angles computed from the digital images, accelerometer data and Xsens data is shown in Figure B-2. Although the loads differ somewhat from the loads carried in the treadmill study, it is apparent that the angles computed from the digital images lie between those computed using accelerometer and Xsens data.
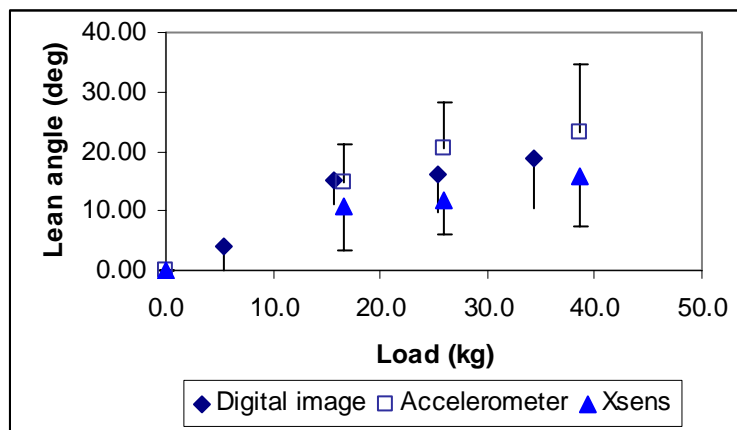

Figure B-2.　Relative forward lean angles computed using upper body accelerations, Xsens angles and digital images. In general, the angles obtained from the digital images fall between the angles computed from the accelerometer and Xsens data.

B.2 Static and Dynamic Forward Lean Angles Computed during the Gait Analysis Study

The average forward body lean angles, computed from the upper body accelerations for all subjects in the gait analysis study, are given in Table B-V. The three accelerometer channels were sampled at 100 Hz synchronously with motion data collected using the Optotrak system and force plate data. Prior to data collection, the accelerometer was calibrated by measuring acceleration due to gravity on each axis. Calibration values are given in Table B-IV.

Table B-IV. Calibration values for the Crossbow accelerometer.

Accelerometer axis	X	Y	Z
Zero-g voltage (V)	2.596	2.497	2.483
Sensitivity (V/g)	0.206	0.204	0.201

The stationary lean angle was computed using 2 sec of accelerometer data as the subject stood upright and the dynamic forward lean angles were computed using 2 sec of data from each of the walking trials – 10 self paced and 10 fixed paced trials. The ten angles for each walking condition were averaged to give the average lean angles. Repeatability of the forward lean angles within subjects was determined using the following equation:

$$r = \frac{S^2 A}{S^2 + S^2 A}$$

where S^2A is the between group variance and S^2 is the within group variance; r ranges from 0 to 1 where a value closer to 1 indicates better repeatability of the data[10]. Single factor ANOVA's were run on the lean angles for each load and each walking condition (self-paced or fixed paced) where subject was the factor. In all cases, the p-values were very small, indicating a significant difference in lean angles between subjects. To compute repeatability, r:

$$S^2 = MS_W$$

$$S^2 A = \frac{MS_B - MS_W}{n_0}$$

where MS_W is the mean square difference within groups and MS_B is the mean square difference between groups, reported by the ANOVA. The r-values for each load and walking condition are given in Table B-VI. The values are all very close to 1, indicating that the lean angles measured for different trials on the same subject are repeatable.

Table B-V. Average forward body lean angles computed for all subjects for the gait study.

	Computed Angles					Relative Angles			
	Stationary					Stationary			
Sub #	0 kg	16.6 kg	25.9 kg	38.7 kg	Sub #	0 kg	16.6 kg	25.9 kg	38.7 kg
1	-8.43	-1.03	3.01	5.14	1	0	7.40	11.44	13.58
2	-10.44	-10.46	-7.41	-5.75	2	0	0.02	3.02	4.69
3	-10.50	-4.93	-3.27	-0.13	3	0	5.56	7.23	10.37
4	-9.45	-2.32	-3.61	-2.50	4	0	7.12	5.84	6.95
5	-12.75	-7.86	-7.59	-7.82	5	0	4.89	5.16	4.92
6	-8.15	0.69	5.29	5.29	6	0	8.84	13.44	13.44
7	-12.49	-4.46	-2.61	7.03	7	0	8.03	9.88	19.53
8	-8.18	-3.10	-3.41	1.32	8	0	5.08	4.77	9.50
9	-4.98	8.14	3.01	17.35	9	0	13.11	7.99	22.33
10	-17.03	-9.35	-10.36	-13.75	10	0	7.68	6.67	3.29
11	-9.40	1.44	5.00	10.62	11	0	10.85	14.40	20.02
12	-8.20	4.25	5.86	5.74	12	0	12.45	14.06	13.94
Avg	**-10.00**	**-2.42**	**-1.34**	**1.88**	**Avg**	**0**	**7.59**	**8.66**	**11.88**
Std Dev	**2.92**	**5.29**	**5.37**	**8.16**	**Std Dev**	**0**	**3.44**	**3.74**	**6.12**
	Self Paced Walking					Self Paced Walking			
1	-5.35	7.57	10.28	10.52	1	0	12.91	15.63	15.87
2	-5.35	-2.23	0.16	5.21	2	0	3.11	5.50	10.56
3	-6.59	-0.53	0.31	2.56	3	0	6.05	6.90	9.15
4	-2.89	0.85	3.98	5.17	4	0	3.75	6.88	8.06
5	-7.36	-2.43	0.02	0.27	5	0	4.93	7.38	7.62
6	-7.37	1.39	9.89	9.89	6	0	8.76	17.26	17.26
7	-0.72	6.53	2.18	14.18	7	0	7.26	2.90	14.91
8	-6.37	-2.68	-0.49	2.19	8	0	3.69	5.88	8.56
9	-0.85	15.95	17.45	22.54	9	0	16.80	18.31	23.39
10	-10.63	-1.09	-1.78	-3.29	10	0	9.54	8.85	7.34
11	-3.11	8.65	14.03	13.54	11	0	11.76	17.14	16.65
12	2.53	12.85	14.74	14.21	12	0	10.32	12.21	11.68
Avg	**-4.51**	**3.74**	**5.90**	**8.08**	**Avg**	**0**	**8.24**	**10.40**	**12.59**
Std Dev	**3.47**	**6.12**	**6.64**	**7.04**	**Std Dev**	**0**	**4.06**	**5.18**	**4.80**
	Fixed Paced Walking					Fixed Paced Walking			
1	-5.14	7.29	11.69	11.50	1	0	12.43	16.83	16.64
2	-8.20	-2.66	-1.85	4.76	2	0	5.54	6.35	12.96
3	-6.48	-0.83	1.22	2.69	3	0	5.65	7.70	9.17
4	-2.90	2.41	7.75	4.69	4	0	5.31	10.65	7.58
5	-8.76	-2.32	0.86	1.19	5	0	6.44	9.62	9.95
6	-5.68	2.70	9.55	9.55	6	0	8.38	15.23	15.23
7	1.53	8.85	4.82	15.72	7	0	7.32	3.29	14.19
8	-6.39	-2.51	-1.13	2.55	8	0	3.88	5.27	8.94
9	-2.94	12.05	13.94	17.98	9	0	14.99	16.87	20.91
10	-9.57	0.66	-1.65	-2.28	10	0	10.23	7.92	7.29
11	-2.77	9.03	13.93	15.21	11	0	11.80	16.70	17.98
12	4.69	12.62	16.86	14.64	12	0	7.93	12.17	9.95
Avg	**-4.38**	**3.94**	**6.33**	**8.18**	**Avg**	**0**	**8.33**	**10.72**	**12.57**
Std Dev	**4.04**	**5.51**	**6.53**	**6.46**	**Std Dev**	**0**	**3.23**	**4.62**	**4.25**

---

[10] This method of assessing repeatability is included in notes on Repeatability by David Gray, California State University Northridge. See http://www.csun.edu/~dgray/BE528/528Fall2004.html

Table B-VI. Within subject repeatability computed for the forward lean angles for all load and walking conditions.

Load		0 kg	16.6 kg	25.9 kg	38.7 kg
Self-paced	*r-value*	0.954	0.978	0.974	0.983
Fixed paced	*r-value*	0.949	0.975	0.975	0.974

B.3 Comparison of Static and Dynamic Lean Angles

The average static and dynamic lean angles computed from upper body accelerations are given in Table B-VII and shown in Figure B-3, where a negative angle represents a backwards tilt and a positive angle represents a forwards lean.

Table B-VII. Forward lean angles computed from upper body accelerations during both standing (static) and walking (dynamic).

Changing Speed Tests								
	static		3.22 km/h		4.83 km/h		6.44 km/h	
Load	Average	Std dev	Average	Std dev	Average	Std dev	Average	Std dev
0	-15.71	7.68	-8.21	10.72	-7.33	10.29	-6.15	10.43
16.6	-8.02	18.58	1.06	11.40	2.97	9.81	1.95	7.03
25.9	0.28	11.67	7.97	10.15	9.07	10.60	7.85	7.47
38.7	2.83	15.69	19.46	14.79	18.82	13.64	15.85	14.03
Changing Incline Tests								
	Static		0 deg		5 deg		10 deg	
Load	Average	Std dev	Average	Std dev	Average	Std dev	Average	Std dev
0.0	-13.17	7.73	-8.79	11.53	-6.53	11.83	-5.50	13.50
16.6	-2.81	9.14	3.91	8.53	8.30	8.31	11.22	10.60
25.9	4.44	13.27	11.81	11.87	14.17	11.25	16.44	10.35
38.7	-0.72	11.42	9.06	9.52	11.20	8.78	13.63	9.55
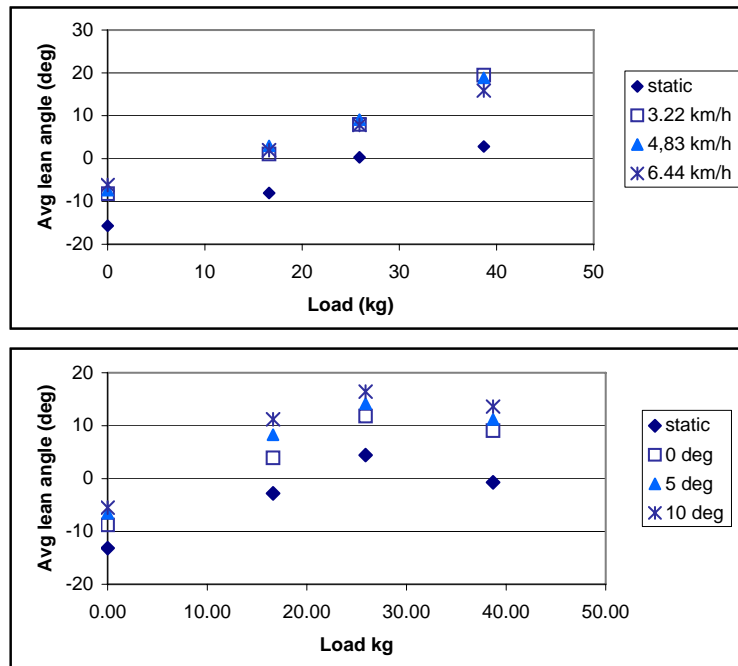
Figure B-3. Forward lean angles computed from upper body accelerations during changing speed (top) and changing incline (bottom) tests.

It is apparent from Table B-VII and Figure B-3, that at each load, there is more forward lean when the subjects are walking than when they are standing. T-tests were run on the static versus walking forward lean angles for all speeds and inclines. In all cases, the static lean angle was significantly different from the walking lean angle ($p < 0.05$). The same effect was noted with the data from the gait analysis study. When the actual (not relative) lean angle computed from the upper body accelerations was considered, the forward lean was significantly different during walking than during standing ($p < 0.05$), as shown in Figure B-4. The forward lean angles for the two walking cases – self-paced and fixed paced – were not significantly different. Again, there was no difference in standing versus walking forward lean angle for the relative lean angles.
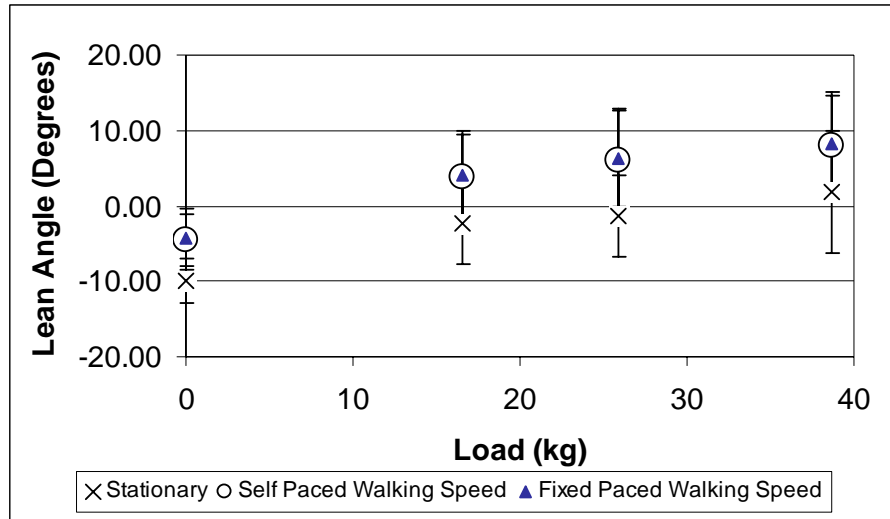
Figure B-4. Forward lean angles for standing, self-paced walking and fixed paced walking computed from upper body accelerations.

These results indicate that, on average, individuals lean forward when walking, both when carrying a load and when carrying no load. This effect is independent of the forward body lean due to backpack load carriage, since it is not apparent in the relative lean angles in which the zero load angles have been subtracted to give a reference angle of 0° for the no load condition.

Appendix C – Energy Cost Prediction Models

Six models were created for the prediction of $\dot{V}O_2$ during load carriage using data collected in the previous study (Morin et al., 2004) – $\dot{V}O_2$ sampled at 20s intervals, upper body accelerations (sampled at 100 Hz) and heart rate, recorded at 1 min. intervals. The first model involved HR only as the independent variable. The second involved load, speed and incline as the independent variables. Models 3-6 involved upper body acceleration parameters with the inclusion of HR in Model 5 and load in Model 6. The test conditions, under which the data were recorded, are given in Table C-I. The measured parameters – HR and rms values of upper body accelerations – are plotted against measured $\dot{V}O_2$ in Figure C-1.

Table C-I. Test conditions for the treadmill study; two tests were completed on each experimental day.

Test	Load (kg)	Speed (km/h)	Incline (deg)
A1	0	3.22, 4.83, 6.44	0
A2	38.7	3.22, 4.83, 6.44	0
B1	0	4.83	0, 5, 10
B2	38.7	4.83	0, 5, 10
C1	16.6	3.22, 4.83, 6.44	0
C2	25.9	3.22, 4.83, 6.44	0
D1	16.6	4.83	0, 5, 10
D2	25.9	4.83	0, 5, 10
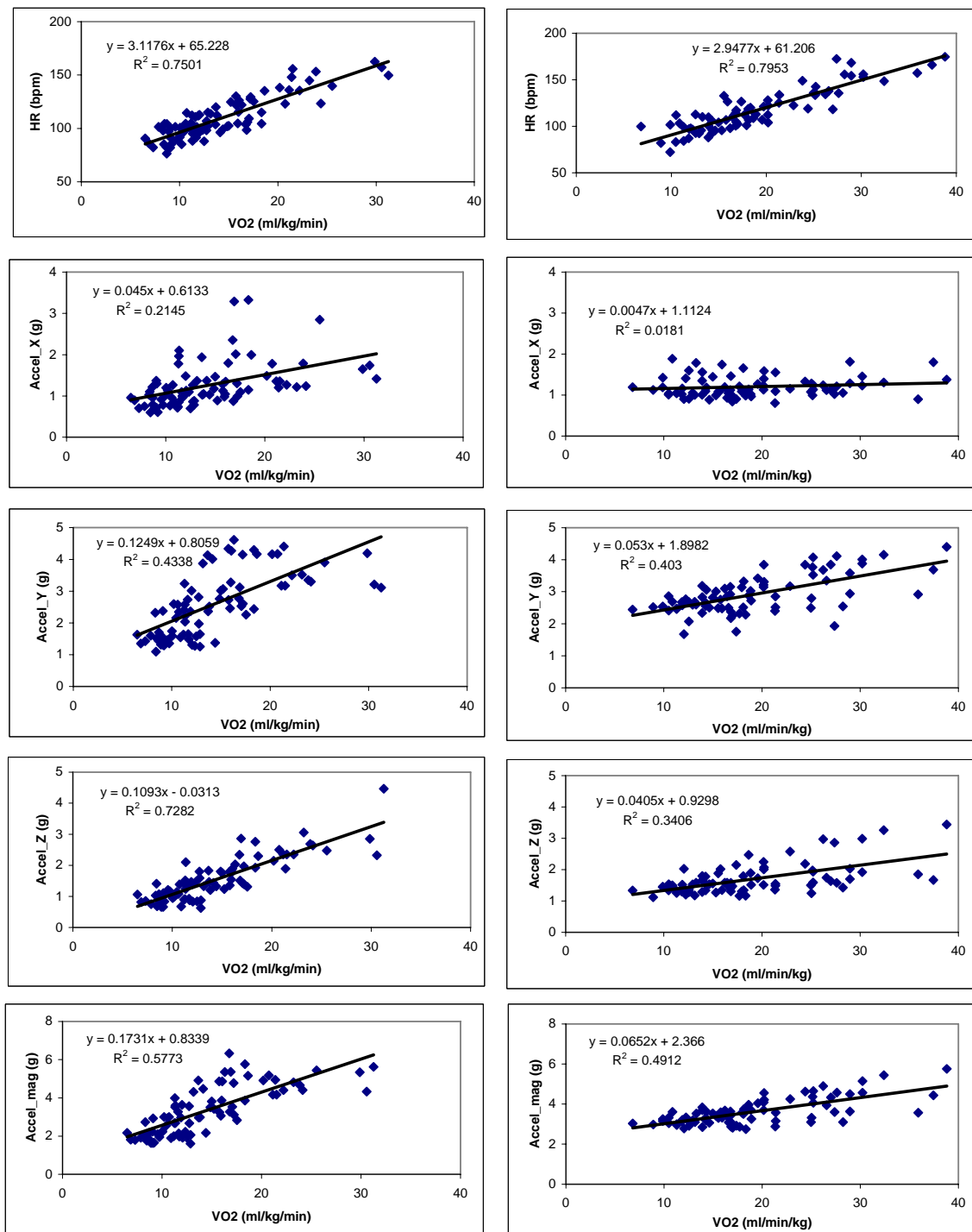
Figure C-1. Measured parameters versus $\dot{V}O_2$ for the changing speed (left) and changing incline (right) tests. All values have been averaged over the final four minutes of each test condition.

C.1 Graphical Analysis of Energy Cost Models

The models generated to predict $\dot{V}O_2$ from the known parameters and/or measured variables were analysed to assess their validity. The correlation coefficient was computed for each model, however this measures the strength of the linear relationship between variables (in our case between the predicted and measured $\dot{V}O_2$) but not the agreement between them (Bland and Altman, 1986). If the predicted values agree well with the measured values, a plot of predicted vs. measured values will lie along a line of slope 1 and intercept 0. The validity of a model is better assessed by considering the characteristics of the residuals: the difference between the measured values and the predicted values. In the Bland-Altman plot, the residuals are plotted against the average of the measured and predicted values. The plot provides information on how large the differences between the measured and predicted values are and whether or not the differences are random or vary in some systematic way. Residuals can also be plotted against the independent variables in the model to determine the sufficiency of the functional part of the model. If the residuals vary randomly with respect to the independent variables, the model fits the data well and the variance not explained by the model is random (NIST/SEMATECH, 2005; sec. 4.4.4.1). Residual plots can also be used to assess whether the standard deviation in the random errors is constant across the range of the independent variables, such that the data are of equal quality for generating a model (NIST/SEMATECH, 2005; sec. 4.4.4.2). The distribution of the residuals determines the limits on the acceptable errors. If the residuals are normally distributed, upper and lower bounds are set at [mean ± 2×(standard deviation)] (Bland and Altman, 1986). Residuals can be tested for normality by plotting the histogram and the normal probability plot, which is a plot of the residual values versus values from a standard normal distribution (NIST/SEMATECH, 2005; sec. 4.4.4.5). The skewness and kurtosis of the distribution can be computed, where a normal distribution has a skewness of zero and a kurtosis of 3. If the distribution is skewed left, skewness is negative; if the distribution is skewed right, skewness is positive. If kurtosis is >3 the distribution is more peaked; if kurtosis is <3, the distribution is flattened (NIST/SEMATECH, 2005; sec. 1.3.5.11). These graphical tests were done for the six energy cost models and the results are shown below in Figures C-2 to C-25 (plots of the predicted vs measured values and the residual plots were done in Excel; the histogram and normality probability plots were done in SPSS v. 12.0; skewness and kurtosis were computed in SPSS v. 12.0).

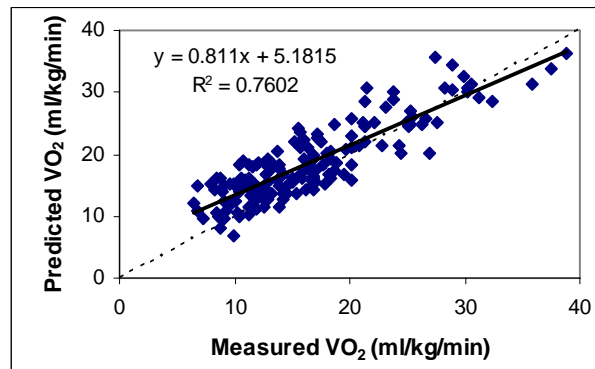**Model 1:** $\dot{V}O_2 = -13.791 + 0.286(HR)$ $\qquad$ **$R^2 = 0.760$**

Figure C-2. Predicted vs measured $\dot{V}O_2$ for Model 1. The solid line is the linear regression, where the equation is shown at the top left. The dashed line is the line of agreement: predicted $\dot{V}O_2$ = measured $\dot{V}O_2$. The mean (standard deviation) of the measured values is 16.69 (6.69) and of the predicted values is 18.68 (6.22).
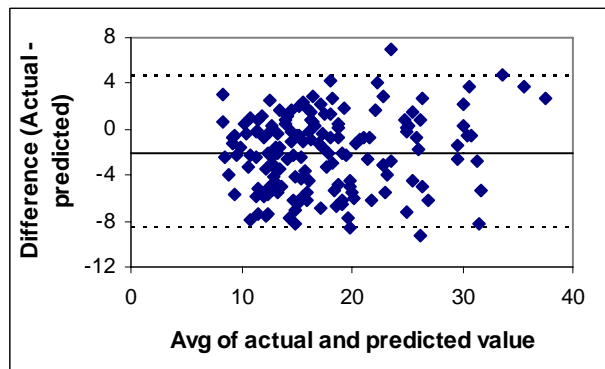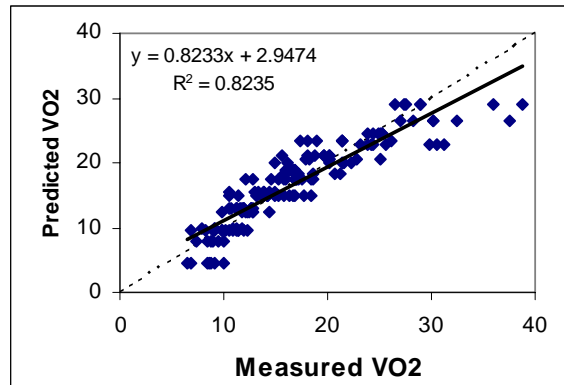

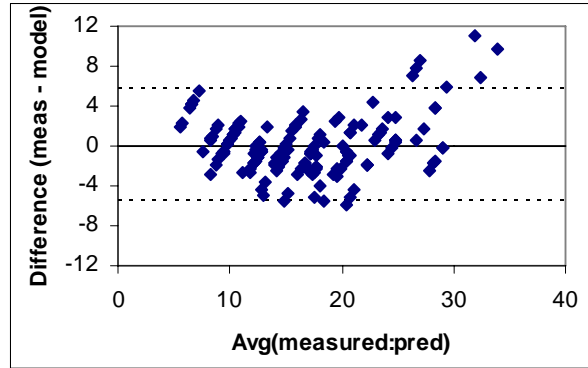**Figure C-3.** Bland-Altman plot for Model 1. The solid line is the mean of the residuals (−2.04); the dashed lines are the mean ± 2×std dev (−8.63, 4.55).
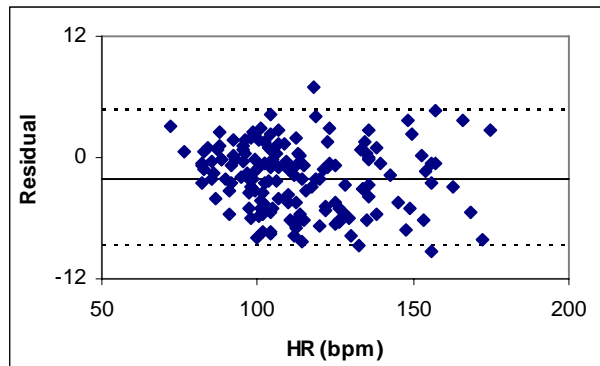
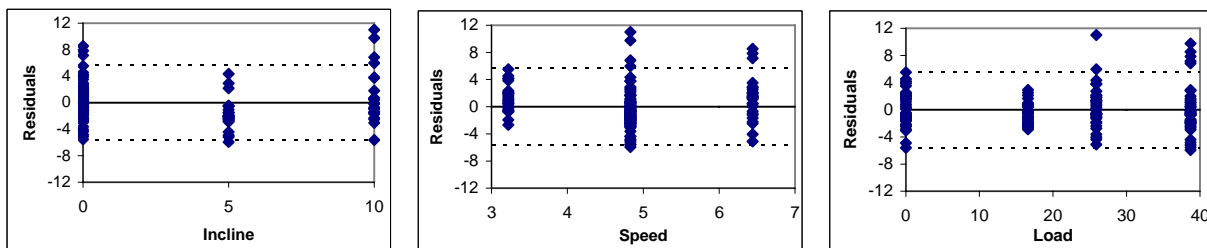**Figure C-4.** Residuals versus the independent variable (HR) for Model 1. The solid and dashed lines are as in Fig. C-3.
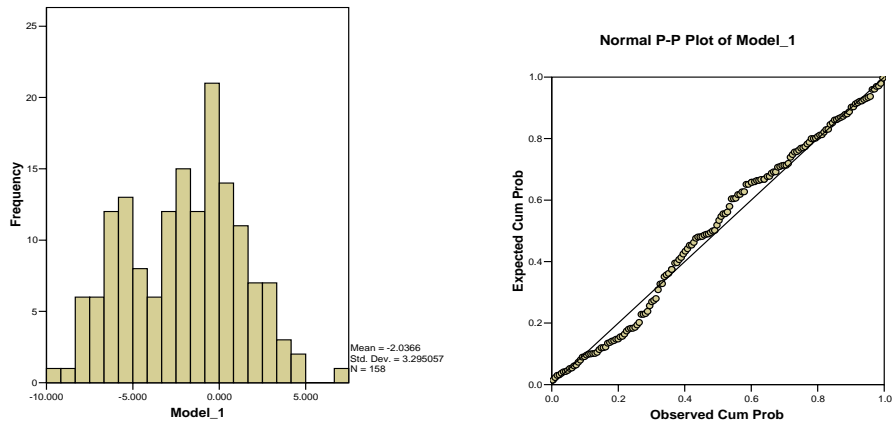
Figure C-5.   Histogram and normal probability plot of the residuals of Model 1. The residuals are normally distributed, but the distribution is not zero mean. The distribution is not skewed (skewness = −0.052), but is flattened (kurtosis = −0.632).

Model 2: $\dot{V}O_2 = -5.79 + 1.148(I) + 3.202(S) + 0.204(L)$ **$R^2 = 0.823$**
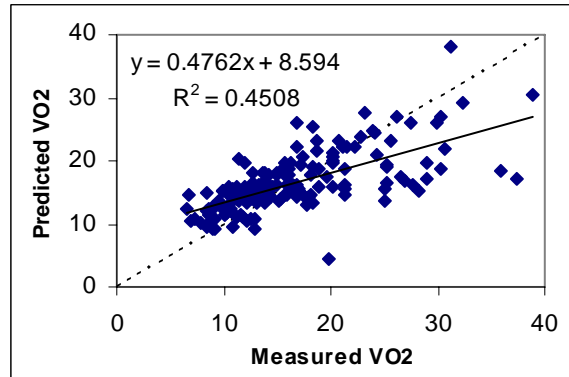

Figure C-6.   Predicted vs measured $\dot{V}O_2$ for Model 2. The solid line is the linear regression, where the equation is shown at the top left. The dashed line is the line of agreement. The mean (standard deviation) of the measured values is 16.69 (6.69) and of the predicted values is 16.69 (6.07).
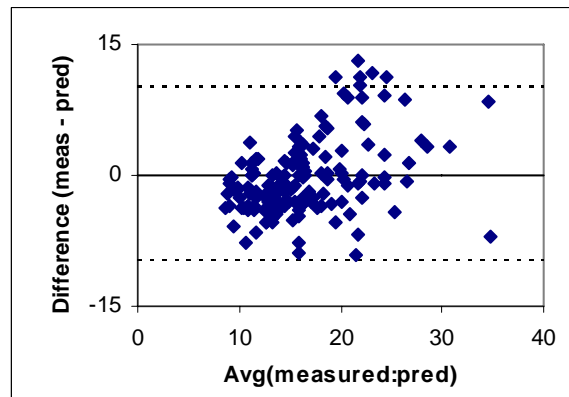
Figure C-7. Bland-Altman plot for Model 2. The solid line is the mean of the residuals (0.0014); the dashed lines are the mean ± 2×std dev (−5.62, 5.62).

Figure C-8. Residuals versus the independent variables (load, speed and incline) for Model 2. The solid and dashed lines are as in Fig. C-7.
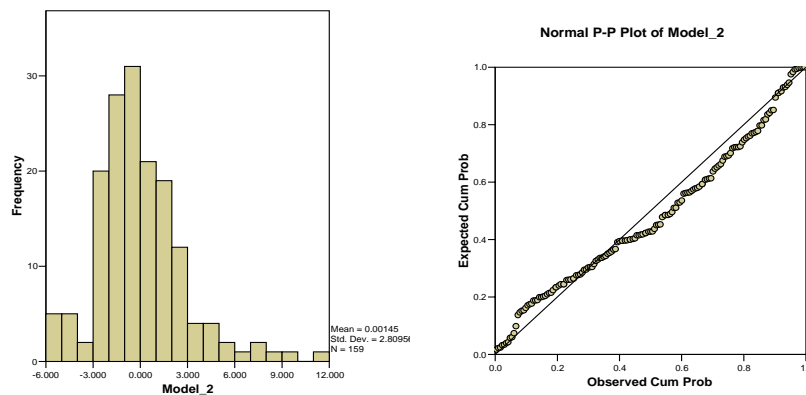
Figure C-9. Histogram and normal probability plot of the residuals of Model 2. The mean of the distribution is zero. The distribution is slightly skewed right (skewness = 0.995), and the shape is normal (kurtosis = 2.223).

Model 3: $\dot{V}O_2 = 7.579(\text{AccelZ}) + 4.345$ $\quad$ $\mathbf{R^2 = 0.482}$

Figure C-10. Predicted vs measured $\dot{V}O_2$ for Model 3. The solid line is the linear regression, where the equation is shown at the top left. The dashed line is the line of agreement. The mean (standard deviation) of the measured values is 16.69 (6.69) and of the predicted values is 16.5 (4.74).

Figure C-11. Bland-Altman plot for Model 3. The solid line is the mean of the residuals (0.099); the dashed lines are the mean $\pm 2 \times$std dev (-9.81, 10.01).
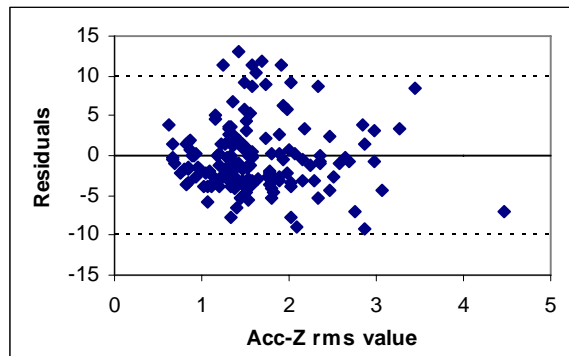
Figure C-12. Residuals versus the independent variable (AccelZ) for Model 3. The solid and dashed lines are as in Fig. C-11.
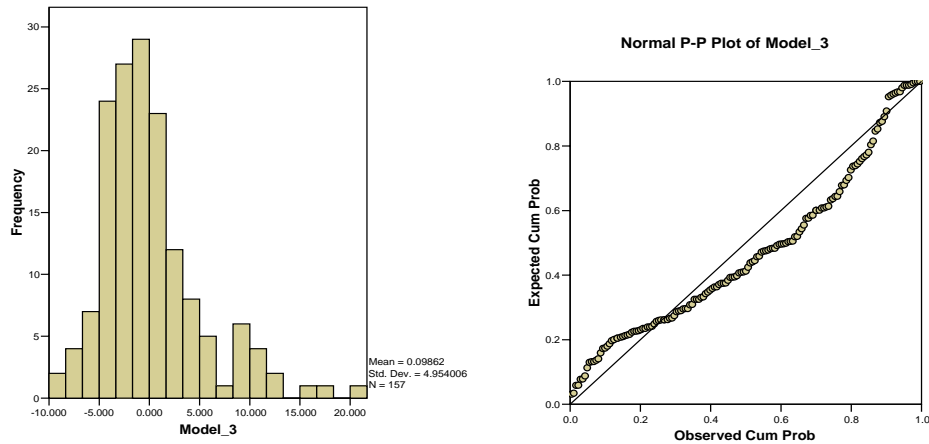
Figure C-13. Histogram and normal probability plot of the residuals of Model 3. The mean of the distribution is close to zero. The distribution is skewed right (skewness = 1.346) and the shape is normal (kurtosis = 2.702). Note the deviation in the normal probability plot.

Model 4: $\dot{V}O_2 = 2.627 + 5.9(\text{AccelZ}) + 2.801(\text{AccelY}) - 2.65(\text{AccelX})$ **R^2 = 0.554**
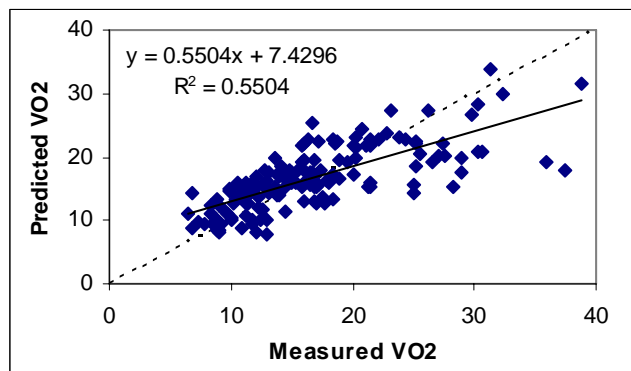

Figure C-14. Predicted vs measured $\dot{V}O_2$ for Model 4. The solid line is the linear regression, where the equation is shown at the top left. The dashed line is the line of agreement. The mean (standard deviation) of the measured values is 16.69 (6.69) and of the predicted values is 16.53 (4.96).
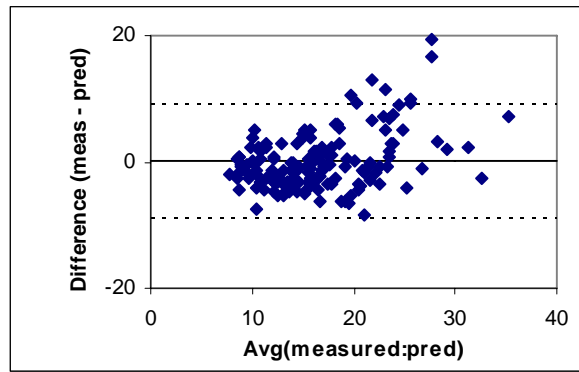
Figure C-15. Bland-Altman plot for Model 4. The solid line is the mean of the residuals (0.0007); the dashed lines are the mean ± 2×std dev (−8.97, 8.97).
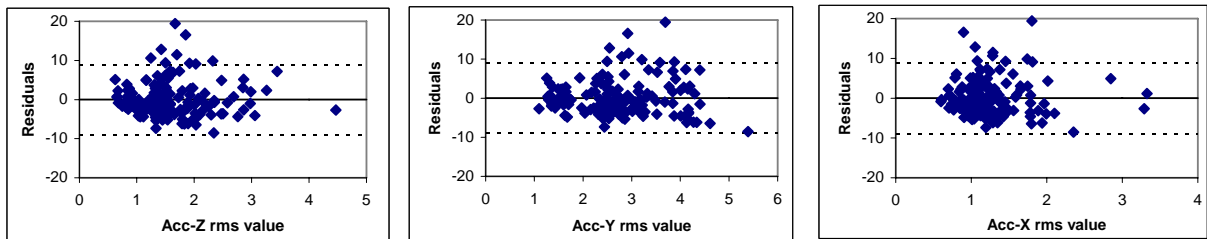

Figure C-16. Residuals versus the independent variables (AccelZ, AccelY and AccelX) for Model 4. The solid and dashed lines are as in Fig. C-15.
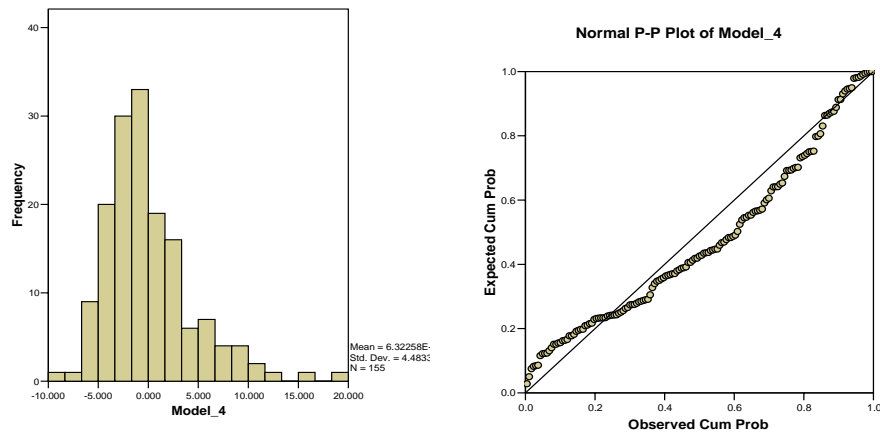

Figure C-17. Histogram and normal probability plot of the residuals of Model 4. The mean of the distribution is close to zero. The distribution is skewed right (skewness = 1.373), and the shape is normal (kurtosis = 2.85). Note the deviation in the normal probability plot.

Model 5: $\dot{V}O_2 = -13.652 + 0.212(\mathrm{HR}) + 0.186(\mathrm{AccelZ}) + 1.16(\mathrm{AccelY})$ $\mathbf{R^2 = 0.811}$
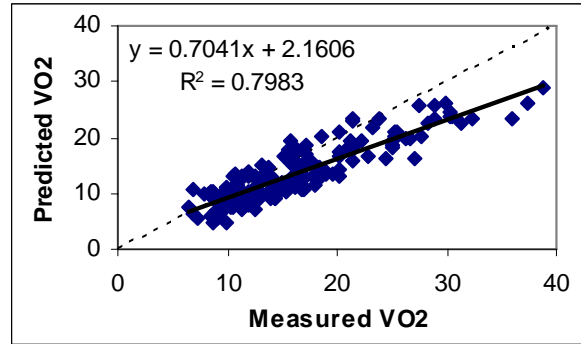

Figure C-18. Predicted vs measured $\dot{V}O_2$ for Model 5. The solid line is the linear regression, where the equation is shown at the top left. The dashed line is the line of agreement. The mean (standard deviation) of the measured values is 16.69 (6.69) and of the predicted values is 13.8 (5.27).

Figure C-19. Bland-Altman plot for Model 5. The solid line is the mean of the residuals (2.73); the dashed lines are the mean $\pm$ 2$\times$std dev (-3.44, 8.9).
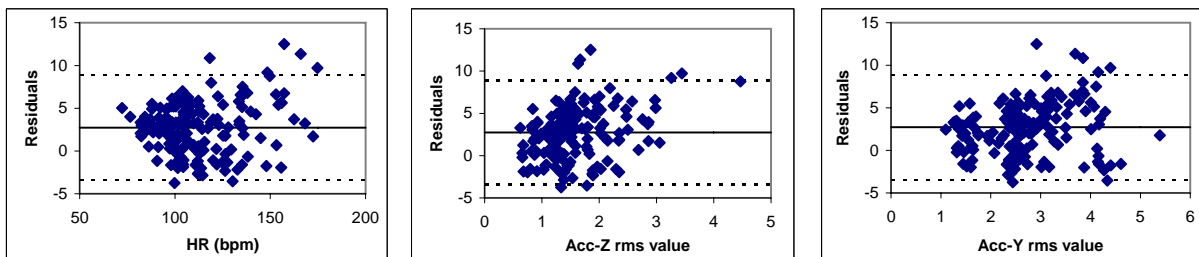
Figure C-20. Residuals versus the independent variables (HR, AccelZ and AccelY) for Model 5. The solid and dashed lines are as in Fig. C-19.

Figure C-21. Histogram and normal probability plot of the residuals of Model 5. The mean of the distribution is not zero (mean = 2.73). The distribution is not skewed (skewness = 0.283), but is flattened (kurtosis = 0.181).

Model 6: $\dot{V}O_2 = -2.35 + 3.871(\text{AccelZ}) + 0.185(\text{L}) + 3.233(\text{AccelY})$　　　　$\mathbf{R^2 = 0.683}$
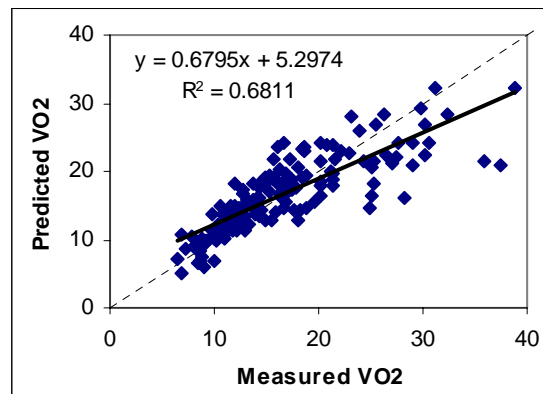
Figure C-22. Predicted vs measured $\dot{V}O_2$ for Model 6. The solid line is the linear regression, where the equation is shown at the top left. The dashed line is the line of agreement. The mean (standard deviation) of the measured values is 16.69 (6.69) and of the predicted values is 16.53 (5.51).
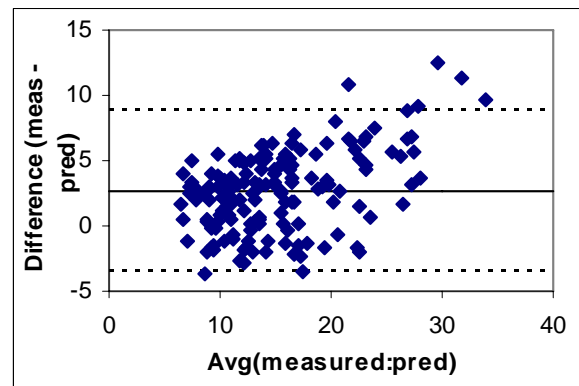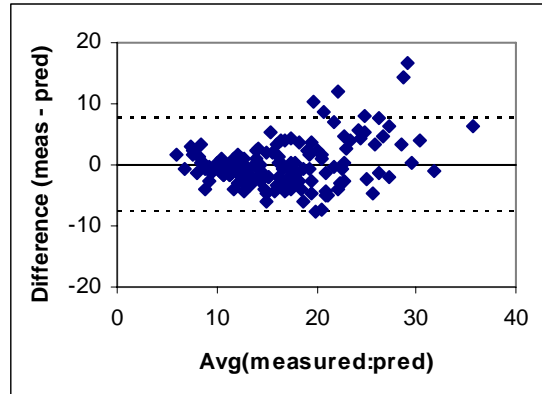
Figure C-23. Bland-Altman plot for Model 6. The solid line is the mean of the residuals (−0.0006); the dashed lines are the mean ± 2×std dev (−7.55, 7.55).
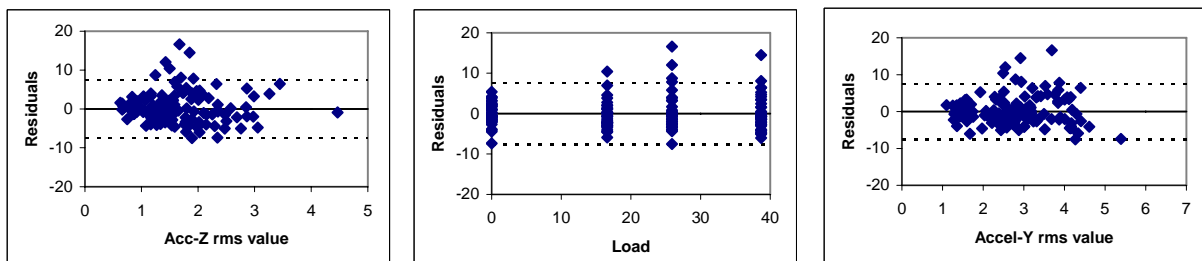
Figure C-24. Residuals versus the independent variables (HR, AccelZ and AccelY) for Model 6. The solid and dashed lines are as in Fig. C-23.
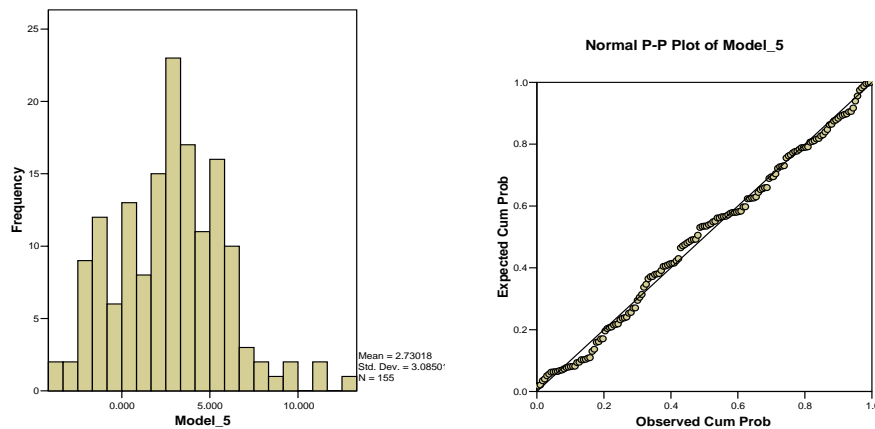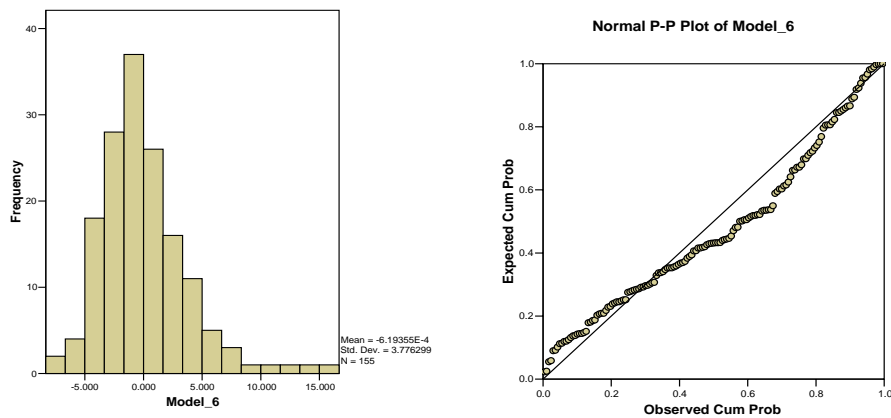

Figure C-25. Histogram and normal probability plot of the residuals of Model 6. The distribution is zero mean (mean = −0.0006) and is skewed right (skewness = 1.383) and slightly peaked (kurtosis = 3.439).

In Model 1, in which HR is related to measured $\dot{V}O_2$, there seems to be good agreement between measured and predicted $\dot{V}O_2$ values, as the slope of the regression line on the predicted versus measured $\dot{V}O_2$ plot is close to 1. However, the mean of the predicted values is higher than the mean of the measured values and the residual mean is −2.04. This indicates that there is a bias error, or a constant error across the range of measured $\dot{V}O_2$, in the predicted $\dot{V}O_2$. There is no apparent structure in the Bland-Altman or residual versus HR plots, and only one residual value falls outside the statistical bounds, indicating that, except for the bias error, the model fits the data well. The residuals are normally distributed (although the distribution is flattened) so the upper and lower bounds on the residuals (mean ± 2×SD) are acceptable. Model 2, based on incline, speed and load, also agrees well with the measured data, and the mean value of the predicted $\dot{V}O_2$ is very close to the mean value of the measured $\dot{V}O_2$ (the mean of the residuals is 0.0014). On the Bland-Altman plot, however, several values lie above the upper bound for the residuals. These occur at the upper range of the $\dot{V}O_2$ values and examination of the plot of predicted versus measured $\dot{V}O_2$ reveals that $\dot{V}O_2$ is under-predicted at the high values. The spread in the residuals is not constant across incline, speed and load, indicating that the standard deviation of the errors is not constant across the range of the independent variables. Models 3 through 6 all involve using the rms values of the upper body accelerations as independent variables in the models. Considering the predicted vs measured $\dot{V}O_2$ plots, a common characteristic appears to be under-prediction of $\dot{V}O_2$ particularly for the higher measured $\dot{V}O_2$ values. There is an upward trend in the Bland-Altman plot for all models, but the slope of the trend decreases from Model 3 to Model 6 (the slopes are 0.405, 0.339, 0.25 and 0.212 for Models 3, 4, 5 and 6 respectively), indicating that the added variables have improved the fit of the models. In all models however, there are a number of residuals above the upper bound. The predicted vs measured $\dot{V}O_2$ is plotted for the changing speed tests only for Models 3-6 in Fig. C-26. It is apparent that the agreement between predicted and measured $\dot{V}O_2$ is much better for these models when the values for the changing incline tests are removed. Thus, upper body accelerations can be used to reliably predict energy cost under conditions of changing speed of walking and different loads carried, but the effect of changes in terrain on energy cost is not reflected in upper body accelerations.
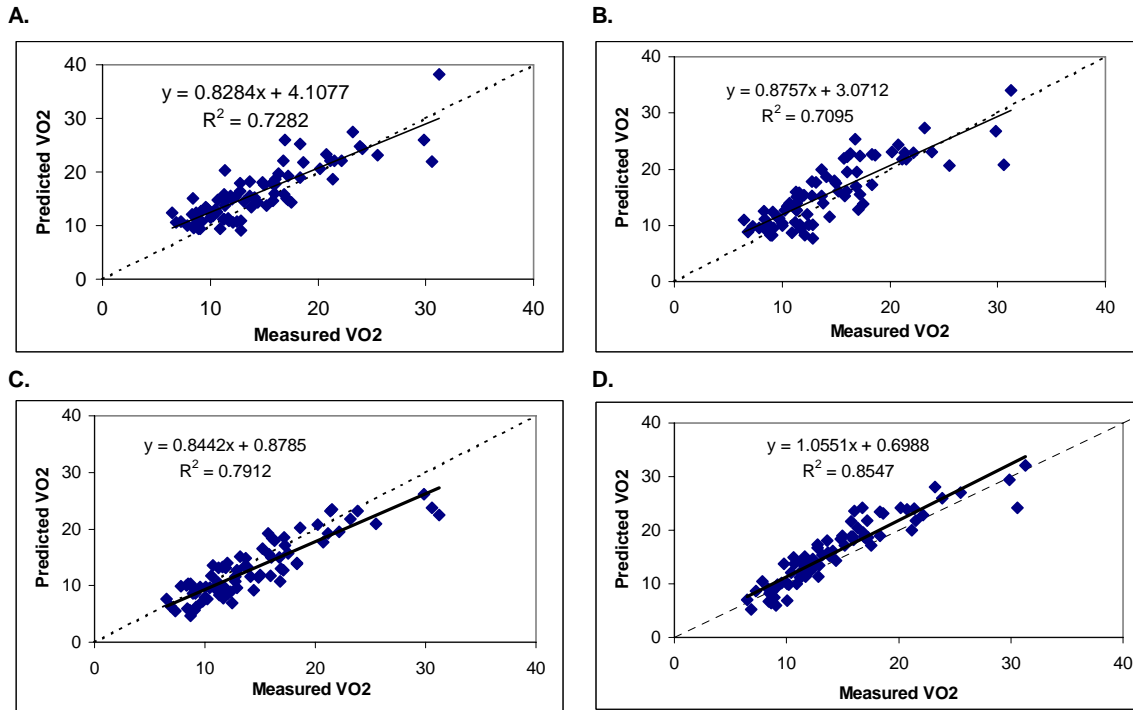
A.

B.

C.

D.

Figure C-26. Predicted vs measured $\dot{V}O_2$ for A. Model 3; B. Model 4; C. Model 5 and D. Model 6 for changing speed tests only. The agreement between the predicted and measured values is very good for all models.

Appendix D

60N Shoulder Strap Tension, 0 N Waist Belt Tension

15 kg

Walking Speed	COG Position Low	COG Position Med	COG Position High
4 kph	15kg60N0N1L4kph.txt	15kg60N0N2M4kph.txt	15kg60N0N3H4kph.txt
5 kph	15kg60N0N1L45ph.txt	15kg60N0N2M5kph.txt	15kg60N0N3H5kph.txt
6 kph	15kg60N0N1L46ph.txt	15kg60N0N2M6kph.txt	15kg60N0N3H6kph.txt

25 kg

Walking Speed	COG Position Low	COG Position Med	COG Position High
4 kph	25kg60N0N1L4kph.txt	25kg60N0N2M4kph.txt	25kg60N0N3H4kph.txt
5 kph	25kg60N0N1L45ph.txt	25kg60N0N2M5kph.txt	25kg60N0N3H5kph.txt
6 kph	25kg60N0N1L46ph.txt	25kg60N0N2M6kph.txt	25kg60N0N3H6kph.txt

35 kg

Walking Speed	COG Position Low	COG Position Med	COG Position High
4 kph	35kg60N0N1L4kph.txt	35kg60N0N2M4kph.txt	35kg60N0N3H4kph.txt
5 kph	35kg60N0N1L45ph.txt	35kg60N0N2M5kph.txt	35kg60N0N3H5kph.txt
6 kph	35kg60N0N1L46ph.txt	35kg60N0N2M6kph.txt	35kg60N0N3H6kph.txt

100 N Shoulder Strap Tension, 0 N Waist Belt Tension

15 kg

Walking Speed	COG Position Low	COG Position Med	COG Position High
4 kph	15kg100N0N1L4kph.txt	15kg100N0N2M4kph.txt	15kg100N0N3H4kph.txt
5 kph	15kg100N0N1L45ph.txt	15kg100N0N2M5kph.txt	15kg100N0N3H5kph.txt
6 kph	15kg100N0N1L46ph.txt	15kg100N0N2M6kph.txt	15kg100N0N3H6kph.txt

25 kg

Walking Speed	COG Position Low	COG Position Med	COG Position High
4 kph	25kg100N0N1L4kph.txt	25kg100N0N2M4kph.txt	25kg100N0N3H4kph.txt
5 kph	25kg100N0N1L45ph.txt	25kg100N0N2M5kph.txt	25kg100N0N3H5kph.txt
6 kph	25kg100N0N1L46ph.txt	25kg100N0N2M6kph.txt	25kg100N0N3H6kph.txt

35 kg

Walking Speed	COG Position Low	COG Position Med	COG Position High
4 kph	35kg100N0N1L4kph.txt	35kg100N0N2M4kph.txt	35kg100N0N3H4kph.txt
5 kph	35kg100N0N1L45ph.txt	35kg100N0N2M5kph.txt	35kg100N0N3H5kph.txt
6 kph	35kg100N0N1L46ph.txt	35kg100N0N2M6kph.txt	35kg100N0N3H6kph.txt

60 N Shoulder Strap Tension, 60 N Waist Belt Tension

15 kg

Walking Speed	COG Position Low	COG Position Med	COG Position High
4 kph	15kg60N60N1L4kph.txt	15kg60N60N2M4kph.txt	15kg60N60N3H4kph.txt
5 kph	15kg60N60N1L45ph.txt	15kg60N60N2M5kph.txt	15kg60N60N3H5kph.txt
6 kph	15kg60N60N1L46ph.txt	15kg60N60N2M6kph.txt	15kg60N60N3H6kph.txt

25 kg

Walking Speed	COG Position Low	COG Position Med	COG Position High
4 kph	25kg60N60N1L4kph.txt	25kg60N60N2M4kph.txt	25kg60N60N3H4kph.txt
5 kph	25kg60N60N1L45ph.txt	25kg60N60N2M5kph.txt	25kg60N60N3H5kph.txt
6 kph	25kg60N60N1L46ph.txt	25kg60N60N2M6kph.txt	25kg60N60N3H6kph.txt

35 kg

Walking Speed	COG Position Low	COG Position Med	COG Position High
4 kph	35kg60N60N1L4kph.txt	35kg60N60N2M4kph.txt	35kg60N60N3H4kph.txt
5 kph	35kg60N60N1L45ph.txt	35kg60N60N2M5kph.txt	35kg60N60N3H5kph.txt
6 kph	35kg60N60N1L46ph.txt	35kg60N60N2M6kph.txt	35kg60N60N3H6kph.txt

100 N Shoulder Strap Tension, 60 N Waist Belt Tension

15 kg

Walking Speed	COG Position Low	COG Position Med	COG Position High
4 kph	15kg100N60N1L4kph.txt	15kg100N60N2M4kph.txt	15kg100N60N3H4kph.txt
5 kph	15kg100N60N1L45ph.txt	15kg100N60N2M5kph.txt	15kg100N60N3H5kph.txt
6 kph	15kg100N60N1L46ph.txt	15kg100N60N2M6kph.txt	15kg100N60N3H6kph.txt

25 kg

Walking Speed	COG Position Low	COG Position Med	COG Position High
4 kph	25kg100N60N1L4kph.txt	25kg100N60N2M4kph.txt	25kg100N60N3H4kph.txt
5 kph	25kg100N60N1L45ph.txt	25kg100N60N2M5kph.txt	25kg100N60N3H5kph.txt
6 kph	25kg100N60N1L46ph.txt	25kg100N60N2M6kph.txt	25kg100N60N3H6kph.txt

35 kg

Walking Speed	COG Position Low	COG Position Med	COG Position High
4 kph	35kg100N60N1L4kph.txt	35kg100N60N2M4kph.txt	35kg100N60N3H4kph.txt
5 kph	35kg100N60N1L45ph.txt	35kg100N60N2M5kph.txt	35kg100N60N3H5kph.txt
6 kph	35kg100N60N1L46ph.txt	35kg100N60N2M6kph.txt	35kg100N60N3H6kph.txt

DOCUMENT CONTROL DATA

(Security classification of the title, body of abstract and indexing annotation must be entered when the overall document is classified)

1. ORIGINATOR (The name and address of the organization preparing the document, Organizations for whom the document was prepared, e.g. Centre sponsoring a contractor's document, or tasking agency, are entered in section 8.)	2. SECURITY CLASSIFICATION (Overall security classification of the document including special warning terms if applicable.)
Publishing: DRDC Toronto Performing: Ergonomics Research Group Mechanics Group, Queen's University, Kingston, Ontario, Canada, K7L 3N6 Monitoring: Contracting: DRDC Toronto	UNCLASSIFIED

3. TITLE (The complete document title as indicated on the title page. Its classification is indicated by the appropriate abbreviation (S, C, R, or U) in parenthesis at the end of the title)

Development of a Dynamic Biomechanical Model for Load Carriage: Phase VI: Assessing Physiological and Biomechanical Loading Using the Portable Measurement System and the Dynamic Biomechanical Model (U)
Élaboration d'un modèle biomécanique dynamique pour le transport de charges – Phase VI : Évaluation des charges biomécaniques et physiologiques à l'aide du système de mesure portatif et du modèle biomécanique dynamique (U)

4. AUTHORS (First name, middle initial and last name. If military, show rank, e.g. Maj. John E. Doe.)

E. Morin; S.A. Reid ; J.M. Stevenson; A. Lee; C. Hare

5. DATE OF PUBLICATION (Month and year of publication of document.) December 2007	6a NO. OF PAGES (Total containing information, including Annexes, Appendices, etc.) 101	6b. NO. OF REFS (Total cited in document.) 36

7. DESCRIPTIVE NOTES (The category of the document, e.g. technical report, technical note or memorandum. If appropriate, enter the type of document, e.g. interim, progress, summary, annual or final. Give the inclusive dates when a specific reporting period is covered.)

Contract Report

8. SPONSORING ACTIVITY (The names of the department project office or laboratory sponsoring the research and development – include address.)

Sponsoring:

Tasking:

9a. PROJECT OR GRANT NO. (If appropriate, the applicable research and development project or grant under which the document was written. Please specify whether project or grant.)	9b. CONTRACT NO. (If appropriate, the applicable number under which the document was written.) 7711–0–7863/02–TOR
10a. ORIGINATOR'S DOCUMENT NUMBER (The official document number by which the document is identified by the originating activity. This number must be unique to this document) DRDC Toronto CR 2008–009	10b. OTHER DOCUMENT NO(s). (Any other numbers under which may be assigned this document either by the originator or by the sponsor.)

11. DOCUMENT AVAILABILITY (Any limitations on the dissemination of the document, other than those imposed by security classification.)

Unlimited distribution

12. DOCUMENT ANNOUNCEMENT (Any limitation to the bibliographic announcement of this document. This will normally correspond to the Document Availability (11), However, when further distribution (beyond the audience specified in (11) is possible, a wider announcement audience may be selected.))

Unlimited announcement

DOCUMENT CONTROL DATA
(Security classification of the title, body of abstract and indexing annotation must be entered when the overall document is classified)

13. ABSTRACT (A brief and factual summary of the document. It may also appear elsewhere in the body of the document itself. It is highly desirable that the abstract of classified documents be unclassified. Each paragraph of the abstract shall begin with an indication of the security classification of the information in the paragraph (unless the document itself is unclassified) represented as (S), (C), (R), or (U). It is not necessary to include here abstracts in both official languages unless the text is bilingual.)

(U) In this work, factors affecting the physiological cost of load carriage and models for the estimation of metabolic energy cost during load carriage were examined in detail. The dynamic biomechanical model (DBM), designed to analyse the effects of rucksack parameters on forces experienced by a pack wearer, was used to create a stand–alone interactive software tool.

It was shown that tri–axial accelerations of the upper torso can be used in static and dynamic conditions to determine alterations in posture and gait, including: heel strike and toe off, forward lean angle, double support time and stride duration. These findings will permit assessment of gait in the field using the portable measurement system, allowing assessment of gait parameters over long durations, under varying terrain and loads. Terrain characteristics are also likely to be reflected in signal parameters other than the rms values examined in this work, permitting further improvement of the predictive models without requiring specific field data such as load, speed and topography. The ability to measure gait alterations using upper body accelerations merits further investigation as the present work was limited in this area.

Models to predict metabolic cost during load carriage under conditions of variable speed, load and incline were developed. A model similar to Pandolf's (Pandolf et al. 1977), using field specific data: load, speed and incline, had the highest correlation coefficient (r2 = 0.823) but under–predicted energy cost both at low values and at high values of measured VO2. A second model using upper body acceleration alone showed reasonable predictive ability (r2 = 0.554) but under predicted VO2 at high energy cost levels. Review of the results showed that the energy effect of incline is not captured in the rms acceleration parameters used in the model. Heart rate is well correlated to metabolic cost and a model using it and acceleration parameters successfully achieved the predictive power of the model based on load, speed and incline with r2 = 0.811.

The Dynamic Biomechanical Model body of work consists of a general dynamic biomechancial model of human backpack load carriage based on the characteristics of the Canadian Clothe the Soldier Rucksack with the ability to assess injury risk potential across as range of activities and loads. Output from this program is expected to provide input to a load carriage limit predictive equation.

(U) Résumé analytique

Dans cette étude, les facteurs qui ont une incidence sur le coût physiologique lié au transport de charges et sur les modèles servant à évaluer la dépense d'énergie métabolique durant le transport de charges ont été examinés en détail. Le modèle biomécanique dynamique (MBD), élaboré dans le but d'analyser les effets des paramètres relatifs aux havresacs sur les forces ressenties par le porteur d'un sac, a été utilisé pour créer un outil logiciel interactif autonome.

Il a été démontré que les accélérations triaxiales de la partie supérieure du torse peuvent être utilisées dans des conditions statiques et dynamiques pour déterminer les changements au niveau de la posture et de la démarche, y compris l'impact du talon au sol et le décollement des orteils, l'angle d'inclinaison avant, la durée du double appui et la durée des enjambées. Ces résultats permettront d'évaluer la démarche sur le terrain à l'aide du système de mesure portatif ainsi que les paramètres relatifs à la démarche sur une longue période, sur différents terrains et avec des charges variées. Les caractéristiques des terrains doivent également pouvoir être prises en considération dans les paramètres des signaux autres que les valeurs quadratiques moyennes examinées

dans cette étude, en vue d'améliorer davantage les modèles prédictifs sans recourir à des données de terrain précises comme la charge, la vitesse et la topographie. La capacité à mesurer les changements dans la démarche en utilisant les accélérations du haut du corps mérite une analyse plus poussée, la présente étude ayant à peine effleuré cet aspect.

Des modèles servant à prédire la dépense d'énergie métabolique durant le transport de charges dans des conditions de vitesse, de charge et d'inclinaison variables ont été élaborés. Un modèle similaire à celui de Pandolf (Pandolf et coll., 1977), qui utilise des données de terrain précises, par exemple la charge, la vitesse et l'inclinaison, avait le coefficient de corrélation le plus élevé (r2 = 0,823), mais une dépense d'énergie sous−estimée à des valeurs mesurées de VO2 faibles et élevées. Un deuxième modèle utilisant seulement une accélération du haut du corps a montré une valeur prédictive raisonnable (r2 = 0,554), mais une valeur de VO2 sous−estimée à des niveaux de dépense énergétique élevés. Un examen des résultats montre que l'effet de l'énergie liée à l'inclinaison n'est pas pris en considération dans les valeurs quadratiques moyennes des paramètres d'accélération utilisés dans le modèle. Il existe une bonne corrélation entre le rythme cardiaque et la dépense métabolique; un modèle qui tient compte de cette corrélation ainsi que des paramètres d'accélération a montré la valeur prédictive du modèle basée sur la charge, la vitesse et l'inclinaison avec un coefficient de corrélation r2 = 0,811.

Le modèle biomécanique dynamique consiste en un modèle biomécanique dynamique général de transport de charges dans un havresac par un être humain, basé sur les caractéristiques du havresac du programme canadien Habillez le soldat (HLS), qui permet d'évaluer les risques de blessures potentiels en fonction d'une gamme d'activités et de charges. On s'attend à ce que les données issues de ce programme soient utilisées dans une équation prédictive des limites de transport de charges.

14. KEYWORDS, DESCRIPTORS or IDENTIFIERS (Technically meaningful terms or short phrases that characterize a document and could be helpful in cataloguing the document. They should be selected so that no security classification is required. Identifiers, such as equipment model designation, trade name, military project code name, geographic location may also be included. If possible keywords should be selected from a published thesaurus, e.g. Thesaurus of Engineering and Scientific Terms (TEST) and that thesaurus identified. If it is not possible to select indexing terms which are Unclassified, the classification of each should be indicated as with the title.)

(U) Clothe the Soldier; CTS; Load carriage system; load carriage simulator; compliance tester; pressure measurement system; Dynamic Biomechanical Model; portable measurement system; Human Performance Assessment; human performance evaluation; Portable Data Acquisition system

UNCLASSIFIED